Thermodynamic properties of a CO_2 −rich mixture $CO_2 + CH_3OH$ in conditions of interest for carbon dioxide capture and storage technology and other applications

Clara Rivas[1], Beatriz Gimeno[1], Ramón Bravo[2], Manuela Artal[1], Javier Fernández[1], Sofía Teresa Blanco[1], María Inmaculada Velasco[*1]

[1]*Departamento de Química Física, Facultad de Ciencias, Universidad de Zaragoza, 50009 Zaragoza, Spain*

[2]*Departamento de Física Aplicada, Facultad de Física, Universidad de Santiago de Compostela, 15782 Santiago de Compostela, Spain*

*Corresponding author: curra@unizar.es

ABSTRACT

Methanol can be an impurity in transported and stored anthropogenic CO_2 in carbon dioxide capture and storage technology; likewise, methanol is one of the most useful CO_2 modifiers for supercritical processes. Therefore reliable values of thermodynamic properties of CO_2 −rich mixtures $CO_2 + CH_3OH$ are needed. We measured the following properties of a $CO_2 + CH_3OH$ mixture with $x_{CO_2} = 0.9700$ in dense phase at six temperatures from 263.15K to 313.15 K:

- The speed of sound, c, up to 194.49 MPa, using a double-path pulse-echo method at 5 MHz, for which a repeatability study gave an overall standard uncertainty of c, $u(c) = 5.9 \times 10^{-4} \cdot c$.
- The density, ρ, at pressures ≤ 20.00 MPa using a vibrating-tube densimeter with a standard uncertainty, $u(\rho) = 0.4\ \mathrm{kg/m^3}$.

Combining our c and ρ experimental values and the isobaric specific heat capacity, c_p, from the GERG equation of state (EoS), we calculated ρ, c_p, the volume-dependent solubility parameter, δ_V, and the Joule-Thomson coefficient, μ_{JT}, at pressures ≤195.0 MPa. We are the first to report the adaptation for compressed gases of a calculation method based on numerical integration previously used only for liquids. The experimental and calculated values

were compared with those from the PC-SAFT and GERG EoSs, allowing us to validate both EoSs to represent the experimental properties of the system under most conditions studied and the calculation method up to 195.0 MPa.

Keywords: CO_2, methanol, density, speed of sound, PC-SAFT EoS, GERG EoS

1. Introduction

Carbon dioxide capture and storage (CCS) is considered one of the most important technologies to reduce the world´s emissions of greenhouse gases. In the International Energy Agency´s two-degree scenario (2DS), CCS is expected to help reduce global $\mathrm{CO_2}$ emissions by storing approximately 7 gigatons per year by 2050 [1]. This amount is much greater than that used for enhanced oil and gas recovery purposes (approximately 50 megatons per year in the USA [2]). To optimize the process efficiency, the $\mathrm{CO_2}$ will have to be transported from the capture plants to reservoirs predominantly in high-pressure pipelines [3].

CCS technology comprises three main steps: anthropogenic $\mathrm{CO_2}$ capture, transport and storage. The design of each step is influenced by the thermodynamic procedure used to model the fluid behavior [3]. Whether using an existing procedure or developing a new one, experimental data on the physicochemical properties of $\mathrm{CO_2}$ mixtures with the impurities typically present in anthropogenic $\mathrm{CO_2}$ are needed in wider composition, temperature and pressure ranges than those associated with CCS technology [4]. However, the paucity of experimental data precludes the development of a reference model for this technology, especially an equation of state (EoS), which is one of the most critical future challenges [5].

To develop an EoS, the essential data are the volumetric properties (pressure-density-temperature, $p-\rho-T$) and the liquid-vapor equilibrium, VLE, although reliable values for the speed of sound, c, and the isobaric specific heat capacity, c_p are necessary as well. Using acoustic results to formulate EoSs is particularly attractive given that the speed of sound can be measured with outstanding precision over wide temperature and pressure ranges. Furthermore, all the thermodynamic properties of a

fluid can be obtained from speed of sound measurements by integrating the partial differential equations that relate c to other thermodynamic properties [6]. Currently, accurately measuring the speed of sound propagation in high-pressure fluids is one of the standard methods to precisely determine such fluids' thermophysical properties [7].

In practice, reliable $p-\rho-T$ data, among others, are necessary to evaluate parameters related to transport, injection and storage [8]. Moreover, the speed of sound enables detection of the pressure drop along the pipeline and leaks, monitoring of changes in composition and the performance of seismic studies [9, 10, 11].

To estimate the temperature variations at various stages of the process, precise data from additional thermodynamic properties such as c_p and the Joule-Thomson coefficient, μ_{JT}, are required [9,12]. The solubility parameter, δ, provides information about the interactions between the injected fluid and other substances present in the storage reservoir.

All these properties are affected to a great extent by the nature and quantity of the impurities present in the anthropogenic $\mathrm{CO_2}$, which, in turn, depend on the $\mathrm{CO_2}$ source and the capture and conditioning processes [5]. Although the main impurities are $\mathrm{N_2}, \mathrm{H_2}, \mathrm{O_2}, \mathrm{Ar}, \mathrm{SO_2}, \mathrm{NO_x}, \mathrm{CO}$ and water [4, 13], methanol can be present in transported and injected anthropogenic $\mathrm{CO_2}$ because of its use as a hydrate inhibitor and as a residue from pipeline drying. Thus, quantification of the effect of this impurity on the thermodynamic properties that influence CCS processes is necessary.

Furthermore, supercritical $\mathrm{CO_2}$, $\mathrm{ScCO_2}$, is the most widely used supercritical solvent in a broad range of applications, and methanol is one of the most common modifiers added to enhance the solvating power of $\mathrm{ScCO_2}$ to target polar species [14]. The

80 solvent strength of a supercritical fluid solvent is related to its density, and it may be
81 quantitatively represented by the solubility parameter [15]. In addition, c_p and μ_{JT} of
82 $\mathrm{CO_2} + \mathrm{CH_3OH}$ system acting as the mobile phase affect to resolution properties in
83 supercritical fluid chromatography [16].
84 Density and VLE have been widely studied in the literature [17, 18, 19, 20, 21, 22, 23,
85 24, 25, 26, 27, 28, 29, 30, 31,32 33, 34, 35, 36, 37] for the $\mathrm{CO_2} + \mathrm{CH_3OH}$ system,
86 however we note that little information is available on its volumetric behavior at $T \leq$
87 313 K and at mole fractions of $\mathrm{CO_2}$, $x_{\mathrm{CO_2}}$, greater than 0.75 [19, 20, 21, 32, 34].
88 δ values have been obtained at $T \geq 313$ K [14, 38, 39, 40]; however, no data for c, c_p
89 or μ_{JT} are available in the literature.
90 The aim of this work was to conduct an extensive thermodynamic study of a $\mathrm{CO_2}$ −rich
91 mixture with $\mathrm{CH_3OH}$ ($x_{\mathrm{CO_2}} = 0.9700$) under T and p conditions compatible with CCS
92 and other applications. We therefore:
93 i) Adapted and used an experimental apparatus to accurately measure the speed
94 of sound in mixtures containing sufficiently dense compressed gases. We also
95 determined the uncertainty of the experimental speed of sound
96 measurements for the system $\mathrm{CO_2} + \mathrm{CH_3OH}$.
97 ii) Experimentally measured the following properties for the $\mathrm{CO_2} + \mathrm{CH_3OH}$
98 mixture with $x_{\mathrm{CO_2}} = 0.9700$:
99 -The speed of sound, $p - c - T$, between 263.16 K and 313.15 K and at
100 pressures up to 194.49 MPa.
101 - The density, $p - \rho - T$, from 263.15 K to 313.15 K and up to 20.00 MPa.
102 iii) Adapted and validated a calculation method to obtain ρ and c_p values and
103 derived properties such as the volume-dependent solubility parameter, δ_V ,

and μ_{JT} for systems containing compressed gases at pressures up to 195.0 MPa. All properties were obtained for $CO_2 + CH_3OH$ with $x_{CO_2} = 0.9700$ in the working temperature range. Several authors [41, 42, 43, 44, 45] have used the same fundamental approach to liquid compounds; however, this work represents its first application to compressed gases.

iv) Compared either the experimental results or the calculated values of the aforementioned thermodynamic properties with two different formulation EoS: PC-SAFT [46, 47] and GERG [48, 49].

In summary, in this article we implement an experimental setup to measure *c* in mixtures containing compressed gases. We present the experimental results for the speed of sound (at pressures up to 194.49 MPa), and density (up to 20.00 MPa) for the mixture $CO_2 + CH_3OH$ ($x_{CO_2} = 0.9700$); together, these results allow us to evaluate the predictive power of the PC-SAFT and GERG EoSs for these properties. From our *c* data and both our ρ and the GERG EoS c_p at a reference pressure, we calculate ρ, c_p, δ_V, and μ_{JT} for pressures up to 195.0 MPa. This method of calculating thermodynamic properties up to high pressures, which is applied here to compressed gases for the first time, is validated by comparing the results with the values obtained from the PC-SAFT and GERG EoSs.

2. Materials and methods

2.1. Chemicals

Methanol from Sigma-Aldrich (biotech. grade, mole fraction 0.9993) and carbon dioxide from Air Liquide (mole fraction > 0.99998) were used without further

126 purification. The details, including purities and sources of the materials used in this
127 work are listed in Table 1.

128 2.2. Speed of sound data acquisition: Experimental setup and procedure

129 To determine speeds of sound, we used a 5 MHz ultrasonic pulse device previously
130 described for its application to pure fluids [50]. It was originally designed to work with
131 liquids, and we demonstrated that it is also adequate for sufficiently dense
132 compressed gases [50]. The device operates between 253 K and 473 K and from
133 atmospheric pressure to 200 MPa, with standard uncertainties of $u(T) = 0.015$ K and
134 $u(p) = 0.02$ MPa, respectively.

135 The $CO_2 + CH_3OH$ mixtures were prepared in a variable-volume cell provided by Top
136 Industrie S.A.S. with a maximum volume of 0.51 L and a maximum working pressure of
137 30 MPa. The cell was first evacuated, and methanol was the first component added to
138 the evacuated cell. Next, CO_2 was injected using an ISCO model 260D syringe pump for
139 a chromatography instrument; this pump operates at pressures up to 50 MPa. After
140 the mixture was prepared, it was transferred to a syringe pump by pushing the
141 embolus of the cell with an inert gas. It was then transferred from the syringe pump to
142 the experimental setup in several steps. This method allowed us to accumulate enough
143 fluid mass to reach pressures as high as 195.0 MPa using the manual pump in the
144 installation. The mixture was homogenized by stirring inside the variable-volume cell,
145 the syringe pump and the manual pump; it was homogenized using a recirculation
146 pump inside the setup.

147 The masses of the different components were determined by successive weighing in a
148 mass comparator from Sartorius, model CCE 2004, with a repeatability better than

149 0.0002 g. The mole fraction of the component that was first introduced, x_1, was
150 determined by the relation

151 $$x_1 = \left[\frac{(m_2 - m_1)}{M_1}\right] / \left[\frac{(m_3 - m_2)}{M_2} + \frac{(m_2 - m_1)}{M_1}\right] \quad (1)$$

152 where m_1 is the empty cell mass, m_2 and m_3 are the masses after the first and second
153 components were added, respectively, and M_1 and M_2 are the molar masses of the
154 first and second components, respectively. The standard uncertainty in the mole
155 fraction was calculated to be $u(x) = 2 \times 10^{-6}$ using the following:

156 $$u^2(x) = [(\partial x/\partial m_1)u(m)]^2 + [(\partial x/\partial m_2)u(m)]^2 + [(\partial x/\partial m_3)u(m)]^2 \quad (2)$$

157 where $u(m) = 2 \times 10^{-4}$ g is the uncertainty of the balance.

158 2.3. Volumetric data acquisition: Experimental setup and procedure.

159 The apparatus and the experimental procedure used to measure densities were
160 previously described [8]. In this setup, T ranges from 263 K to 473 K $\pm$ 0.006 K and p
161 ranges between atmospheric pressure and 70 MPa with 0.025% FS precision. The main
162 component is an Anton Paar DMA HPM vibrating-tube densimeter connected to an
163 MPDS V3 evaluation unit.

164 **3. Calculation method of thermodynamic properties up to high pressures**

165 Various methods have been proposed in the literature to obtain other thermodynamic
166 properties from the speed of sound [51], thus exploiting the high precision of its
167 experimental determination. These methods use experimental data of c obtained at
168 high pressures and several temperatures and ρ and c_p both at a reference pressure $p^{\neq}$
169 and as a function of temperature. From these data, calculated values of ρ, the isobaric

thermal expansivity, α_p, the isothermal compressibility, κ_T, and c_p are obtained as functions of pressure and temperature. In liquid systems $p^{\neq}$ is equal to atmospheric pressure [7, 41, 42, 43, 44, 45, 52, 53]. The method we used is based on these studies, except that $p^{\neq}$ must be above atmospheric pressure to ensure that the fluid is in a dense phase along all working pressure and temperature ranges; thus, $p^{\neq}$ depends on the studied system. Moreover, at the chosen $p^{\neq}$ value, the experimental density $\rho^{\neq}$ obtained at $p^{\neq}$must correlate well with *T*. In this method, the input thermodynamic properties are correlated using the following equations:

$$(p - p^{\neq})/MPa = \sum_{i=1}^{3} \sum_{j=0}^{2} a_{ij} \{(c - c^{\neq})/(m \cdot s^{-1})\}^i (T/K)^{-j} \quad (3)$$

$$c^{\neq}/(m \cdot s^{-1}) = \sum_{j=0}^{2} b_j (T/K)^j \quad (4)$$

$$c_p^{\neq}(J \cdot kg^{-1} \cdot K^{-1}) = \sum_{j=0}^{3} c_j (T/K)^j \quad (5)$$

$$\rho^{\neq}(kg \cdot m^{-3}) = \sum_{j=0}^{3} d_j (T)/K^j. \quad (6)$$

The calculated thermodynamic properties of the system are obtained for a given composition up to high pressures by numerical integration of the following system of partial differential equations:

$$\left.\begin{aligned} c^{-2} &= (\partial\rho/\partial p)_T - \left(T/\rho^2 c_p\right)(\partial\rho/\partial T)_p^2 \\ \left(\partial c_p/\partial p\right)_T &= -(T/\rho^3)\left[2(\partial\rho/\partial T)_p^2 - \rho(\partial^2\rho/\partial T^2)_p\right] \quad . \end{aligned}\right\} \quad (7)$$

The solution to the system (7) is obtained using the initial conditions $\rho^{\neq}(T)$ and ${c_p}^{\neq}(T)$ and a simple predictor-corrector algorithm [43] with step lengths Δp =0.1 MPa and ΔT =5 K. The values of $\rho^{\neq}(T)$ were determined experimentally, whereas ${c_p}^{\neq}(T)$ values were calculated with the GERG EoS [48, 49] using REFPROP 9 [54]. The values of

δ_V [55, 56, 57] and μ_{JT} were calculated up to high pressures using the preceding and the following equations:

$$\delta_V^2 = \left(\frac{\partial U}{\partial V}\right)_T = T\left(\frac{\partial p}{\partial T}\right)_V - p = T\frac{\alpha_p}{\kappa_T} - p \tag{8}$$

$$\mu_{JT} = \left(\frac{\partial T}{\partial p}\right)_H = -\frac{1}{c_p}\left[T\frac{(\partial p/\partial T)_V}{(\partial p/\partial V)_T} + V\right] = \frac{(T\alpha_p - 1)}{\rho c_p} \quad . \tag{9}$$

4. Equations of state

In this work, we compared both our experimental data (c, ρ, ~~p_b, ρ_L~~), and the calculated data previously explained ($\rho, c_p, \delta_V, \mu_{JT}$) with data obtained from the PC-SAFT and the GERG EoS using VLXE [58] and REFPROP 9 [54] software, respectively.

4.1. PC-SAFT EoS

The PC-SAFT EoS [46, 47] describes the Helmholtz adimensional energy, $\tilde{a}$, as the sum of several contributions: ideal gas (id), hard chain (hc), dispersive attraction (dis), association ($assoc$) and multipolar interactions (QQ: quadrupole − quadrupole, DD: dipole − dipole, QD: quadrupole−dipole).

$$\tilde{a} = \tilde{a}^{id} + \tilde{a}^{hc} + \tilde{a}^{dis} + \tilde{a}^{assoc} + (\tilde{a}^{QQ} + \tilde{a}^{DD} + \tilde{a}^{QD}) \, . \tag{10}$$

In this model, three geometrical parameters are needed to describe the non-associated and non-polar pure components: the segment number, m; the segment diameter, σ; and the segment energy parameter, ε. Generally, these parameters are calculated from VLE and density data; however, in such cases the critical region is not correctly represented. An alternative is to recalculate the parameters from the pure compounds' critical temperatures and pressures [17].

The mixing parameters σ_{ij} and ε_{ij} are obtained from the Berthelot-Lorentz rules, which include an adjustable binary interaction parameter, k_{ij}:

$$\sigma_{ij} = \frac{1}{2}\left(\sigma_i + \sigma_j\right) \tag{11}$$

$$\varepsilon_{ij} = \sqrt{\varepsilon_i \varepsilon_j}\left(1 - k_{ij}\right) \tag{12}$$

where the subscripts i and j refer to each of the compounds present in the mixture.

When pure compounds exhibit association, two additional parameters are required: the association volume, $\kappa^{A_iB_i}$, and the association energy, $\varepsilon^{A_iB_i}$. These parameters can be obtained from experimental hydrogen-bonding enthalpies and entropies of the pure compounds or from molecular simulations. Moreover, an association scheme must be defined.

For mixtures of such compounds, the cross-association parameters, $\kappa^{A_iB_j}$ and $\varepsilon^{A_iB_j}$, can be calculated using the following combination rules:

$$\kappa^{A_iB_j} = \sqrt{\kappa^{A_iB_i}.\kappa^{A_jB_j}} \tag{13}$$

$$\varepsilon^{A_iB_j} = \frac{1}{2}\left(\varepsilon^{A_iB_i} + \varepsilon^{A_jB_j}\right). \tag{14}$$

The interactions present in the mixtures between a self-associated compound and another non-self-associated compound, which has either proton donor sites or proton acceptor sites (e.g., CO_2), were named *induced association* by Kleiner and Sadowski [59]. In this case, they suggested a simple approach: the association energy parameter, $\varepsilon^{A_iB_i}$, of the non-self-associating compound is zero, and the association volume

parameter, $\kappa^{A_iB_i}$, of this component is assumed to be equal to the value of the associating component in the mixture:

$$\kappa^{A_iB_j} = \kappa^{assoc.comp}; \qquad \varepsilon^{A_iB_j} = \frac{\varepsilon^{assoc.comp}}{2} \tag{15}$$

A detailed explanation of this model applied to the $CO_2 + CH_3OH$ system is given in a previous work [17], where we studied the VLE and the critical region of this system. For this study, the geometrical parameters of the pure compounds were recalculated from their critical points, and a temperature-dependent binary interaction parameter, $k_{ij}(T)$, was introduced. For methanol, we used a 2B association scheme (i.e., two association sites: a one-electron donor and a one-electron acceptor). Because of the presence of specific interactions between the carbon atom of CO_2 and the oxygen atom of alcohol and CO_2–alcohol hydrogen bonding, we treated this system as *induced association*. We then used $\varepsilon^{A_iB_i} = 0$ and $\kappa^{A_iB_i} = \kappa^{methanol}$ and a 2C association scheme (i.e., two negative sites that are active only when mixed with a molecule with at least one positive or neutral site) for CO_2. Multipole interactions were not considered. This procedure is also that used in the present study.

Neither the PC-SAFT EoS nor cubic EoSs adequately predict density at moderate and high pressures. To enhance the precision in the density calculation, some authors have recalculated the geometrical parameters by introducing the density in the objective function and even varying it with pressure [60, 61]. Similar to our earlier work [8], we chose to add the volume translation, Δv_c, for each pure component. We used a constant Δv_c value for all T to avoid unphysical results [62]. Because Δv_c depends on the value of the molar volume of the component, v, we here used a Δv_c value for CO_2

that differs from that used in previous works [8] because we extended the pressure range to 195.0 MPa.

In summary, in applying the PC-SAFT EoS to the $CO_2 + CH_3OH$ system, we used the same procedure as in our previous work [17] except that we added Δv_c to accurately predict the density. Thus, we used a minimum number of parameters (Table S1) to model the investigated thermodynamic properties (vapor−liquid equilibrium, critical locus, speed of sound and density).

4.2. The GERG EoS

The GERG EoS [48, 49] is based on a multifluid approximation where the adimensional Helmholtz energy, $\tilde{a}$, is expressed as the sum of two contributions: an ideal-gas mixture (id) and a residual component (res):

$$\tilde{a} = \tilde{a}^{id} + \tilde{a}^{res} = \sum_{i=1}^{N} x_i\left[\tilde{a}_i^{id} + lnx_i\right] + \sum_{i=1}^{N} x_i\tilde{a}_i^{res} + \Delta\tilde{a}^{res} \quad (16)$$

where the subscript i indicates the pure compound and $\Delta\tilde{a}^{res}$ is the departure function. Initially, this EoS was developed as a reference EoS for natural gas mixtures, and it generally provides better results than other EoSs for systems whose components are implemented in the equation.

Although methanol is not one of the 21 compounds included in the Kunz and Wagner article [49], it has been implemented in the REFPROP 9 software; thus, we were able to use the equation to calculate the thermodynamic properties of the system under investigation in the present work. The calculations are based in the reference EoS for CO_2 [63] and methanol [64] together with the GERG EoS mixture model. The predicted

values are slightly more accurate than those from GERG EoS as published because the pure-component EoSs are more elaborate.

5. Results

5.1. Experimental results obtained using the newly implemented apparatus to measure the speed of sound in mixtures

The system $CO_2 + CH_3OH$ was studied to develop the experimental procedure for mixtures containing sufficiently dense compressed gases and to determine the uncertainty of the speed of sound measurements in those gases. The chosen compositions were $x_{CO_2} =$ (0.7534, 0.8502, 0.9250 and 0.9803) at nominal temperatures of 263.15 K, 298.15 K and 323.15 K and pressures from 6.00 MPa to 190.04 MPa. The $p - c - T$ values used in this section are listed in Table S2.

The overall standard uncertainty of the experimental c measurements, $u(c)$, was calculated from the following equation [65]:

$$u^2(c) = \left[(\partial c/\partial T)_{p,x} u(T)\right]^2 + \left[(\partial c/\partial p)_{T,x} u(p)\right]^2 + \left[(\partial c/\partial x)_{T,p} u(x)\right]^2 + (u^*(c))^2 \qquad (17)$$

where $u(T)$, $u(p)$, and $u(x)$ are given in section 2.2, and $(\partial c/\partial T)_{p,x}$ and $(\partial c/\partial p)_{T,x}$ were obtained from equations (3) and (4). Correlated $c - x$ data for the four mixtures allowed us to evaluate $(\partial c/\partial x)_{T,p}$.

To determine the standard repeatability uncertainty, $u^*(c)$, two mixtures with $x_{CO_2} =$ 0.9250 were prepared. For each one, two isotherms were determined at each of the three temperatures (Table S2). The deviations between the c values of each isotherm for both mixtures are represented in Figure 1. The value determined for $u^*(c)$ was

293 $5.3 \times 10^{-4} \cdot c$, and the overall standard uncertainty of c was $u(c) = 5.9 \times 10^{-4} \cdot c$.
294 The last value lies within the range of standard uncertainties ($3 \times 10^{-4} \cdot c$ to $10 \times$
295 $10^{-4} \cdot c$) obtained by other authors using similar apparatus for liquid mixtures and
296 binary mixtures of compressed gases [43, 65, 66].

297 5.2. Experimental results for the mixture $CO_2 + CH_3OH$ ($x_{CO_2} = 0.9700$)

298 *Speed of sound.* Experimental values $p - c - T$ were measured along six isotherms at
299 nominal temperatures= (263.15, 273.15, 283.15, 293.15, 304.21 and 313.15) K and at
300 pressures from 3.28 MPa to 194.49 MPa (Figure 2, Table S3). The standard uncertainty
301 was $u(c) = 5.9 \times 10^{-4} \cdot c$, as previously indicated. The speed of sound increases as
302 pressure increases and as temperature decreases. No values were found in the
303 literature for this system.

304 *Density.* The density was measured at the same nominal temperatures as the speed of
305 sound and the pressure ranged from 4.00 to 20.00 MPa. The experimentally
306 determined density values of the six isotherms correspond to dense phase of the
307 mixture. The isotherms at temperatures from 263.15 K to 304.21 K are subcritical and
308 that at 313.15 K is supercritical. The standard uncertainty in the experimental
309 determination of the density was $u(\rho)$= 0.4 $\mathrm{kg \cdot m^{-3}}$, which was obtained following
310 the procedure described in the Supplementary material (S.M.) (pp S11). Similar to the
311 speed of sound, values of ρ in the liquid phase of this mixture also increase with
312 increasing pressure and with decreasing temperature (Figure 3, Table S4).

313 Despite the abundance of density data in the literature, we could quantitatively
314 compare our values only with those of Berger and Deye ($x_{CO_2} = 0.9777$ at 313.15 K)

315 [20] and Cao et al. ($x_{CO_2} = 0.9657$-0.9760 at 313.15 K) [32], where the deviations
316 $MRD_\rho = 1.30\%$ and 5.52%, respectively. Our results are consistent with the remainder
317 of the literature data at $T \leq 313$ K and at $x_{CO_2} > 0.75$ [19, 20, 21, 32, 34].

318 5.3. Results from the thermodynamic property calculation method for the mixture
319 $CO_2 + CH_3OH$ (x_{CO_2}= 0.9700) at high pressures

320 From our experimental $p - c - T$ and $\rho^{\neq} - T$ data and from our calculated $c_p^{\neq} - T$
321 values (GERG EoS), we obtained ρ, c_p, δ_V and μ_{JT} for temperatures from 263.15 K to
322 313.15 K and for pressures up to 195.0 MPa using the aforementioned calculation
323 method (Table S5 and Figure 4 a-d). Equations (3) to (6) of this method were applied
324 with $p^{\neq}$= 14.0 MPa and with the values of the parameters a_{ij}, b_j, c_j and d_j given in
325 Table ~~1~~2.

326 *Density.* Because we have experimental values for ρ for pressures up to 20.00 MPa and
327 calculated values starting from 14.0 MPa, we compared the values in the overlapping
328 range from 14.0 MPa to 20.0 MPa. The experimental and calculated values agreed
329 well, with an $MRD_\rho = 0.075\%$. We compared our calculated density values with the
330 experimental data of Berger and Deye [20]; the deviation is MRD_ρ= 0.35%. Our results
331 are consistent with the experimental data of Maiwald et al. [34].

332 *Isobaric specific heat capacity.* The calculated values of this property vary between
333 2734.6 J·kg^{-1}·K^{-1} (14.0 MPa, 313.15 K) and 1551.6 J·kg^{-1}·K^{-1} (195.0 MPa, 313.15 K). The
334 variation of c_p with pressure diminishes gradually as temperature decreases, showing
335 a crossing region at approximately 1865 J·kg^{-1}·K^{-1} and 35 MPa. No c_p data for the
336 studied mixture were found in the literature.

337 *Volume-dependent solubility parameter.* The calculated values for δ_V increase as
338 pressure increases and temperature decreases. We found solubility parameter, δ, data
339 in the literature for $T \geq 313.15$ K [14, 38, 39, 40], which cannot be compared with our
340 δ_V values because of the different included effects and the temperature or
341 composition.

342 *Joule-Thomson coefficient.* The evolution of μ_{JT} values with pressure and temperature
343 is similar to that of c_p. The greatest variation with pressure is shown for the
344 supercritical isotherm (0.82597 K·MPa^{-1} at 14.0 MPa and -0.33179 K·MPa^{-1} at 195.0
345 MPa) and the lowest variation corresponds to 263.15 K, which causes a crossing of all
346 isotherms in the vicinity of -0.25 K·MPa^{-1} and 100 MPa. The Joule-Thomson coefficient
347 changes its sign for the five upper isotherms in the pressure range studied. No μ_{JT}
348 values were found in the literature.

349 **6. Discussion**

350 The repeatability and overall standard uncertainty results obtained in this work,
351 together with the agreement with the data from the literature, allow us to use our
352 experimental c and ρ data to evaluate whether the PC-SAFT and GERG EoSs properly
353 predict the studied thermodynamic behavior for $\mathrm{CO_2} + \mathrm{CH_3OH}$. If the two EoSs are
354 successful, we will use both to validate the method for calculating ρ, δ_v, c_P and μ_{JT} up
355 to 195.0 MPa.

356 6.1. Experimental results for $\mathrm{CO_2} + \mathrm{CH_3OH}$ ($x_{\mathrm{CO_2}} = 0.9700$)

357 *Speed of sound* ($p \leq 194.49$ MPa; $263.16 \leq T \leq 313.15$ K). We observed that the PC-
358 SAFT EoS tends to underestimate the speed of sound when we compared the

359 experimental and EoS results (Figure S1); we also observed that the divergence
360 increases with decreasing temperature. The calculated value of the average PC-SAFT
361 EoS deviation for all isotherms is $\overline{MRD_c} = 2.77\%$ (Table S6). The GERG EoS values of c
362 are always greater than the experimental values, with the largest deviations at low
363 pressures (Figure S1). The average value of the GERG EoS deviations for all isotherms is
364 slightly lower than that from the PC-SAFT EoS, $\overline{MRD_c} = 2.65\%$ (Table S6).

365 To calculate the overall standard uncertainty in the speed of sound, u_c, experimental
366 values of c for four mixtures of $\mathrm{CO_2} + \mathrm{CH_3OH}$ ($0.7534 \leq x_{CO_2} \leq 0.9803$) were
367 determined. All of them were modeled to investigate possible trends with respect to
368 composition. The PC-SAFT EoS deviations are similar for all mixtures. However, the
369 GERG EoS provides better results than the PC-SAFT EoS for the two $\mathrm{CO_2}$ −richest
370 mixtures and significantly higher deviations with increasing $x_{\mathrm{CH_3OH}}$. Thus, the GERG
371 EoS $\overline{MRD_c}$ is 2.07% for $x_{\mathrm{CO_2}} = 0.9803$ and 14.1% for $x_{\mathrm{CO_2}} = 0.7534$ (Table S7).

372 *Density* ($p \leq 20.00$ MPa; 263.15K $\leq T \leq$ 313.15 K*).* Deviations in density values
373 increase with increasing temperature and decreasing pressure for both EoSs (Figure
374 S2). The PC-SAFT EoS predicts that the density values will be lower than the
375 experimental values for subcritical isotherms. For this EoS, the largest deviations are
376 observed at T= 313.15 K, near the critical point of the mixture ($T_c \cong 310$ K [17])
377 (Figure S2). The mean value of all PC-SAFT EoS deviations is $\overline{MRD_\rho} = 3.81\%$ (Table S6).
378 The GERG EoS overestimates ρ with a significantly lower $\overline{MRD_\rho} = 0.52\%$, although its
379 deviation is more than double that of the PC-SAFT EoS at the supercritical
380 temperature, $\left(MRD_\rho\right)_{max} = 23\%$. Density data from literature show similar or higher

deviations with PC-SAFT EoS predictions than our experimental data and greater differences with GERG EoSs than our values (Table S8).

On the basis of the deviations between the experimental values and those calculated by each EoS for the four properties, we conclude that both equations are valid to represent the behavior of this system under most of the studied conditions. However, we observed exceptions, such as the evaluation of the density near the critical point of the mixture, where the deviations were significant for both EoSs, and the GERG EoS's prediction for the speed of sound within mixtures with $x_{\mathrm{CO_2}} < 0.97$.

The experimental results are a useful contribution to the body of scientific knowledge because no c data have been reported and because volumetric information at $T \leq 313$ K and $x_{\mathrm{CO_2}} > 0.75$ is scarce. Accurate values for these properties are needed to evaluate several parameters related to transport, injection and storage in CCS technology and also for other applications. In addition, these values will allow the research community to develop and improve EoSs in the future.

6.2. Calculated results for $\mathrm{CO_2} + \mathrm{CH_3OH}$ ($x_{\mathrm{CO_2}} = 0.9700$) up to 195.0 MPa

Given the satisfactory results obtained in the previous section, we will use both EoSs to discuss our results calculated from the experimental data at pressures up to 195.0 MPa. The calculated ρ, c_P, δ_V and μ_{JT} values are compared with those obtained from the PC-SAFT and GERG EoSs (Figures S3-S6) at temperatures from 263.15 K to 313.15 K and at pressures from 14.0 MPa to 195.0 MPa. The deviations thus obtained are expressed as $MRD_x(\%)$ or AAD in Table S89.

Density. Figure S3 shows the deviations between the calculated ρ values and those from both EoSs. Our obtained values are greater than the values obtained using the PC-SAFT EoS at pressures below 40-60 MPa, whereas they are lower at higher pressures; the average deviations obtained for each isotherm are nearly equal, and $\overline{MRD_\rho} = 1.90\%$. In relation to the GERG EoS, we obtain deviations no higher than 1%, with an average value $\overline{MRD_\rho} = 0.46\%$, where our calculated values are usually higher than the predicted values.

Isobaric specific heat capacity. A comparison of the calculated values with those from the two EoSs (Figure S4) shows that calculated values are higher than the values predicted by the PC-SAFT EoS. The deviations are significant and generally increase with increasing pressure, with an average value of $\overline{MRD_{c_p}} = 10.3\%$. Deviations of the values calculated using the GERG EoS are much lower than those calculated using the PC-SAFT EoS, with an average value of $\overline{MRD_{c_p}} = 2.47\%$. The calculated crossing region for this property ($c_p \cong 1865$ J·kg^{-1}·K^{-1} and $p \cong 35$ MPa) agrees better with predictions from the GERG EoS ($c_p \cong 1780$ J·kg^{-1}·K^{-1} and $p \cong 55$ MPa) than with predictions from the PC-SAFT EoS ($c_p \cong 1460$ J·kg^{-1}·K^{-1} and $p \cong 155$ MPa).

Volume-dependent solubility parameter. In Figure 5, δ_V values are represented as a function of ρ for pure $\mathrm{CO_2}$ [50], for the $\mathrm{CO_2} + \mathrm{CH_3OH}$ mixture studied in this work and for six $\mathrm{CO_2} + \mathrm{CO}$, $\mathrm{CO_2} + \mathrm{CH_4}$, $\mathrm{CO_2} + \mathrm{H_2}$ and $\mathrm{CO_2} + \mathrm{CO} + \mathrm{H_2}$ mixtures from the literature [8]. The graph shows a good $\delta_V - \rho$ correlation at densities less than $\cong 1050$ $\mathrm{kg \cdot m^{-3}}$, as shown in a previous study [8]. This result indicates that in this density range, different systems at various T or p conditions, but with the same density, will have the same δ_V. For $\rho > 1050\ \mathrm{kg \cdot m^{-3}}$, deviations between the δ_V values for the

$CO_2 + CH_3OH$ mixture and those for pure CO_2 depend on T; however, these deviations are not greater than those observed for other systems in other regions of the graph.

Our δ_V data are lower than the values obtained from the PC-SAFT EoS in the full range of pressures, with larger deviations at both higher pressures and higher temperatures, with an $\overline{MRD_{\delta_V}} = 3.28\%$. The GERG deviations are smaller than those obtained from the PC-SAFT EoS, and their average value is $\overline{MRD_{\delta_V}} = 1.60\%$. Comparisons with both EoSs are shown in Figure S5.

Joule-Thomson coefficient. Because the numerical values of this property were so small, deviations were expressed as AADs. The PC-SAFT EoS deviations are much larger than those from the GERG EoS, as shown in Figure S6, which is reflected in the average values of $\overline{AAD_{\mu_{JT}}} = 0.056$ K/MPa from the PC-SAFT EoS and $\overline{AAD_{\mu_{JT}}} = 0.013$ K/MPa from the GERG EoS. The crossing region obtained from the calculation method ($\mu_{JT} \cong$ -0.25 K/MPa and $p \cong$100 MPa) differs more from that predicted by the PC-SAFT EoS ($\mu_{JT} \cong$ -0.43 K/MPa and $p \cong$220 MPa) than that from the GERG EoS ($\mu_{JT} \cong$ -0.32 K/MPa and $p \cong$180 MPa).

We consider the obtained results adequate in the comparison between the calculated values of the four properties ρ, c_P, δ_V and μ_{JT} and the data provided by both EoSs, except for c_P and μ_{JT} in relation to the PC-SAFT EoS.

7. Conclusions

An ultrasonic pulse apparatus and the experimental procedure were adapted to measure the speed of sound in mixtures containing compressed gases, and c was

447 measured for four $CO_2 + CH_3OH$ mixtures (x_{CO_2} = 0.7534, 0.8502, 0.9250 and 0.9803)
448 at nominal temperatures T = (263.15, 298.15, and 323.15) K and at pressures up to
449 190.04 MPa. The overall standard uncertainty of the experimental speed of sound was
450 evaluated for the $CO_2 + CH_3OH$ system, where the contributions of temperature,
451 pressure, composition and repeatability were taken into account. The obtained value,
452 $u_c = 5.9 \times 10^{-4} \cdot c$, is within values reported in the literature.

453 The speed of sound was experimentally determined for the $CO_2 + CH_3OH$ mixture
454 with x_{CO_2} = 0.9700 at nominal T = (263.15, 273.15, 283.15, 293.15, 304.21 and
455 313.15) K and at pressures from 3.28 MPa to 194.49 MPa. The density of the mixture in
456 dense phase was measured at the same nominal temperatures, including five
457 subcritical and one supercritical, and at pressures up to 20.00 MPa.

458 This system was modeled with two different formulation EoSs: PC-SAFT and GERG.
459 From the obtained deviations, we conclude that both equations are valid to represent
460 the studied experimental thermodynamic properties of the system except for in the
461 critical region and, in the case of the GERG EoS, the speed of sound in the mixtures
462 poorest in CO_2.

463 Values of , c_p, δ_V and μ_{JT} were calculated in the *T* range from 263.15 K to 313.15 K and
464 from 14.0 MPa to 195.0 MPa for the $CO_2 + CH_3OH$ mixture with x_{CO_2} = 0.9700. For
465 this calculation, we used a method based on numerical integration and previously used
466 for liquid systems by adapting it for compressed gases. The values thus obtained were
467 compared with those obtained from the PC-SAFT and GERG EoSs. The results of this
468 comparison, together with the agreement between our experimental and calculated
469 densities in the overlapping pressure range, validate the calculation method.

Therefore, we have achieved the aim of this work, which was to comprehensively study the thermodynamics of a CO_2 − rich mixture of $CO_2 + CH_3OH$ at T and p conditions of interest for CCS technology and other applications. The results reported in this paper are a useful contribution to mitigate the lack of information in the literature on the thermodynamic behavior of such mixtures. Acoustic, volumetric, c_p and μ_{JT} data are important for the calculation of several parameters related to transport, injection and storage in CCS and for supercritical processes. In addition, these data will allow the future improvement, development and validation of new theoretical models for this technology. Neither of the two studied EoSs satisfactorily represents all the properties studied in this work, although the GERG EoS correctly predicts the system behavior at high pressures.

Acknowledgements

This research received funding from the Ministry of Economy and Competitiveness of Spain ENE2013-44336-R and from the Government of Aragon and the European Social Fund.

Appendix A. Supplementary material

Supplementary material for this article can be found in the online version.

488

References

[1] IEA, Energy Technology Perspectives, 2012. Pathways to a clean energy system.

[2] US DOE, 2010. Interagency Task Force on Carbon Capture and Storage. Washington, DC, USA.

[3] Aursand, P., Hammer, M., Munkejord, S.T., Wilhelmsen, Ø., 2013. Pipeline transport of CO_2 mixtures: Models for transient simulation. International Journal of Greenhouse Gas Control, 15, 174-185. doi: 10.1016/j.ijggc.2013.02.012

[4] Løvseth, S.W., Skaugen, G., Jacob Stang, H.G., Jakobsen, J.P., Wilhelmsen, Ø., Span, R., Wegge, R., 2013. CO_2Mix Project: Experimental determination of thermo physical properties of CO_2 −rich mixtures. Energy Procedia, 37, 2888–2896. doi: 10.1016/j.egypro.2013.06.174.

[5] Li, H., Jakobsen, J. P., Wilhelmsen, O., Yan, J., 2011. PVTxy properties of CO_2 mixtures relevant for CO_2 capture, transport and storage: Review of available experimental data and theoretical models. Applied Energy, 88, 3567-3579. doi: 10.1016/j.apenergy.2011.03.052

[6] Estrada-Alexanders, A.F., Trusler, J.P.M., Zarari, M.P., 1995. Determination of thermodynamic properties from the speed of sound. International Journal of Thermophysics, 16, 663-673. Doi: 10.1007/BF01438851.

[7] Chorazewski, M., Postnikov, E.B., 2015. Thermal properties of compressed liquids: Experimental determination via an indirect acoustic technique and modeling using the volume fluctuations approach. International Journal of Thermal Sciences, 90, 62-69. doi: 10.1016/j.ijthermalsci.2014.11.028.

[8] Blanco, S.T., Rivas, C., Bravo, R., Fernández, J., Artal, M., Velasco, I., 2014. Discussion of the influence of CO and CH_4 in CO_2 transport, injection, and storage for CCS technology. Environmental Science & Technology, 48, 10984-10992. doi: /10.1021/es502306k.

[9] Lund, H., Flåtten, T., Munkejord, S.T., 2011. Depressurization of carbon dioxide in pipelines – models and methods. Energy Procedia, 4, 2984-2991. doi: 10.1016/j.egypro.2011.02.208.

[10] Diamantonis, N.I., Boulougouris, G.C., Tsangaris, D.M., El Kadi, M.J., Saadawi, H., Negahban, S., Economou, I.G., 2013. Thermodynamic and transport property models for carbon capture and sequestration (CCS) processes with emphasis on CO_2transport. Chemical Engineering Research and Design, 91, 1793-1806. doi: 10.1016/j.cherd.2013.06.017.

[11] Woolley, R.M., Fairweather, M., Wareing, C.J., Proust, C., Hebrard, J., Jamois, D., Narasimhamurthy, V.D., Storvik, I.E., Skjold, T., Falle, S.A.E.G., Brown, S., Mahgerefteh, H., Martynov, S., Gant, S.E., Tsangaris, D.M., Economou, I.G., Boulougouris, G.C., Diamantonis, N.I., 2014. An integrated, multi-scale modelling approach for the simulation ofmultiphase dispersion from accidental CO_2 pipeline releases inrealistic terrain. International Journal of Greenhouse Gas Control, 27, 221-238. doi: 10.1016/j.ijggc.2014.06.001.

[12] Ziabakhsh-Ganji, Z., Kooi, H., 2014. Sensitivity of Joule–Thomson cooling to impure CO_2 injection in depleted gas reservoirs. Applied Energy 113, 434-451. doi: 10.1016/j.apenergy.2013.07.059.

[13] Porter, R. T. J., Fairweather, M., Pourkashanian, M., Woolley, R. M., 2015. The range and level of impurities in CO_2 streams from different carbon capture sources International Journal of Greenhouse Gas Control, 36, 161–174. doi:10.1016/j.ijggc.2015.02.016.

[14] Huang, Z., Li, J.H., Li, H.S., Teng, L.J., Kawi, S., Lai, M.W., 2013a. Effects of polar modifiers on supercritical extraction efficiency fororganic template removal from mesoporous MCM-41 materials. The Journal of Supercritical Fluids, 82 , 96-105. doi: 10.1016/j.supflu.2013.06.012.

[15] Huang, Z., Li, J-H., Li, H-S., Miao, H., Kawi, S., Goh, A. H., 2013. Separation and Purification Technology, 118, 120-126. doi: 10.1016/j.seppur.2013.06.047.

[16] Gritti, F., Guiochon, G., 2013. Effect of methanol concentration on the speed-resolution properties in adiabatic supercritical fluid chromatography. Journal of Chromatography A, 1314 , 255-265. doi: 10.1016/j.chroma.2013.07.082

[17] Gil, L., Blanco, S.T., Rivas, C., Laga, E., Fernández, J., Artal, M., Velasco, I., 2012. Experimental determination of the critical loci for {n-C_6H_{14} or CO_2+alkan-1-ol} mixtures. Evaluation of their critical and subcritical behavior using PC-SAFT EoS. The Journal of Supercritical Fluids, 71, 26-44. doi: 10.1016/j.supflu.2012.07.008.

[18] Francis, A.W., 1954. Ternary Systems of Liquid Carbon Dioxide. Chemische Berichte, 87, 1099-1114.

[19] Brunner, E., Hültenschmidt, W., Schlichthärle, G., 1987. Fluid mixtures at high pressures IV. Isothermal phase equilibria in binary mixtures consisting of (methanol + hydrogen or nitrogen or methane or carbon monoxide or carbon dioxide). The Journal of Chemical Thermodynamics, 19, 273-291. doi:10.1016/0021-9614(87)90135-2.

[20] Berger, T.A., Deye, J.F., 1990. Composition and density effects using methanol/carbon dioxide in packed column supercritical fluid chromatography. Analytical Chemistry, 62, 1181-1185. doi: 10.1021/ac00210a017

[21] Yong, Y., Zhangli, J., Kunyuan, L., Huanzhang, L., 1992. Determination and correlation of saturated liquid density for binary systems of carbon dioxide with acetone, ethyl ether and methanol. Journal of Chemical Engineering of Chinese Universities, 1.

[22] Langenfeld, J. J., Hawthorne, S. B., Miller, D. J., Tehrani, J., 1992. Method for determining the density of pure and modified supercritical fluids. Analytical Chemistry, 64, 2263-2266 .

[23] Galicia-Luna, L. A., Richon, D., Renon, H., 1994. New Loading Technique for a Vibrating Tube Densimeter and Measdurements of Liquid Densities up to 39.5 MPa for Binary and Ternary Mixtures of the Carbon Dioxide-Methanol-Propane System. Journal of Chemical Engineering Data, 39, 424-31

[24] Kodama, D., Kubota, N., Yamaki, Y., Tanaka, H., Kato, M., 1996. High Pressure Vapor-Liquid Equilibria and Density Behaviors for Carbon Dioxide+ Methanol System at 313.15 K. Netsu Bussei, 10, 16-20.

[25] Chang, C.J., Day, C-Y., Ko, C-M., Chiu, K-L., 1997. Densities and P-x-y diagrams for carbon dioxide dissolution in methanol, ethanol, and acetone mixtures. Fluid Phase Equilibria, 131, 243-258.

[26] Chang, C.J., Chiu, K.-L., Day, C.-Y., 1998. A new apparatus for the determination of P-x-y diagrams and Henry's constants in high pressure alcohols with critical carbon dioxide. Journal of Supercritical Fluids, 12, 223-237

[27] Kodama, D., Kubota, N., Yamaki, Y., Tanaka, H., Kato, M., 1998. Partial Molar Volumes of Methanol and Ethanol at Infinite Dilution in Supercritical Carbon Dioxide. Netsu Bussei, 12, 186-190.

[28] Goldfarb, D.L., Fernández, D.P, Corti, H., 1999. Dielectric and volumetric properties of supercritical carbon dioxide (1) + methanol (2) mixtures at 323.15 K. Fluid Phase Equilibria, 158, 1011-1019.

[29] Smith, R.L., Sung, B. L., Suzuki, S., Saito, C., Inomata, H, Arai, K., 2002. Densities of Carbon Dioxide + Methanol Mixtures at Temperatures from 313.2 to 323.2 K and at pressures from 10 to 20 MPa. Journal of Chemical Engineering, 47, 608-612.

[30] Bezanehtak, K., Combes, G. B., Dehghani, F., Foster, N. R., Tomasko, D. L., 2002. Vapor-Liquid Equilibrium for Binary Systems of Carbon Dioxide + Methanol, Hydrogen + Methanol, and Hydrogen + Carbon Dioxide at High Pressures. Journal of Chemical Engineering Data, 47, 161-168

[31] Zhang, J.C., Wu, X.Y., Cao, W.L., 2002. Phase equilibrium properties of supercritical carbon dioxide in binary system. Chemical Journal of Chinese Universities, 23, 10-13.

[32] Cao, W., Li, X., Zhang, J., 2004. Partial molar volumes of solutes and molecular interaction in binary mixed CO2-cosolvent supercritical fluids. Huagong Xuebao, 55 (7), 1614-1620.

[33] Sih, R., Dehghani, F., Foster, N.R., 2007. Viscosity measurements on gas expanded liquid systems-Methanol and carbon dioxide. Journal of Supercritical Fluids, 41, 148-157.

[34] Maiwald, M., Li, H., Schnabel, T., Braun, K., Hasse, H., 2007. On-line ^{1}H NMR spectroscopic investigation of hydrogen bonding in supercritical and near critical CO_2–methanol up to 35 and 403 K. The Journal of Supercritical Fluids*, 43,* 267-275. doi: 10.1016/j.supflu.2007.05.009.

[35] Aida, T., Aizawa, T., Kanakubo, M., Nanjo, H., 2010. Relation between Volume Expansion and Hydrogen Bond Networks for CO2-Alcohol Mixtures at 40 ºC. Journal of Physical Chemistry, B., 114, 13628-13636.

[36] Kariznovi, M., Nourozieh, H., Abedi, J., 2013. Experimental measurements and predictions of density, viscosity, and carbon dioxide solubility in methanol, ethanol, and 1-propanol. Journal of Chemical Thermodynamics, 57, 408-415.

[37] Jalili, A.H., Shokouhi, M., Samani, F., Hosseini-Jenab, M., 2015. Measuring the solubility of CO2 and H2S in sulfolane and the density and viscosity of saturated liquid binary mixtures of (sulfolane + CO2) and (sulfolane + H2S) Journal of Chemical Thermodynamics, 85, 13-25.

[38] Sajilata, M.G., Bule, M.V., Chavan, P., Singhal, R.S., Kamat, M.Y., 2010. Development of efficient supercritical carbon dioxide extraction methodology for zeaxanthin from dried biomass of *Paracoccus zeaxanthinifaciens.* Separation and Purification Technology, 71, 173-177. doi: 10.1016/j.seppur.2009.11.017.

[39] Bule, M.V., Singhal, R.S., 2012. Development of a protocol for supercritical carbon dioxide extraction of ubiquinone-10 from dried biomass of *Pseudomonas diminuta.* Bioprocess and Biosystems Engineering, 35, 809-816. doi: 10.1007/ s00449-011-0661-5.

[40] Huang, Z., Li, J.H., Li, H.S., Miao, H., Kawi, S., Goh, A.H., 2013b. Effect of the polar modifiers on supercritical extraction efficiency for template removal from hexagonal mesoporous silica materials: Solubility parameter and polarity

considerations. Separation and Purification Technology, 118, 120-126. doi: 10.1016/j.seppur.2013.06.047.

[41] Piñeiro, M.M., Plantier, F., Bessières, D., Legido, J.L., Daridon, J.L., 2004. High-pressure speed of sound measurements in methyl nonafluorobutyl ether and ethyl nonafluorobutyl ether. Fluid Phase Equilibria, 222–223, 297-302. doi:10.1016/j.fluid.2004.06.013.

[42] González-Salgado, D., Troncoso, J., Plantier, F., Daridon, J.L., Bessières, D., 2006. Study of the volumetric properties of weakly associated alcohols by means of high-pressure speed of sound measurements. The Journal of Chemical Thermodynamics, 38, 893-899. doi:10.1016/j.jct.2005.10.002.

[43] Dávila, M.J., Trusler, J.P.M., 2009. Thermodynamic properties of mixtures of *N*-methyl-2-pyrrolidinone and methanol at temperatures between 298.15 K and 343.15 K and pressures up to 60 MPa. The Journal of Chemical Themodynamics, 41, 35-45. doi:10.1016/j.jct.2008.08.003.

[44] Dzida, M., Waleczek, L., 2010. Speed of sound, density, and heat capacity for (2-methyl-2-butanol + heptane) at pressures up to 100 MPa and temperatures from (293 to 318) K. Experimental results and theoretical investigations. The Journal of Chemical Thermodynamics, 42, 312–322. doi:10.1016/j.jct.2009.09.001.

[45] Peleties, F., Segovia, J.J., Trusler, J.P.M., Vega-Maza, D., 2010. Thermodynamic properties and equation of state of liquid di-isodecyl phthalate at temperature between (273 and 423) K and at pressures up to 140 The Journal of Chemical Themodynamics,42, 631-639. doi:10.1016/j.jct.2009.12.002.

[46] Gross, J., Sadowski, G., 2001. Perturbed-Chain SAFT: An equation of state based on a perturbation theory for chain molecules. Industrial & Engineering Chemical Research, 40, 1244-1260. doi: 10.1021/ie0003887.

[47] Gross, J., Sadowski, G., 2002. Application of the Perturbed-Chain SAFT equation of state to associating systems. Industrial & Engineering Chemical Research, 41, 5510-5515. doi: 10.1021/ie010954d.

[48] Kunz, O., Klimeck, R., Wagner, W., Jaeschke, M., 2007. The GERG-2004 wide-range equation of state for natural gases and other mixtures; GERG TM15; Fortschr.-Ber. VDI, Reihe 6, Nr. 557, VDI Verlag: Düsseldorf.

[49] Kunz, O., Wagner, W., 2012. The GERG-2008 Wide-Range Equation of state for natural gases and other mixtures: An expansion of GERG-2004. The Journal of Chemical & Engineering Data, 57, 3032-3091. doi: 10.1021/je300655b.

[50] Velasco, I., Rivas, C., Martínez-López, J. F., Blanco, S. T., Otín, S., Artal, M., 2011. Accurate values of some thermodynamic properties for carbon dioxide, ethane, propane, and some binary mixtures. The Journal of Physical Chemistry B, 115, 8216-8230. doi 10.1021/jp202317n.

[51] Estrada-Alexanders, A.F., Justo, D., 1995. New method for deriving accurate thermodynamic properties from speed-of-sound. The Journal of Chemical Thermodynamics, 36, 419-429. doi:10.1016/j.jct.2004.02.002.

[52] Davis, L.A., Gordon, R.B., 1967. Compression of mercury at high pressure. The Journal of Chemical Physics, 46, 2650-2660. doi: 10.1063/1.1841095.

[53] Sun, T.F., Ten Seldam, C.A., Kortbeek, P.J., Trappeniers, N.J., Biswas, S.N., 1988. Acoustic and Thermodynamic Properties of Ethanol from 273.15 to 333.1 5 K and up to 280 MPa. Physics and Chemistry of Liquids, 18, 107-116. doi: 10.1080/00319108808078584.

[54] Lemmon, E. W.; Huber, M. L.; McLinden, M. O., 2010. NIST Standard Reference Database 23: Reference Fluid Thermodynamic and Transport Properties-REFPROP, Version 9.0, National Institute of Standards and Technology, Standard Reference Data Program, Gaithersburg.

[55] Hildebrand, J. H., Scott, R. L., 1950. The Solubility of Nonelectrolytes; Reinhold: New York.

[56] Hansen, C. M., 1969. The universality of the solubility parameter. Industrial & Engineering Chemistry Product Research and Development, 8 (1), 2−11. doi: 10.1021/i360029a002.

[57] Bagley, E. B., Nelson, T. P., Scigliano, J. M., 1971. Three-dimensional solubility parameters and their relationship to internal pressure measurements in polar and hydrogen bonding solvents. Journal of Paint Technology, 43 (555), 35−42.

[58] Laursen, T. VLXE ApS. Scion-DTU, Diplomvej, Denmark, 2012.

[59] Kleiner, M., Sadowski, G., 2007. Modeling of polar systems using PCP-SAFT: An approach to account for induced-association interactions. The Journal of Physical Chemistry C, 111, 15544-15553. doi: 10.1021/jp072640v.

[60] Diamantonis, N.I., Economou, I.G., 2011. Evaluation of statistical associating fluid theory (SAFT) and perturbed chain-saft equations of state for the calculation of thermodynamic derivative properties of fluids related to carbon capture and sequestration. Energy & Fuels, 25, 3334–3343. doi: 10.1021/ef200387p.

[61] Tapriyal, D., Enick, R., McHugh, M., Gamwo, I. K., Morreale, B., 2012. High temperature, high pressure equation of state density correlations and viscosity correlations; NETL-TRS-1-2012; National Energy Technology Laboratory.

[62] Pfohl, O., 1999. Evaluation of an improved volume translation for the prediction of hydrocarbon volumetric properties. Fluid Phase Equilibria, 163, 157-159.

[63] Span, R. and Wagner, W., 1996. A New Equation of State for Carbon Dioxide Covering the Fluid Region from the Triple-Point Temperature to 1100 K at Pressures up to 800 MPa. J. Phys. Chem. Ref. Data, 25(6), 1509-1596. doi:10.1063/1.555991.

[64] de Reuck, K.M., Craven, R.J.B., 1993. Methanol, International Thermodynamic Tables of the Fluid State - 12, IUPAC, Blackwell Scientific Publications, London.

[65] Lin, C.W., Trusler, J.P.M., 2014. Speed of sound in (carbon dioxide + propane) and derived sound speed of pure carbon dioxide at temperatures between (248 and 373) K and at pressures up to 200 MPa. The Journal of Chemical & Engineering Data, 59, 4099–4109. doi: 10.1021/je5007407.

[66] Ball, S.J., Trusler, J.P.M., 2001. Speed of sound of n-hexane and n-hexadecane at temperatures between 298 and 373 K and pressures up to 100 MPa.

International Journal of Thermophysics, 22, 427-443. doi: 10.1023/A:1010770730612.

Table 1. The sources and mole fraction purity of the materials used in this paper.

Chemical Name	Source	Mole Fraction Purity	Purification Method
methanol	Sigma Aldrich	0.9993[a]	None
carbon dioxide	Air Liquide	>0.99998[a]	None

[a] The mole fraction was given by the supplier

Table 2. Parameters in equations (3)−(6) for the correlation for the density, isobaric heat capacity, and speed of sound of $CO_2 + CH_3OH$ with $x_{CO_2} = 0.9700$ and MRD (%) values.

Parameters	*Equation (3)*
a_{10}	$1.803588 \cdot 10^{0}$
a_{11}	$-1.057660 \cdot 10^{3}$
a_{12}	$1.613456 \cdot 10^{5}$
a_{20}	$-2.893926 \cdot 10^{-3}$
a_{21}	$1.590804 \cdot 10^{0}$
a_{22}	$-2.057073 \cdot 10^{2}$
a_{30}	$2.153084 \cdot 10^{-6}$
a_{31}	$-1.154812 \cdot 10^{-3}$
a_{32}	$1.601533 \cdot 10^{-1}$
MRD (%):	0.08
Parameters	*Equation (4)*
b_0	$4.551011383 \cdot 10^{3}$
b_1	$-2.1725446 \cdot 10^{1}$
b_2	$2.7618 \cdot 10^{-3}$
MRD (%):	0.27
Parameters	*Equation(5)*
c_0	$-8.2772910000 \cdot 10^{4}$
c_1	$9.35309155 \cdot 10^{2}$
c_2	$-3.460573 \cdot 10^{0}$
c_3	$4.297499 \cdot 10^{-3}$
MRD (%):	0.11
Parameters	*Equation (6)*
d_0	$5.897805216 \cdot 10^{3}$
d_1	$-5.0584614 \cdot 10^{1}$
d_2	$0.188454 \cdot 10^{0}$
d_3	$-2.526272E \cdot 10^{-4}$
MRD (%):	0.02

$$MRD(\%) = \frac{10^2}{N}\sum_{i=1}^{N}\left|\frac{x_i - x_{fit}}{x_i}\right|$$

x_i: experimental datum; x_{fit}: value obtained for that property at the same state point from the corresponding correlating equation; N: number of points.

Figure captions:

Figure 1. Deviations between the *c* values in two mixtures (1, 2) $CO_2 + CH_3OH$ with $x_{CO_2} = 0.9250$, at three temperatures, *T*, and versus pressure, *p*. Each mixture was measured twice at each temperature. ■, *T*=263.15 K; ▲,*T*=298.15 K; and ✸,*T*= 323.15 K.

Figure 2. Experimental speeds of sound, c, versus pressure, p, for $CO_2 + CH_3OH$ with $x_{CO_2} = 0.9700$ at several temperatures: ■, *T*=263.15 K; ●, *T*=273.15 K; ▲, *T*=283.15 K; ▼, *T*=293.15 K; ◆, *T*=304.21 K; ✸, *T*=313.15 K.

Figure 3. Experimental densities, ρ, versus pressure, p, for $CO_2 + CH_3OH$ with $x_{CO_2} = 0.9700$ at several temperatures: ■, *T*=263.15 K; ●, *T*=273.15 K; ▲, *T*=283.15 K; ▼, *T*=293.15 K; ◆, *T*=304.21 K; ✸, *T*=313.15 K.

Figure 4. (a) Calculated densities, ρ; (b) calculated isobaric specific heat capacities, c_p; (c) calculated volume-dependent solubility parameters, δ_V; (d) calculated Joule-Thomson coefficients, μ_{JT}, versus pressure, p, for the mixture $CO_2 + CH_3OH$ with $x_{CO_2} = 0.9700$ at several temperatures; (a) and (c): ■, *T*= 263.15 K; ●, *T*= 273.15 K; ▲, *T*= 283.15 K; ▼, *T*= 293.15 K; ◆, *T*= 304.21 K; ✸, *T*= 313.15 K; (b) and (d): ●, *T*=263.15 K; ●, *T*=273.15 K; ●, *T*=283.15 K; ●, *T*=293.15 K; ●, *T*=304.21 K; ●, *T*=313.15 K.

Figure 5. Volume-dependent solubility parameter, δ_V, versus density, ρ, for pure CO_2 [50] (line); $CO_2 + CH_3OH$ with $x_{CO_2} = 0.9700$ at several temperatures: ●, *T*=263.15 K; ●, *T*=273.15 K; ●, *T*=283.15 K; ●, *T*=293.15 K; ●, *T*=304.21 K; ●, *T*=313.15 K; $CO_2 + CO$, $CO_2 + CH_4$, $CO_2 + H_2$ and $CO_2 + CO + H_2$ mixtures (yellow) [8].

Thermodynamic properties of a CO_2-rich mixture $CO_2 + CH_3OH$ in conditions of interest for carbon dioxide capture and storage technology and other applications

Clara Rivas[1], Beatriz Gimeno[1], Ramón Bravo[2], Manuela Artal[1], Javier Fernández[1], Sofía Teresa Blanco[1], María Inmaculada Velasco[*1]

[1]*Departamento de Química Física, Facultad de Ciencias, Universidad de Zaragoza, 50009 Zaragoza, Spain*

[2]*Departamento de Física Aplicada, Facultad de Física, Universidad de Santiago de Compostela, 15782 Santiago de Compostela, Spain*

*Corresponding author: curra@unizar.es

SUPPLEMENTARY MATERIAL

TABLE OF CONTENTS

Table S1. Parameters used to model the CO_2 + CH_3OH system with the PC-SAFT EoS.

Pure Compound Parameter	CO_2	CH_3OH
T_c / K[a]	304.21	512.90
P_c / MPa[a]	7.383	8.094
V_c / (10^{-6}m^3·mol^{-1})[b]	94	117
ω[b]	0.2236	0.5643
(m/M) / (mol·g^{-1})[a]	0.04834	0.05273
σ / Å[a]	2.8251	3.3264
ε / K[a]	163.76	175.20
$\kappa^{A_iB_i}$[a]	0.035176[c]	0.035176
$\varepsilon^{A_iB_i}$ / K[a]	0	2899.5
Association scheme[a]	2C	2B
Δv_c / (10^{-3}m^3·kg^{-1})[d]	0.085	0.229
Binary interaction parameter CO_2 - CH_3OH[a]: $k_{ij} = -0.323 + 2.88 \times 10^{-4}\, T$		

[a] Gil, L., Blanco, S.T., Rivas, C., Laga, E., Fernández, J., Artal, M., Velasco, I., 2012. Experimental determination of the critical loci for {n-C_6H_{14} or CO_2+alkan-1-ol} mixtures. Evaluation of their critical and subcritical behavior using PC-SAFT EoS. The Journal of Supercritical Fluids, 71, 26-44. doi: 10.1016/j.supflu.2012.07.008.

[b] DIPPR Chemical Database, 2009.

[c] Kleiner, M., Sadowski, G., 2007. Modeling of polar systems using PCP-SAFT: An approach to account for induced-association interactions. The Journal of Physical Chemistry C, 111, 15544-15553. doi: 10.1021/jp072640v.

[d] This work. Ranges: T = 263-313 K; p = up to 195.0 MPa.

Table S2. Experimental speeds of sound, c, in CO_2 + CH_3OH mixtures in dense phase at several compositions, x_{CO_2}, temperatures T and pressures p.

p/MPa	c/(m·s^{-1})	p/MPa	c/(m·s^{-1})	p/MPa	c/(m·s^{-1})
$x_{CO_2} = 0.7534$					
T= 263.18 K		T= 298.13 K		T= 323.15 K	
6.06	735.8	10.08	529.7	25.00	585.5
9.71	770.9	14.98	600.9	29.95	635.7
14.73	813.5	20.03	657.7	35.04	680.4
20.16	854.1	30.03	746.7	40.00	719.1
24.94	886.4	34.98	783.5	45.07	755.0
30.09	918.5	40.05	817.8	50.42	789.8
35.00	946.9	45.02	848.9	55.12	818.2
40.02	974.0	50.07	878.2	60.11	846.6
44.82	998.5	54.89	904.5	65.81	876.8
49.95	1023.2	60.23	932.1	70.22	899.1
55.09	1046.8	64.68	953.8	75.22	923.1
59.88	1067.8	70.03	978.8	90.00	988.1
64.88	1088.8	75.55	1003.2	100.23	1029.0
70.36	1110.8	80.53	1024.4	109.96	1065.3
75.34	1130.0	90.43	1064.1	120.58	1102.5
80.26	1148.4	99.83	1098.9	140.52	1166.6
89.76	1182.3	110.32	1136.1	160.41	1224.7
100.04	1216.8	120.12	1168.5	180.46	1278.6
110.59	1250.3	139.11	1226.8		
119.81	1278.1	159.59	1284.3		
141.28	1338.3	180.37	1338.1		
159.89	1386.5				
179.55	1433.7				
$x_{CO_2} = 0.8502$					
T= 263.19 K		T= 298.13 K		T= 323.15 K	
6.00	691.2	15.06	554.0	24.96	549.5
9.88	731.2	20.00	613.8	30.02	602.8
14.65	773.8	24.94	663.5	35.10	648.9
19.85	814.7	30.00	707.4	40.05	688.4
24.99	850.9	35.06	746.3	45.01	724.5

29.69	881.1		40.03	780.8		49.92	757.3
35.02	912.8		45.00	812.9		55.04	788.7
40.08	940.7		50.08	843.0		59.98	817.2
44.91	965.8		54.91	869.9		64.84	843.5
50.17	991.7		59.95	896.4		69.88	869.3
55.23	1015.1		65.10	922.0		75.11	894.6
60.10	1036.7		69.93	944.8		80.18	918.0
64.65	1056.0		75.12	968.2		89.68	959.3
70.03	1078.0		79.99	989.0		99.90	1000.3
74.38	1095.2		89.88	1029.2		109.76	1037.3
80.05	1116.4		100.01	1067.3		119.51	1071.6
90.05	1152.6		109.89	1102.7		139.89	1137.2
100.54	1187.6		119.50	1135.1			
110.23	1218.2		140.06	1198.2			
120.05	1247.8		160.55	1255.2			
140.15	1303.4		178.27	1301.3			
150.27	1329.1						

p/MPa	c/(m·s^{-1})	p/MPa	c/(m·s^{-1})	p/MPa	c/(m·s^{-1})	p/MPa	c/(m·s^{-1})
$x_{CO_2} = 0.9250$							
T= 263.13 K		T= 263.13 K		T= 263.14 K		T= 263.14 K	
7.97	694.6	7.97	693.1	7.97	694.8	7.97	695.2
9.99	715.1	10.00	714.3	10.02	715.9	9.96	715.4
14.94	760.5	14.96	759.3	14.99	761.0	14.95	760.8
20.00	800.7	19.99	799.6	20.02	800.7	19.99	801.0
24.97	836.0	24.98	835.1	24.99	836.3	24.97	836.4
29.99	868.4	29.96	867.4	30.00	868.9	29.96	868.8
34.99	898.5	35.00	897.7	34.98	898.5	34.95	898.5
39.95	926.1	39.97	925.5	39.99	926.5	39.99	926.8
44.97	952.1	44.98	951.6	45.03	952.7	45.04	952.8
49.97	977.0	49.97	976.2	49.95	977.1	49.96	977.1
54.99	1000.3	54.95	999.5	55.01	1000.5	54.98	1000.5
59.99	1022.6	59.95	1021.6	59.95	1022.5	59.97	1022.9
64.98	1043.7	65.00	1043.0	64.97	1043.9	64.97	1044.2
69.96	1063.9	70.00	1063.4	69.99	1064.1	69.95	1064.3
74.96	1083.5	74.96	1082.7	74.97	1083.7	74.99	1084.1
80.00	1102.6	79.98	1101.6	80.00	1102.8	79.99	1102.8

90.00	1138.2	89.99	1137.3	89.95	1138.4	90.02	1138.8
99.99	1171.5	100.00	1170.8	100.00	1171.8	99.98	1172.1
109.98	1203.2	109.97	1202.4	109.98	1203.3	110.00	1203.8
119.98	1233.2	119.95	1232.3	120.00	1233.4	119.98	1233.5
129.98	1261.7	129.99	1260.9	130.00	1262.0	130.01	1262.1
139.97	1288.8	139.98	1288.1	139.98	1289.1	140.01	1289.5
149.95	1315.0	149.97	1314.1	149.95	1315.1	150.00	1315.4
159.97	1340.0	159.98	1339.2	159.96	1340.2	159.95	1340.4
170.01	1364.1	170.04	1363.4	169.98	1364.2	169.96	1364.5
180.02	1387.5	180.00	1386.5	179.99	1387.5	179.97	1388.0
190.00	1409.9	190.01	1409.0	190.02	1409.9	190.00	1410.3
T = 298.13 K		T = 298.13 K		T = 298.13 K		T = 298.13 K	
14.98	537.1	14.99	536.5	14.97	538.3	14.99	539.1
19.95	600.2	20.00	599.6	20.00	601.7	19.96	602.2
24.97	651.7	24.99	651.3	25.00	652.9	25.00	653.0
29.98	696.1	30.01	695.5	29.99	696.8	29.95	696.6
34.99	735.2	35.02	734.8	35.00	736.1	35.00	736.1
39.99	770.5	39.99	770.1	39.98	771.2	40.00	771.3
45.02	803.0	44.98	802.5	45.00	803.5	44.96	802.0
49.99	832.8	49.98	832.4	50.01	833.6	49.98	833.5
55.00	860.7	54.95	860.2	54.94	860.9	54.97	861.2
60.00	887.0	59.97	886.8	60.02	887.7	60.01	887.7
64.96	911.8	65.01	911.9	64.95	912.0	64.99	912.4
69.98	935.3	69.96	935.2	69.97	935.8	70.00	936.0
74.96	957.7	74.97	957.9	75.00	958.5	74.97	958.4
79.99	979.4	79.99	979.4	79.95	979.9	79.97	979.7
89.96	1019.7	90.00	1020.0	90.00	1020.4	89.98	1020.4
100.04	1057.3	99.99	1057.5	99.97	1057.9	100.01	1057.5
109.95	1092.7	109.99	1092.8	109.99	1093.2	109.98	1093.2
120.00	1126.0	119.99	1125.8	119.93	1126.0	119.96	1126.1
129.97	1157.2	129.96	1157.1	130.00	1157.5	129.97	1157.6
139.99	1187.1	139.98	1186.8	140.03	1187.4	139.98	1187.3
149.95	1215.3	149.99	1215.1	149.96	1215.5	149.95	1215.7
159.99	1242.6	159.98	1242.2	159.97	1242.8	159.96	1242.8
170.01	1268.7	169.99	1268.1	169.98	1268.9	169.97	1268.9
180.02	1293.8	179.99	1293.2	180.06	1294.1	180.02	1294.0

190.01	1317.9	189.94	1316.8	189.97	1317.8	189.95	1317.9
T= 323.14 K		T= 323.14 K		T= 323.14 K		T= 323.14 K	
25.00	537.5	24.96	536.3	24.98	537.5	24.96	537.4
29.99	591.2	29.99	590.7	29.99	591.5	29.98	591.2
34.99	637.5	34.96	636.5	34.96	637.2	34.98	637.4
39.98	678.0	39.98	677.9	40.00	678.2	39.99	678.6
44.98	714.6	45.00	714.7	44.98	714.8	44.98	714.8
49.98	748.4	49.98	748.2	49.96	748.0	50.00	748.4
54.98	779.1	55.00	779.3	55.01	779.4	54.96	779.2
59.99	808.2	59.98	807.9	59.98	808.1	60.03	808.2
64.97	835.2	64.97	835.3	64.99	835.4	64.97	835.1
69.97	860.9	69.98	861.0	69.99	860.9	69.97	860.8
74.99	885.2	75.00	885.4	75.06	885.5	74.95	885.0
80.00	908.4	79.99	908.5	79.99	908.4	79.97	908.3
90.00	951.8	90.00	952.0	89.99	951.7	89.99	951.7
99.95	991.5	100.00	992.1	100.01	991.8	100.01	991.7
109.99	1029.0	109.98	1029.1	109.96	1028.8	109.98	1028.9
119.99	1063.9	119.97	1063.9	119.97	1063.8	119.99	1063.9
129.96	1096.8	129.99	1096.8	130.02	1096.9	129.98	1096.8
139.99	1128.0	139.96	1128.0	140.00	1128.1	139.99	1128.1
149.96	1157.6	149.98	1157.7	149.99	1157.7	150.01	1157.8
160.01	1186.0	160.00	1187.0	160.05	1186.2	159.99	1186.2
169.98	1213.1	170.01	1213.2	169.94	1213.1	169.98	1213.3
180.00	1239.1	180.10	1239.2	179.96	1239.4	180.00	1239.5
190.00	1264.3	189.98	1263.9	190.05	1264.6	190.01	1264.5

p/MPa	c /(m·s^{-1})	p/MPa	c /(m·s^{-1})	p/MPa	c /(m·s^{-1})
$x_{CO_2} = 0.9803$					
T= 263.18 K		T= 298.14 K		T= 323.16 K	
6.04	643.4	44.94	798.0	69.98	855.3
7.92	666.1	50.05	829.6	74.96	879.8
10.19	691.8	54.98	857.8	79.95	903.2
14.95	747.6	60.14	885.4	89.64	945.6
20.05	788.0	64.99	909.9	99.69	986.1
24.99	823.9	70.21	935.0	110.36	1025.6
29.91	856.8	75.30	958.1	120.03	1059.8
34.86	887.4	80.24	979.6	129.97	1092.5

39.91	916.3	89.80	1018.7	140.23	1124.5
44.98	943.5	100.45	1059.1	150.14	1153.8
50.17	969.0	109.89	1092.5		
55.00	992.2	120.16	1126.5		
60.14	1015.5	130.40	1158.4		
64.76	1035.7	139.81	1185.8		
70.16	1058.2	150.17	1215.7		
75.41	1078.8	160.47	1243.6		
79.75	1095.2				
89.94	1132.1				
99.68	1165.0				
109.95	1197.7				
120.70	1230.1				
140.78	1286.1				
160.95	1337.6				
179.55	1382.1				

$u_T = 0.015$ K; $u_p = 0.02$ MPa; $u_c = 5.9 \times 10^{-4} c$

Table S3. Experimental speeds of sound, c, in the CO_2 + CH_3OH mixture with x_{CO_2} = 0.9700 in dense phase at temperatures T and pressures p.

p /MPa	c /(m·s^{-1})	p /MPa	c /(m·s^{-1})	p /MPa	c /(m·s^{-1})	p /MPa	c /(m·s^{-1})
T = 263.16 K		T = 273.15 K		T = 283.14 K		T = 293.13 K	
3.28	626.2	5.00	570.5	14.01	615.2	20.01	624.7
3.80	633.5	6.02	581.6	20.00	679.8	24.93	674.5
5.05	649.7	6.04	581.0	25.01	725.0	29.99	718.7
6.02	661.8	10.00	634.7	29.94	763.8	34.94	755.3
6.17	664.3	14.90	688.9	34.98	799.7	39.99	791.4
8.10	687.5	19.91	735.5	39.94	831.8	44.94	822.9
10.02	706.8	24.94	776.2	45.09	862.8	49.97	852.5
14.96	752.4	29.98	812.6	50.15	890.9	54.90	879.8
19.89	792.8	35.03	845.6	55.02	916.3	59.94	906.0
24.92	829.4	39.99	875.6	59.83	940.2	64.95	930.5
29.96	862.5	44.95	903.5	64.95	964.2	69.95	953.8
34.89	892.6	49.96	929.9	70.15	987.4	74.98	976.0
39.94	921.0	54.97	954.7	74.97	1007.9	80.02	997.6
44.89	947.0	60.00	978.4	79.68	1027.1	90.01	1037.3
49.99	972.3	64.95	1000.7	90.23	1067.9	100.01	1074.3
54.91	995.6	69.99	1022.2	99.95	1102.7	109.95	1108.7
60.01	1018.3	74.93	1042.5	109.90	1136.3	120.04	1141.7
65.09	1039.8	80.12	1062.9	120.08	1168.8	140.05	1201.9
69.97	1059.9	90.14	1100.0	140.09	1227.7	160.04	1256.5
75.00	1079.5	99.97	1134.2	159.98	1281.0	178.78	1303.9
80.15	1098.9	110.03	1167.0	180.05	1330.2		
90.13	1134.4	120.15	1198.3				
100.14	1168.0	139.94	1255.0				
110.06	1199.3	159.79	1307.2				
119.96	1228.9	180.53	1357.4				
140.00	1284.7						
159.90	1335.8						
179.99	1383.3						
194.49	1415.5						
T = 304.19 K		T = 313.15 K					
24.95	621.0	31.89	648.6				

29.96	668.7	34.94	674.9
34.88	709.6	39.99	714.5
39.93	747.2	44.94	749.7
44.97	781.3	49.94	782.0
50.02	812.8	54.96	812.2
54.97	841.5	60.14	841.3
59.97	868.6	65.17	867.7
65.10	894.9	70.01	891.8
70.23	919.7	75.17	916.2
75.54	944.1	80.06	938.2
79.98	963.6	90.00	980.1
90.07	1005.1	100.11	1019.5
100.04	1043.2	109.90	1055.1
109.90	1078.3	120.04	1089.6
119.96	1112.5	140.11	1152.5
140.09	1173.8	159.96	1208.8
159.77	1228.8	179.84	1260.7
180.45	1282.0		

$u_T = 0.015$ K; $u_p = 0.02$ MPa; $u_c = 5.9 \times 10^{-4} c$

Calculation procedure for the combined uncertainty of the experimental values of density

From a calibration with pure CO_2, and taking into account the uncertainty in the vibrational period, τ, $u_\tau = 2\times10^{-5}$ ms (Bouchot and Richon, 2001), the combined uncertainty in density, u_ρ, was calculated for the studied mixtures using the error propagation law and the following equation:

$$\rho(p,T) = \rho_{ref}(p,T)\frac{\left(\frac{K(p,T)}{K_0(T)}\right)\tau^2(p,T)-\tau_0^2(T)}{\left(\frac{K(p,T)}{K_0(T)}\right)\tau_{ref}^2(p,T)-\tau_0^2(T)} \quad (1)$$

where $\rho(p,T)$ is the density of the inner fluid to be determined at pressure p and temperature T; $\rho_{ref}(p,T)$ is the density of the reference fluid at pressure p and temperature T; $K(p,T)$ is the transversal stiffness of the vibrating tube at pressure p and temperature T; $K_0(T)$ is the transversal stiffness of the vibrating tube under vacuum and at temperature T; $\tau(p,T)$ is the period of the vibrating tube with inner fluid determined at pressure p and temperature T; $\tau_{ref}(p,T)$ is the period of the vibrating tube with the reference fluid at pressure p and temperature T; $\tau_0(T)$ is the period of the vibrating tube under vacuum and at temperature T.

Bouchot, C., Richon, D., 2001. An enhanced method to calibrate vibrating tube densimeters. Fluid Phase Equilibria, 191, 189-208. doi: 10.1016/S0378-3812(01)00627-6.

Table S4. The $p-\rho-T$ experimental data for the CO_2 + CH_3OH mixture with x_{CO_2} = 0.9700 in dense phase at temperatures T and pressures p. ~~The bubble pressures, p_b, and densities of the liquid phase at VLE, ρ_L, at the studied subcritical temperatures are included~~. **Modificar , añadir y/o quitar valores de densidad y añadir fase densa y supercrítica según formato**

p/MPa	ρ/(kg·m^{-3})					
	T=263.15 K	T=273.15 K	T=283.15 K	T=293.15 K	T=304.21 K	T=313.15 K
20.000	1052.99	1015.77	979.19	937.71	889.20	846.53
19.975	1052.91	1015.70	979.04	937.60	888.98	846.29
19.950	1052.83	1015.60	978.96	937.48	888.82	846.10
19.925	1052.75	1015.50	978.84	937.36	888.67	845.91
19.900	1052.67	1015.41	978.72	937.17	888.48	845.69
19.875	1052.59	1015.31	978.64	937.05	888.28	845.47
19.850	1052.50	1015.29	978.49	936.93	888.12	845.27
19.825	1052.45	1015.19	978.42	936.81	887.96	845.06
19.800	1052.34	1015.08	978.31	936.69	887.80	844.89
19.775	1052.28	1014.98	978.19	936.57	887.64	844.64
19.750	1052.26	1014.88	978.07	936.44	887.40	844.43
19.725	1052.13	1014.86	977.97	936.26	887.24	844.25
19.700	1052.08	1014.76	977.89	936.18	887.09	844.02
19.675	1052.02	1014.66	977.74	936.00	886.92	843.84
19.650	1051.89	1014.56	977.66	935.88	886.76	843.59
19.625	1051.83	1014.47	977.51	935.75	886.54	843.37
19.600	1051.77	1014.44	977.43	935.62	886.37	843.19
19.575	1051.69	1014.34	977.29	935.49	886.21	842.96
19.550	1051.58	1014.24	977.22	935.36	886.04	842.75
19.525	1051.53	1014.15	977.10	935.24	885.78	842.53
19.500	1051.45	1014.05	976.99	935.12	885.62	842.31
19.475	1051.35	1013.95	976.85	934.91	885.46	842.08
19.450	1051.29	1013.91	976.74	934.79	885.28	841.84
19.425	1051.21	1013.82	976.66	934.64	885.12	841.61
19.400	1051.12	1013.72	976.53	934.51	884.95	841.40
19.375	1051.04	1013.61	976.42	934.38	884.78	841.18
19.350	1050.96	1013.58	976.34	934.24	884.60	840.94
19.325	1050.88	1013.48	976.18	934.10	884.43	840.71

19.300	1050.80	1013.37	976.10	933.97	884.25	840.49
19.275	1050.72	1013.27	976.02	933.83	884.07	840.27
19.250	1050.63	1013.25	975.85	933.70	883.86	840.03
19.225	1050.56	1013.15	975.76	933.56	883.65	839.82
19.200	1050.47	1013.04	975.66	933.42	883.48	839.61
19.175	1050.39	1012.93	975.52	933.29	883.30	839.32
19.150	1050.31	1012.83	975.44	933.14	883.11	839.12
19.125	1050.23	1012.77	975.31	933.01	882.92	838.87
19.100	1050.15	1012.70	975.18	932.87	882.73	838.61
19.075	1050.07	1012.60	975.08	932.74	882.62	838.38
19.050	1049.99	1012.49	974.98	932.60	882.43	838.15
19.025	1049.91	1012.45	974.90	932.45	882.19	837.93
19.000	1049.82	1012.37	974.74	932.30	882.06	837.72
18.975	1049.74	1012.26	974.63	932.14	881.88	837.47
18.950	1049.66	1012.15	974.55	931.99	881.68	837.22
18.925	1049.58	1012.05	974.41	931.90	881.49	837.02
18.900	1049.50	1011.94	974.28	931.74	881.28	836.78
18.875	1049.42	1011.88	974.17	931.59	881.09	836.55
18.850	1049.34	1011.81	974.07	931.43	880.89	836.28
18.825	1049.09	1011.70	973.96	931.25	880.78	836.06
18.800	1049.06	1011.59	973.84	931.17	880.58	835.84
18.775	1048.93	1011.49	973.72	931.01	880.38	835.62
18.750	1048.93	1011.46	973.60	930.86	880.19	835.38
18.725	1048.85	1011.35	973.46	930.69	879.99	835.15
18.700	1048.83	1011.25	973.35	930.61	879.76	834.94
18.675	1048.74	1011.15	973.21	930.46	879.61	834.69
18.650	1048.64	1011.10	973.11	930.29	879.38	834.43
18.625	1048.58	1010.99	973.03	930.13	879.24	834.20
18.600	1048.53	1010.88	972.90	929.97	879.03	833.97
18.575	1048.43	1010.82	972.76	929.88	878.87	833.75
18.550	1048.31	1010.70	972.62	929.71	878.68	833.50
18.525	1048.28	1010.58	972.54	929.53	878.46	833.28
18.500	1048.20	1010.52	972.43	929.45	878.30	833.03
18.475	1048.11	1010.41	972.30	929.27	878.11	832.80
18.450	1048.04	1010.33	972.17	929.11	877.88	832.53
18.425	1047.96	1010.26	972.05	928.95	877.73	832.31

18.400	1047.88	1010.15	971.98	928.85	877.50	832.11
18.375	1047.82	1010.03	971.85	928.68	877.36	831.85
18.350	1047.75	1009.93	971.73	928.50	877.14	831.62
18.325	1047.69	1009.88	971.57	928.38	876.99	831.37
18.300	1047.62	1009.76	971.48	928.22	876.78	831.12
18.275	1047.55	1009.68	971.39	928.06	876.56	830.86
18.250	1047.47	1009.61	971.25	927.94	876.35	830.62
18.225	1047.37	1009.49	971.16	927.75	876.22	830.35
18.200	1047.31	1009.44	970.99	927.66	876.00	830.13
18.175	1047.23	1009.33	970.91	927.46	875.78	829.87
18.150	1047.15	1009.21	970.80	927.35	875.58	829.59
18.125	1047.07	1009.17	970.66	927.16	875.42	829.36
18.100	1046.98	1009.05	970.52	927.05	875.20	829.11
18.075	1046.90	1008.93	970.43	926.86	875.05	828.84
18.050	1046.85	1008.81	970.31	926.67	874.83	828.60
18.025	1046.79	1008.76	970.18	926.56	874.62	828.35
18.000	1046.66	1008.63	970.08	926.42	874.46	828.10
17.975	1046.58	1008.58	969.94	926.25	874.23	827.85
17.950	1046.51	1008.47	969.80	926.13	874.01	827.61
17.925	1046.44	1008.41	969.69	925.93	873.87	827.38
17.900	1046.37	1008.28	969.60	925.82	873.63	827.14
17.875	1046.32	1008.22	969.46	925.61	873.48	826.87
17.850	1046.26	1008.10	969.37	925.49	873.25	826.64
17.825	1046.11	1008.05	969.25	925.35	873.02	826.41
17.800	1046.04	1007.92	969.12	925.19	872.83	826.17
17.775	1045.97	1007.82	968.98	925.03	872.68	825.94
17.750	1045.89	1007.74	968.88	924.87	872.45	825.67
17.725	1045.81	1007.61	968.78	924.70	872.29	825.45
17.700	1045.77	1007.56	968.64	924.55	872.08	825.17
17.675	1045.69	1007.42	968.48	924.40	871.84	824.95
17.650	1045.61	1007.37	968.40	924.26	871.68	824.71
17.625	1045.52	1007.24	968.24	924.11	871.44	824.46
17.600	1045.44	1007.11	968.15	923.94	871.23	824.21
17.575	1045.33	1007.06	968.06	923.77	871.06	823.99
17.550	1045.28	1006.92	967.90	923.64	870.86	823.71
17.525	1045.20	1006.86	967.82	923.48	870.66	823.52

17.500	1045.12	1006.76	967.66	923.34	870.48	823.28
17.475	1045.04	1006.68	967.57	923.17	870.29	823.11
17.450	1044.94	1006.55	967.41	922.99	870.09	822.87
17.425	1044.87	1006.50	967.31	922.85	869.89	822.65
17.400	1044.79	1006.36	967.17	922.71	869.69	822.42
17.375	1044.71	1006.30	967.09	922.50	869.42	822.18
17.350	1044.63	1006.19	966.97	922.33	869.28	821.98
17.325	1044.55	1006.10	966.85	922.18	869.01	821.73
17.300	1044.44	1006.03	966.70	922.01	868.87	821.48
17.275	1044.39	1005.90	966.60	921.85	868.66	821.23
17.250	1044.31	1005.78	966.51	921.70	868.43	821.00
17.225	1044.22	1005.70	966.36	921.53	868.20	820.77
17.200	1044.14	1005.63	966.25	921.40	867.99	820.54
17.175	1044.06	1005.49	966.11	921.27	867.77	820.32
17.150	1043.98	1005.42	965.97	921.10	867.63	820.09
17.125	1043.90	1005.30	965.87	920.92	867.40	819.79
17.100	1043.82	1005.21	965.75	920.73	867.20	819.55
17.075	1043.74	1005.11	965.62	920.59	866.99	819.27
17.050	1043.64	1005.04	965.46	920.44	866.78	819.06
17.025	1043.57	1004.89	965.37	920.29	866.56	818.81
17.000	1043.49	1004.82	965.28	920.08	866.34	818.55
16.975	1043.40	1004.73	965.14	919.95	866.12	818.28
16.950	1043.33	1004.60	964.99	919.71	865.90	818.05
16.925	1043.24	1004.53	964.88	919.55	865.70	817.80
16.900	1043.17	1004.40	964.79	919.43	865.51	817.54
16.875	1043.08	1004.31	964.65	919.22	865.26	817.27
16.850	1043.01	1004.25	964.49	919.06	865.05	817.00
16.825	1042.91	1004.09	964.40	918.90	864.86	816.74
16.800	1042.82	1004.01	964.28	918.73	864.63	816.46
16.775	1042.75	1003.93	964.16	918.57	864.47	816.22
16.750	1042.68	1003.86	964.00	918.41	864.20	815.94
16.725	1042.57	1003.75	963.92	918.24	864.02	815.67
16.700	1042.51	1003.63	963.77	918.08	863.76	815.43
16.675	1042.38	1003.55	963.66	917.90	863.56	815.12
16.650	1042.33	1003.43	963.51	917.70	863.26	814.87
16.625	1042.27	1003.31	963.43	917.58	863.08	814.60

16.600	1042.19	1003.23	963.26	917.37	862.90	814.33
16.575	1042.08	1003.15	963.18	917.25	862.62	814.03
16.550	1041.95	1003.07	963.02	917.01	862.42	813.76
16.525	1041.91	1002.92	962.86	916.93	862.21	813.50
16.500	1041.79	1002.82	962.78	916.75	862.01	813.24
16.475	1041.72	1002.73	962.61	916.52	861.85	812.90
16.450	1041.66	1002.64	962.53	916.37	861.65	812.66
16.425	1041.59	1002.55	962.42	916.20	861.43	812.38
16.400	1041.46	1002.44	962.28	916.03	861.22	812.11
16.375	1041.38	1002.35	962.15	915.87	861.01	811.82
16.350	1041.32	1002.26	962.02	915.71	860.83	811.55
16.325	1041.25	1002.16	961.89	915.54	860.63	811.27
16.300	1041.16	1002.05	961.74	915.38	860.35	810.98
16.275	1041.05	1001.95	961.63	915.22	860.20	810.69
16.250	1040.97	1001.84	961.53	915.05	859.97	810.39
16.225	1040.89	1001.73	961.39	914.89	859.74	810.09
16.200	1040.81	1001.64	961.23	914.73	859.52	809.79
16.175	1040.73	1001.55	961.15	914.56	859.32	809.50
16.150	1040.65	1001.44	960.98	914.45	859.07	809.20
16.125	1040.57	1001.34	960.89	914.31	858.84	808.91
16.100	1040.49	1001.23	960.74	914.15	858.66	808.61
16.075	1040.40	1001.14	960.60	913.99	858.44	808.29
16.050	1040.31	1001.03	960.49	913.83	858.19	807.98
16.025	1040.20	1000.92	960.33	913.66	857.95	807.71
16.000	1040.16	1000.82	960.25	913.55	857.77	807.41
15.975	1040.06	1000.74	960.09	913.37	857.56	807.09
15.950	1039.97	1000.59	959.94	913.17	857.32	806.83
15.925	1039.88	1000.50	959.84	913.04	857.08	806.51
15.900	1039.79	1000.44	959.71	912.90	856.93	806.23
15.875	1039.70	1000.33	959.55	912.75	856.68	805.91
15.850	1039.61	1000.25	959.43	912.52	856.41	805.58
15.825	1039.51	1000.09	959.30	912.36	856.20	805.27
15.800	1039.43	1000.03	959.19	912.19	855.96	804.99
15.775	1039.35	999.93	959.05	912.03	855.71	804.65
15.750	1039.26	999.85	958.89	911.86	855.49	804.34
15.725	1039.19	999.76	958.78	911.74	855.30	804.02

15.700	1039.10	999.63	958.62	911.59	855.06	803.73
15.675	1039.02	999.52	958.52	911.37	854.81	803.42
15.650	1038.94	999.41	958.37	911.21	854.57	803.12
15.625	1038.86	999.34	958.22	911.01	854.39	802.79
15.600	1038.78	999.22	958.13	910.88	854.15	802.47
15.575	1038.70	999.11	957.97	910.70	853.89	802.17
15.550	1038.61	999.03	957.84	910.48	853.64	801.84
15.525	1038.53	998.89	957.72	910.31	853.40	801.53
15.500	1038.45	998.79	957.56	910.23	853.20	801.17
15.475	1038.37	998.71	957.47	910.14	852.92	800.87
15.450	1038.28	998.63	957.32	910.03	852.70	800.53
15.425	1038.19	998.50	957.17	909.89	852.43	800.19
15.400	1038.07	998.38	957.07	909.68	852.22	799.88
15.375	1038.01	998.30	956.93	909.52	851.98	799.54
15.350	1037.91	998.19	956.78	909.37	851.79	799.22
15.325	1037.80	998.14	956.66	909.22	851.51	798.91
15.300	1037.72	997.98	956.56	909.03	851.23	798.53
15.275	1037.66	997.89	956.42	908.85	851.04	798.26
15.250	1037.56	997.80	956.27	908.66	850.76	797.89
15.225	1037.50	997.66	956.18	908.49	850.56	797.52
15.200	1037.39	997.57	956.01	908.32	850.30	797.19
15.175	1037.31	997.49	955.88	908.18	850.04	796.89
15.150	1037.23	997.37	955.77	907.99	849.76	796.56
15.125	1037.15	997.24	955.60	907.83	849.56	796.20
15.100	1037.07	997.16	955.44	907.60	849.30	795.80
15.075	1036.96	997.08	955.36	907.46	849.02	795.50
15.050	1036.90	996.94	955.20	907.32	848.76	795.16
15.025	1036.78	996.84	955.09	907.15	848.51	794.78
15.000	1036.74	996.75	954.95	906.96	848.29	794.40
14.975	1036.63	996.65	954.79	906.77	848.00	794.09
14.950	1036.51	996.51	954.68	906.59	847.71	793.74
14.925	1036.42	996.43	954.57	906.44	847.52	793.37
14.900	1036.34	996.34	954.41	906.27	847.24	793.03
14.875	1036.25	996.27	954.28	906.06	846.98	792.64
14.850	1036.17	996.12	954.14	905.88	846.73	792.31
14.825	1036.09	996.02	954.02	905.68	846.50	791.96

14.800	1036.01	995.94	953.88	905.48	846.19	791.65
14.775	1035.93	995.81	953.73	905.36	845.96	791.25
14.750	1035.83	995.70	953.62	905.15	845.72	790.91
14.725	1035.77	995.62	953.48	904.95	845.44	790.55
14.700	1035.62	995.50	953.32	904.75	845.17	790.23
14.675	1035.52	995.37	953.17	904.58	844.86	789.86
14.650	1035.44	995.29	953.08	904.42	844.61	789.51
14.625	1035.36	995.18	952.93	904.20	844.38	789.10
14.600	1035.28	995.07	952.75	904.05	844.14	788.78
14.575	1035.19	994.96	952.59	903.82	843.90	788.43
14.550	1035.11	994.85	952.51	903.67	843.58	788.05
14.525	1035.03	994.75	952.37	903.44	843.34	787.73
14.500	1034.95	994.65	952.19	903.28	843.08	787.34
14.475	1034.86	994.54	952.09	903.13	842.78	787.01
14.450	1034.70	994.42	951.93	902.92	842.52	786.66
14.425	1034.62	994.35	951.77	902.77	842.27	786.27
14.400	1034.54	994.23	951.61	902.56	842.04	785.88
14.375	1034.46	994.12	951.51	902.38	841.72	785.52
14.350	1034.38	994.00	951.37	902.18	841.49	785.15
14.325	1034.30	993.90	951.20	902.05	841.24	784.77
14.300	1034.22	993.82	951.12	901.83	840.92	784.39
14.275	1034.13	993.70	950.96	901.66	840.68	784.01
14.250	1033.97	993.58	950.80	901.48	840.43	783.65
14.225	1033.90	993.50	950.70	901.31	840.12	783.28
14.200	1033.81	993.38	950.55	901.13	839.87	782.93
14.175	1033.73	993.26	950.39	900.95	839.62	782.55
14.150	1033.65	993.17	950.22	900.70	839.31	782.18
14.125	1033.57	993.06	950.11	900.51	839.03	781.80
14.100	1033.48	992.93	949.98	900.34	838.78	781.44
14.075	1033.38	992.85	949.82	900.17	838.50	781.06
14.050	1033.24	992.70	949.65	899.94	838.19	780.67
14.025	1033.16	992.60	949.51	899.76	837.92	780.28
14.000	1033.08	992.52	949.41	899.55	837.64	779.85
13.975	1032.99	992.38	949.24	899.38	837.35	779.47
13.950	1032.91	992.27	949.10	899.20	837.08	779.11
13.925	1032.83	992.19	948.95	898.97	836.81	778.72

13.900	1032.75	992.09	948.84	898.80	836.51	778.33
13.875	1032.61	991.95	948.67	898.62	836.22	777.93
13.850	1032.53	991.87	948.51	898.41	836.06	777.52
13.825	1032.42	991.75	948.40	898.26	835.86	777.12
13.800	1032.34	991.62	948.24	898.05	835.64	776.72
13.775	1032.26	991.51	948.10	897.85	835.42	776.36
13.750	1032.18	991.40	947.94	897.68	835.20	776.00
13.725	1032.10	991.30	947.78	897.47	834.90	775.57
13.700	1031.97	991.22	947.69	897.29	834.66	775.16
13.675	1031.94	991.05	947.53	897.09	834.42	774.79
13.650	1031.77	990.97	947.37	896.86	834.12	774.36
13.625	1031.69	990.86	947.20	896.67	833.85	773.92
13.600	1031.61	990.73	947.04	896.51	833.60	773.57
13.575	1031.53	990.65	946.94	896.33	833.35	773.15
13.550	1031.45	990.48	946.80	896.13	833.09	772.70
13.525	1031.37	990.40	946.63	895.96	832.83	772.34
13.500	1031.29	990.32	946.47	895.75	832.56	771.93
13.475	1031.14	990.16	946.39	895.52	832.30	771.50
13.450	1031.04	990.07	946.23	895.34	832.03	771.07
13.425	1030.96	989.98	946.06	895.18	831.75	770.69
13.400	1030.88	989.83	945.90	894.97	831.47	770.23
13.375	1030.80	989.75	945.77	894.75	831.19	769.83
13.350	1030.71	989.67	945.66	894.53	830.91	769.37
13.325	1030.63	989.50	945.49	894.36	830.63	768.93
13.300	1030.53	989.42	945.33	894.19	830.33	768.47
13.275	1030.39	989.28	945.17	893.95	830.06	768.04
13.250	1030.31	989.18	945.05	893.74	829.81	767.60
13.225	1030.22	989.10	944.92	893.53	829.50	767.22
13.200	1030.14	988.93	944.76	893.30	829.21	766.75
13.175	1030.06	988.85	944.59	893.13	828.91	766.29
13.150	1029.94	988.76	944.43	892.96	828.59	765.86
13.125	1029.88	988.61	944.27	892.74	828.34	765.37
13.100	1029.73	988.53	944.17	892.50	828.02	764.93
13.075	1029.65	988.39	944.02	892.32	827.74	764.54
13.050	1029.57	988.28	943.86	892.08	827.45	764.07
13.025	1029.49	988.15	943.70	891.90	827.19	763.58

13.000	1029.41	988.04	943.53	891.66	826.85	763.15
12.975	1029.30	987.96	943.37	891.46	826.52	762.72
12.950	1029.20	987.80	943.22	891.25	826.28	762.23
12.925	1029.08	987.71	943.13	891.01	825.97	761.76
12.900	1029.00	987.63	942.96	890.84	825.66	761.30
12.875	1028.92	987.47	942.80	890.60	825.36	760.82
12.850	1028.84	987.38	942.63	890.37	825.02	760.36
12.825	1028.76	987.27	942.47	890.19	824.72	759.98
12.800	1028.60	987.14	942.34	889.94	824.43	759.54
12.775	1028.51	987.06	942.16	889.77	824.13	759.12
12.750	1028.43	986.89	942.06	889.53	823.79	758.68
12.725	1028.35	986.81	941.87	889.29	823.45	758.30
12.700	1028.27	986.65	941.74	889.11	823.18	757.86
12.675	1028.19	986.57	941.57	888.88	822.85	757.39
12.650	1028.09	986.49	941.41	888.63	822.53	756.92
12.625	1027.96	986.39	941.25	888.41	822.23	756.47
12.600	1027.86	986.24	941.08	888.22	821.94	756.00
12.575	1027.78	986.16	940.92	887.98	821.61	755.53
12.550	1027.70	986.00	940.76	887.80	821.24	755.09
12.525	1027.62	985.92	940.59	887.57	820.93	754.59
12.500	1027.53	985.78	940.45	887.33	820.61	754.12
12.475	1027.38	985.67	940.27	887.16	820.29	753.64
12.450	1027.29	985.59	940.19	886.91	819.95	753.18
12.425	1027.21	985.43	940.02	886.67	819.62	752.63
12.400	1027.13	985.35	939.86	886.49	819.29	752.14
12.375	1027.05	985.18	939.70	886.26	818.95	751.63
12.350	1026.96	985.10	939.53	886.09	818.61	751.14
12.325	1026.88	984.94	939.37	885.85	818.27	750.56
12.300	1026.72	984.86	939.21	885.60	817.94	750.05
12.275	1026.64	984.74	939.10	885.36	817.54	749.50
12.250	1026.56	984.61	938.96	885.18	817.23	749.04
12.225	1026.47	984.53	938.80	884.95	816.89	748.48
12.200	1026.39	984.37	938.63	884.70	816.54	747.95
12.175	1026.31	984.29	938.47	884.46	816.22	747.40
12.150	1026.15	984.12	938.31	884.26	815.82	746.78
12.125	1026.07	984.04	938.14	884.05	815.50	746.23

12.100	1025.98	983.94	937.98	883.79	815.17	745.65
12.075	1025.90	983.79	937.82	883.57	814.76	745.12
12.050	1025.75	983.69	937.68	883.38	814.43	744.51
12.025	1025.66	983.55	937.53	883.12	814.08	743.98
12.000	1025.58	983.47	937.33	882.90	813.70	743.38
11.975	1025.50	983.30	937.23	882.66	813.33	742.81
11.950	1025.41	983.22	937.07	882.46	812.98	742.23
11.925	1025.29	983.06	936.92	882.25	812.53	741.62
11.900	1025.19	982.98	936.74	882.00	812.25	741.01
11.875	1025.09	982.81	936.59	881.77	811.83	740.42
11.850	1025.01	982.74	936.43	881.54	811.47	739.81
11.825	1024.93	982.57	936.26	881.34	811.11	739.20
11.800	1024.84	982.49	936.10	881.10	810.74	738.59
11.775	1024.74	982.36	935.94	880.86	810.37	738.01
11.750	1024.60	982.24	935.78	880.63	810.00	737.41
11.725	1024.52	982.08	935.61	880.38	809.62	736.79
11.700	1024.44	982.00	935.45	880.20	809.25	736.24
11.675	1024.35	981.86	935.29	879.95	808.81	735.62
11.650	1024.21	981.75	935.12	879.71	808.41	734.97
11.625	1024.11	981.62	934.96	879.46	808.01	734.36
11.600	1024.03	981.51	934.80	879.30	807.66	733.75
11.575	1023.95	981.37	934.64	879.00	807.30	733.12
11.550	1023.86	981.26	934.47	878.81	806.91	732.54
11.525	1023.75	981.13	934.39	878.56	806.52	731.88
11.500	1023.62	981.02	934.17	878.33	806.12	731.23
11.475	1023.54	980.89	933.98	878.07	805.69	730.56
11.450	1023.46	980.78	933.88	877.85	805.27	729.89
11.425	1023.38	980.69	933.66	877.58	804.93	729.26
11.400	1023.29	980.53	933.49	877.38	804.56	728.58
11.375	1023.13	980.39	933.37	877.16	804.09	727.87
11.350	1023.05	980.29	933.16	876.93	803.73	727.24
11.325	1022.97	980.16	933.08	876.68	803.31	726.55
11.300	1022.89	980.04	932.90	876.43	802.86	725.87
11.275	1022.80	979.94	932.67	876.20	802.50	725.17
11.250	1022.64	979.80	932.51	875.94	802.05	724.50
11.225	1022.56	979.71	932.34	875.70	801.64	723.83

11.200	1022.48	979.55	932.18	875.45	801.23	723.12
11.175	1022.40	979.46	932.02	875.21	800.80	722.44
11.150	1022.29	979.30	931.86	874.96	800.45	721.68
11.125	1022.15	979.16	931.69	874.72	799.99	720.97
11.100	1022.07	979.06	931.58	874.47	799.63	720.27
11.075	1021.99	978.97	931.33	874.22	799.17	719.52
11.050	1021.91	978.82	931.19	873.98	798.73	718.76
11.025	1021.83	978.70	931.03	873.73	798.32	718.03
11.000	1021.66	978.57	930.89	873.49	797.93	717.28
10.975	1021.58	978.49	930.73	873.24	797.53	716.52
10.950	1021.50	978.33	930.57	873.00	797.06	715.71
10.925	1021.42	978.20	930.41	872.75	796.66	714.94
10.900	1021.25	978.08	930.27	872.51	796.21	714.15
10.875	1021.17	978.00	930.06	872.27	795.84	713.33
10.850	1021.09	977.84	929.88	872.01	795.38	712.55
10.825	1021.01	977.76	929.74	871.77	794.91	711.74
10.800	1020.93	977.59	929.62	871.52	794.49	710.93
10.775	1020.76	977.48	929.45	871.28	794.08	710.14
10.750	1020.68	977.35	929.25	871.03	793.67	709.33
10.725	1020.60	977.18	929.16	870.79	793.26	708.50
10.700	1020.52	977.10	929.00	870.54	792.79	707.66
10.675	1020.44	976.94	928.84	870.30	792.32	706.75
10.650	1020.27	976.86	928.76	869.97	791.91	705.90
10.625	1020.19	976.69	928.66	869.76	791.47	705.05
10.600	1020.11	976.61	928.46	869.48	791.05	704.13
10.575	1020.02	976.45	928.27	869.23	790.60	703.29
10.550	1019.87	976.37	928.10	868.99	790.18	702.39
10.525	1019.78	976.20	927.92	868.74	789.73	701.51
10.500	1019.70	976.12	927.78	868.43	789.30	700.62
10.475	1019.62	975.96	927.61	868.24	788.87	699.66
10.450	1019.46	975.88	927.45	867.99	788.38	698.73
10.425	1019.38	975.71	927.34	867.68	787.92	697.78
10.400	1019.30	975.63	927.17	867.43	787.51	696.92
10.375	1019.21	975.47	927.06	867.18	787.08	695.92
10.350	1019.09	975.36	926.79	866.94	786.55	694.91
10.325	1018.97	975.22	926.69	866.67	786.13	693.97

10.300	1018.89	975.11	926.47	866.45	785.65	693.00
10.275	1018.81	974.98	926.30	866.12	785.18	691.93
10.250	1018.68	974.82	926.06	865.87	784.67	690.95
10.225	1018.56	974.73	926.06	865.63	784.17	689.94
10.200	1018.48	974.57	925.75	865.34	783.77	688.80
10.175	1018.34	974.49	925.57	865.06	783.30	687.88
10.150	1018.23	974.34	925.41	864.74	782.79	686.83
10.125	1018.15	974.24	925.24	864.49	782.29	685.84
10.100	1018.07	974.08	925.08	864.22	781.81	684.80
10.075	1017.99	973.99	924.83	864.00	781.33	683.70
10.050	1017.83	973.84	924.71	863.76	780.81	682.54
10.025	1017.74	973.69	924.53	863.50	780.30	681.48
10.000	1017.66	973.59	924.34	863.30	779.86	680.33
9.975	1017.58	973.43	924.18	863.01	779.32	679.10
9.950	1017.47	973.35	924.00	862.76	778.83	677.96
9.925	1017.34	973.18	923.77	862.54	778.36	676.66
9.900	1017.25	973.10	923.69	862.27	777.81	675.44
9.875	1017.17	972.94	923.48	862.00	777.30	674.13
9.850	1017.01	972.82	923.28	861.78	776.81	672.87
9.825	1016.93	972.69	923.15	861.54	776.25	671.58
9.800	1016.85	972.53	922.94	861.24	775.72	670.26
9.775	1016.77	972.43	922.71	860.99	775.20	668.89
9.750	1016.60	972.29	922.58	860.76	774.65	667.47
9.725	1016.52	972.20	922.38	860.54	774.15	666.14
9.700	1016.44	972.04	922.14	860.28	773.62	664.70
9.675	1016.28	971.88	921.97	860.01	773.03	663.21
9.650	1016.19	971.74	921.81	859.74	772.50	661.70
9.625	1016.11	971.63	921.56	859.48	771.96	660.18
9.600	1016.03	971.55	921.39	859.17	771.35	658.64
9.575	1015.87	971.39	921.21	858.84	770.76	657.12
9.550	1015.78	971.22	921.09	858.59	770.22	655.55
9.525	1015.70	971.14	920.85	858.28	769.73	653.94
9.500	1015.54	970.97	920.65	858.02	769.12	652.27
9.475	1015.46	970.81	920.47	857.69	768.60	650.62
9.450	1015.38	970.67	920.32	857.44	768.06	648.90
9.425	1015.30	970.57	920.09	857.09	767.44	646.98

9.400	1015.13	970.45	919.87	856.82	766.88	645.20
9.375	1015.05	970.32	919.69	856.46	766.27	643.26
9.350	1014.97	970.16	919.52	856.22	765.65	641.40
9.325	1014.89	970.00	919.31	855.89	764.98	639.32
9.300	1014.72	969.92	919.11	855.55	764.36	637.48
9.275	1014.64	969.75	918.95	855.22	763.76	635.44
9.250	1014.56	969.64	918.70	854.90	763.15	633.38
9.225	1014.39	969.51	918.60	854.58	762.52	631.20
9.200	1014.31	969.34	918.33	854.32	761.88	629.00
9.175	1014.23	969.18	918.13	854.24	761.24	626.69
9.150	1014.08	969.10	917.90	854.08	760.55	624.11
9.125	1013.99	968.93	917.75	853.85	759.92	621.62
9.100	1013.91	968.77	917.55	853.57	759.25	619.14
9.075	1013.83	968.69	917.31	853.28	758.64	616.77
9.050	1013.66	968.52	917.12	852.98	757.93	615.82
9.025	1013.58	968.36	916.93	852.71	757.25	615.65
9.000	1013.49	968.28	916.73	852.41	756.48	614.77
8.975	1013.35	968.12	916.53	852.08	755.82	611.82
8.950	1013.25	967.95	916.35	851.81	755.11	608.62
8.925	1013.17	967.86	916.16	851.50	754.39	605.47
8.900	1013.03	967.71	916.00	851.22	753.68	602.11
8.875	1012.93	967.54	915.83	850.92	752.97	598.69
8.850	1012.85	967.38	915.64	850.60	752.22	595.00
8.825	1012.76	967.30	915.43	850.29	751.52	591.27
8.800	1012.60	967.13	915.26	849.99	750.73	587.57
8.775	1012.52	966.97	915.04	849.67	749.97	583.53
8.750	1012.41	966.89	914.82	849.37	749.21	579.14
8.725	1012.27	966.72	914.62	849.03	748.50	574.52
8.700	1012.19	966.56	914.39	848.68	747.67	569.34
8.675	1012.05	966.46	914.29	848.37	746.89	563.57
8.650	1011.94	966.32	914.07	848.04	746.10	557.03
8.625	1011.86	966.15	913.87	847.69	745.32	549.94
8.600	1011.73	966.00	913.66	847.40	744.47	541.54
8.575	1011.62	965.91	913.46	847.10	743.65	531.73
8.550	1011.54	965.74	913.26	846.75	742.83	520.86
8.525	1011.44	965.60	913.06	846.37	741.99	507.21

8.500	1011.29	965.50	912.85	845.98	741.14	487.14
8.475	1011.21	965.34	912.59	845.64	740.29	451.83
8.450	1011.04	965.19	912.40	845.30	739.43	424.35
8.425	1010.96	965.04	912.24	844.93	738.51	412.87
8.400	1010.88	964.93	912.07	844.56	737.68	404.39
8.375	1010.74	964.76	911.83	844.16	736.81	394.80
8.350	1010.64	964.68	911.66	843.86	735.91	388.20
8.325	1010.56	964.52	911.44	843.46	735.01	383.07
8.300	1010.39	964.35	911.17	843.12	734.02	378.23
8.275	1010.31	964.23	910.96	842.74	733.11	370.04
8.250	1010.23	964.11	910.76	842.39	732.12	362.01
8.225	1010.06	963.95	910.56	841.97	731.15	354.66
8.200	1009.98	963.78	910.33	841.62	730.14	346.01
8.175	1009.86	963.70	910.09	841.23	729.10	338.22
8.150	1009.74	963.54	909.86	840.87	728.01	331.00
8.125	1009.66	963.38	909.70	840.47	726.93	324.52
8.100	1009.54	963.21	909.45	840.15	725.92	318.40
8.075	1009.41	963.13	909.27	839.71	724.91	312.91
8.050	1009.33	962.97	909.06	839.37	723.78	307.61
8.025	1009.16	962.80	908.88	838.99	722.66	302.83
8.000	1009.08	962.72	908.68	838.63	721.57	298.20
7.975	1009.00	962.56	908.39	838.26	720.37	293.95
7.950	1008.84	962.39	908.15	837.87	719.19	290.04
7.925	1008.76	962.23	908.06	837.51	717.99	286.28
7.900	1008.68	962.15	907.73	837.14	716.69	282.86
7.875	1008.51	961.98	907.57	836.75	715.24	279.50
7.850	1008.43	961.82	907.32	836.36	713.81	276.35
7.825	1008.35	961.66	907.08	835.97	713.07	273.67
7.800	1008.18	961.54	906.89	835.53	712.22	270.83
7.775	1008.10	961.41	906.67	835.15	711.25	267.52
7.750	1007.94	961.25	906.42	834.76	710.22	264.38
7.725	1007.86	961.08	906.26	834.35	709.19	261.37
7.700	1007.76	960.92	906.04	833.94	708.15	258.48
7.675	1007.61	960.84	905.80	833.55	707.01	255.59
7.650	1007.53	960.68	905.61	833.16	705.78	252.83
7.625	1007.38	960.51	905.36	832.79	704.53	250.35

7.600	1007.28	960.35	905.11	832.39	703.26	247.82
7.575	1007.20	960.18	904.94	832.01	701.96	245.41
7.550	1007.04	960.02	904.69	831.58	700.53	243.12
7.525	1006.96	959.94	904.46	831.18	698.94	240.83
7.500	1006.79	959.77	904.30	830.75	697.36	238.63
7.475	1006.71	959.61	904.05	830.36	695.78	236.47
7.450	1006.63	959.45	903.90	829.96	694.09	234.37
7.425	1006.47	959.28	903.64	829.57	692.32	232.26
7.400	1006.39	959.12	903.45	829.18	690.54	230.29
7.375	1006.29	959.00	903.16	828.75	688.48	228.37
7.350	1006.14	958.87	902.98	828.35	686.42	226.52
7.325	1006.06	958.71	902.74	827.94	684.25	224.60
7.300	1005.90	958.55	902.49	827.52	681.81	222.77
7.275	1005.81	958.38	902.25	827.05	678.77	220.98
7.250	1005.73	958.27	902.09	826.63	675.72	219.19
7.225	1005.57	958.14	901.84	826.24	672.39	217.51
7.200	1005.49	957.97	901.57	825.75	669.04	215.83
7.175	1005.38	957.81	901.36	825.40	666.10	214.10
7.150	1005.24	957.65	901.15	824.97		212.47
7.125	1005.16	957.48	900.92	824.56		210.75
7.100	1004.99	957.34	900.68	824.12		209.13
7.075	1004.91	957.15	900.45	823.68		207.48
7.050	1004.82	956.99	900.20	823.25		205.95
7.025	1004.67	956.91	899.99	822.78		204.45
7.000	1004.59	956.75	899.79	822.38		202.97
6.975	1004.42	956.58	899.77	821.88		201.55
6.950	1004.34	956.42	899.65	821.45		200.26
6.925	1004.25	956.25	899.50	821.00		198.62
6.900	1004.09	956.09	899.30	820.51		197.06
6.875	1004.01	955.96	899.09	820.02		195.52
6.850	1003.85	955.82	898.87	819.56		194.01
6.825	1003.77	955.67	898.60	819.09		192.53
6.800	1003.60	955.52	898.37	818.69		191.03
6.775	1003.52	955.35	898.06	818.19		189.56
6.750	1003.36	955.19	897.77	817.70		188.18
6.725	1003.28	955.03	897.56	817.24		186.70

6.700	1003.20	954.86	897.40	816.75	185.33
6.675	1003.03	954.70	897.02	816.32	183.90
6.650	1002.95	954.53	896.90	815.85	182.53
6.625	1002.79	954.37	896.62	815.37	181.21
6.600	1002.70	954.21	896.41	814.85	179.86
6.575	1002.54	954.04	896.11	814.36	178.57
6.550	1002.46	953.88	895.96	813.83	177.22
6.525	1002.29	953.73	895.62	813.39	175.95
6.500	1002.21	953.64	895.37	813.14	174.70
6.475	1002.05	953.47	895.17	812.89	173.46
6.450	1001.97	953.31	894.92	812.60	172.22
6.425	1001.82	953.14	894.67	812.31	170.92
6.400	1001.72	952.98	894.43	812.01	169.69
6.375	1001.64	952.82	894.18	811.72	168.49
6.350	1001.48	952.65	893.89	811.32	167.28
6.325	1001.39	952.49	893.63	810.89	166.14
6.300	1001.23	952.33	893.45	810.41	164.97
6.275	1001.15	952.24	893.14	809.96	163.83
6.250	1000.98	952.08	892.89	809.52	162.62
6.225	1000.90	951.86	892.62	809.03	161.48
6.200	1000.79	951.67	892.35	808.58	160.32
6.175	1000.66	951.59	892.08	808.10	159.08
6.150	1000.58	951.39	891.86	807.59	157.91
6.125	1000.41	951.26	891.52	807.11	156.80
6.100	1000.33	951.10	891.19	806.62	155.70
6.075	1000.17	950.93	890.95	806.14	154.72
6.050	1000.09	950.77	890.62	805.61	154.11
6.025	999.92	950.61	890.33	805.11	153.09
6.000	999.84	950.47	890.13	804.57	152.02
5.975	999.68	950.35	889.92	804.05	150.98
5.950	999.59	950.20	889.55	803.56	149.91
5.925	999.43	950.03	889.31	803.24	148.78
5.900	999.35	949.87	889.08	802.89	147.74
5.875	999.18	949.74	888.77	802.54	146.74
5.850	999.10	949.62	888.54	802.44	145.71
5.825	998.94	949.41	888.24	802.38	144.72

5.800	998.86	949.30	888.01	802.31	143.69
5.775	998.69	949.13	887.67	802.25	142.66
5.750	998.61	948.97	887.39	802.18	141.63
5.725	998.52	948.81	887.09	802.12	140.68
5.700	998.37	948.64	886.80	802.06	139.72
5.675	998.20	948.48	886.49	801.99	138.65
5.650	998.12	948.35	886.26	801.93	137.71
5.625	997.96	948.22	885.95	801.86	136.76
5.600	997.87	948.00	885.62	801.80	135.80
5.575	997.71	947.84	885.37	801.73	134.81
5.550	997.63	947.70	885.04	801.67	133.91
5.525	997.46	947.55	884.80	801.60	132.96
5.500	997.38	947.38	884.47	801.54	132.33
5.475	997.22	947.19	884.26	801.47	131.54
5.450	997.14	947.02	883.98	801.41	130.61
5.425	996.97	946.88	883.67		129.62
5.400	996.89	946.68	883.40		128.73
5.375	996.73	946.51	883.08		127.85
5.350	996.65	946.35	882.83		126.93
5.325	996.48	946.18	882.50		126.04
5.300	996.40	945.95	882.11		125.20
5.275	996.24	945.83	881.83		124.30
5.250	996.15	945.61	881.47		123.41
5.225	995.99	945.45	881.19		122.51
5.200	995.91	945.28	880.55		121.67
5.175	995.74	945.05	880.53		120.77
5.150	995.58	944.88	879.15		119.93
5.125	995.50	944.71	879.85		119.07
5.100	995.34	944.55	878.04		118.23
5.075	995.25	944.38	877.55		117.40
5.050	995.09	944.22	877.03		116.58
5.025	995.01	944.05	876.66		115.71
5.000	994.84	943.89	876.34		114.91
4.975	994.76	943.65	875.92		114.06
4.950	994.60	943.48	875.51		113.26
4.925	994.43	943.32	875.10		112.42

4.900	994.35	943.14	874.62	111.60
4.875	994.19	942.95	874.15	110.79
4.850	994.11	942.76	873.69	110.01
4.825	993.94	942.58	873.19	109.24
4.800	993.78	942.41	871.37	108.41
4.775	993.70	942.00	871.12	107.65
4.750	993.53	941.70	870.94	106.86
4.725	993.45	941.61	870.52	106.07
4.700	993.29	941.48		105.26
4.675	993.21	941.01		104.50
4.650	993.04	940.77		103.74
4.625	992.88	940.60		102.94
4.600	992.80	940.38		102.21
4.575	992.63	940.19		101.44
4.550	992.55	940.03		100.70
4.525	992.39	939.87		99.93
4.500	992.26	939.62		99.17
4.475	992.14	939.46		98.43
4.450	992.03	939.31		97.68
4.425	991.89	939.16		96.95
4.400	991.73	938.98		96.16
4.375	991.65	938.79		95.44
4.350	991.48	938.58		94.71
4.325	991.32	938.39		93.98
4.300	991.18	938.26		93.29
4.275	991.06	937.99		92.57
4.250	990.91	937.82		91.86
4.225	990.83	937.57		91.14
4.200	990.66	937.33		90.43
4.175	990.57	937.13		89.70
4.150	990.42	936.91		88.97
4.125	990.27	936.62		88.26
4.100	990.09	936.34		87.56
4.075	990.12	935.88		86.87
4.050	990.17	935.59		86.19
4.025	990.23	935.35		85.52

4.000	989.70	935.10	84.84
3.975	989.60	934.85	84.14
3.950	989.44	934.68	83.41
3.925	989.27	934.44	82.73
3.900	989.19	934.28	82.06
3.875	989.03	934.03	81.36
3.850	989.03	933.84	80.68
3.825	989.03	933.62	80.21
3.800	988.99	933.38	79.61
3.775	988.91	933.13	78.94
3.750	988.83	932.55	78.29
3.725	988.77	932.22	77.64
3.700	988.74	931.73	76.97
3.675	988.71	931.27	76.30
3.650	988.68	930.96	75.67
3.625	988.65	930.65	75.06
3.600	988.62	930.24	74.39
3.575	988.59	929.75	73.75
3.550	988.56		73.13
3.525	988.53		72.47
3.500	988.50		71.85
3.475	988.46		71.22
3.450	988.43		70.57
3.425	988.40		69.94
3.400	988.37		69.29
3.375	988.34		68.69
3.350	987.90		68.09
3.325	986.83		67.47
3.300	986.71		66.87
3.275	986.67		66.25
3.250	986.64		65.62
3.225	986.60		65.00
3.200	986.48		64.38
3.175	986.30		63.79
3.150	986.11		63.22
3.125	985.76		62.58

3.100	985.35	62.00
3.075	985.05	61.41
3.050	984.79	60.80
3.025	984.70	60.21
3.000	984.79	59.63
2.975	984.76	59.01
2.950	984.44	58.39
2.925	984.48	57.84
2.900	984.42	57.26
2.875	984.13	56.69
2.850	984.08	56.09
2.825	983.95	55.51
2.800	983.90	54.94
2.775		54.38
2.750		53.79
2.725		53.27
2.700		52.66
2.675		52.09
2.650		51.53
2.625		50.95
2.600		50.36
2.575		49.81
2.550		49.22
2.525		48.72
2.500		48.13
2.475		47.54
2.450		46.97
2.425		46.44
2.400		45.92
2.375		45.34
2.350		44.81
2.325		44.24
2.300		43.69
2.275		43.15
2.250		42.64
2.225		42.09

2.200	41.55
2.175	40.98
2.150	40.50
2.125	39.95
2.100	39.41
2.075	38.90
2.050	38.34
2.025	37.85
2.000	37.31
1.975	36.82
1.950	36.27
1.925	35.78
1.900	35.25
1.875	34.74
1.850	34.21
1.825	33.68
1.800	33.20
1.775	32.69
1.750	32.17
1.725	31.66
1.700	31.18
1.675	30.68
1.650	30.15
1.625	29.64
1.600	29.19
1.575	28.64
1.550	28.21
1.525	27.67
1.500	27.19
1.475	26.72
1.450	26.20
1.425	25.71
1.400	25.20
1.375	24.72
1.350	24.25
1.325	23.78

1.300	23.32
1.275	22.83
1.250	22.35
1.225	21.87
1.200	21.41
1.175	20.89
1.150	20.45
1.125	19.97
1.100	19.47
1.075	19.06
1.050	18.59
1.025	18.12
1.000	17.65
0.975	17.17
0.950	16.72
0.925	16.27
0.900	15.81
0.875	15.32
0.850	14.88
0.825	14.40
0.800	13.99
0.775	13.52
0.750	13.09
0.725	12.64
0.700	12.16
0.675	11.74
0.650	11.28
0.625	10.86
0.600	10.41
0.575	10.02
0.550	9.54
0.525	9.09
0.500	8.67
0.475	8.22
0.450	7.72
0.425	7.31

0.400	6.87
0.375	6.44
0.350	6.01
0.325	5.54
0.300	5.15
0.275	4.71
0.250	4.28
0.225	3.83
0.200	3.35
0.175	2.91
0.150	2.48
0.125	2.04
0.100	1.58

~~**Bubble pressures, p_b, and densities of the liquid phase at *VLE*, ρ_L.**~~

	~~T=263.15 K~~	~~T=273.15 K~~	~~T=283.15 K~~	~~T=293.15 K~~	~~T=304.21 K~~	~~T=313.15 K~~
~~p_b / MPa~~	~~2.797~~	~~3.569~~	~~4.711~~	~~5.431~~	~~7.178~~	~~supercritical~~
~~ρ_L / (kg·m^{-3})~~	~~983.90~~	~~929.58~~	~~869.99~~	~~801.36~~	~~666.10~~	

$u_T = 0.006$ K; $u_p = 0.0015$ MPa from 0.1 to 6 MPa; $u_p = 0.0175$ MPa from 6 to 20 MPa;

$u_\rho = 0.2 - 0.4$ kg·m^{-3}

Table S5. Calculated densities, isobaric specific heat capacities, volume-dependent solubility parameters and Joule-Thomson coefficients (ρ, c_p, δ_V, μ_{JT}) for the mixture CO_2 + CH_3OH with x_{CO_2} = 0.9700 in dense phase at pressures p and temperatures T.

p /MPa	ρ /(kg·m^{-3})	c_p (J·K^{-1}·kg^{-1})	δ_V /MPa$^{1/2}$	μ_{JT} (K·MPa^{-1})	ρ /(kg·m^{-3})	c_p (J·K^{-1}·kg^{-1})	δ_V /MPa$^{1/2}$	μ_{JT} /(K·MPa^{-1})
	T = 263.15 K				T = 273.15 K			
14.0	1032.99	2027.8	16.36	-0.0052	992.81	2093.2	15.50	0.0720
15.0	1036.56	2015.5	16.43	-0.0160	997.21	2073.9	15.59	0.0568
16.0	1040.02	2003.9	16.50	-0.0262	1001.45	2056.2	15.68	0.0427
17.0	1043.39	1993.0	16.57	-0.0356	1005.54	2039.7	15.77	0.0296
18.0	1046.65	1982.6	16.63	-0.0445	1009.49	2024.4	15.84	0.0171
19.0	1049.84	1972.8	16.70	-0.0530	1013.31	2010.2	15.92	0.0055
20.0	1052.93	1963.5	16.76	-0.0610	1017.01	1996.8	16.00	-0.0054
21.0	1055.96	1954.6	16.81	-0.0686	1020.60	1984.3	16.07	-0.0156
22.0	1058.91	1946.2	16.87	-0.0757	1024.09	1972.6	16.14	-0.0254
23.0	1061.79	1938.2	16.92	-0.0826	1027.48	1961.6	16.20	-0.0347
24.0	1064.60	1930.5	16.98	-0.0891	1030.78	1951.2	16.27	-0.0433
25.0	1067.36	1923.2	17.02	-0.0954	1034.00	1941.3	16.33	-0.0517
26.0	1070.06	1916.2	17.08	-0.1013	1037.14	1932.0	16.39	-0.0596
27.0	1072.70	1909.5	17.12	-0.1070	1040.20	1923.2	16.45	-0.0670
28.0	1075.29	1903.1	17.17	-0.1124	1043.19	1914.8	16.51	-0.0743
29.0	1077.83	1897.0	17.21	-0.1176	1046.12	1906.9	16.56	-0.0812
30.0	1080.32	1891.2	17.26	-0.1226	1048.98	1899.3	16.61	-0.0877
31.0	1082.77	1885.5	17.30	-0.1274	1051.77	1892.1	16.67	-0.0939
32.0	1085.17	1880.1	17.34	-0.1320	1054.52	1885.3	16.72	-0.0999
33.0	1087.54	1875.0	17.38	-0.1364	1057.20	1878.7	16.76	-0.1058
34.0	1089.86	1870.0	17.43	-0.1406	1059.84	1872.5	16.81	-0.1112
35.0	1092.14	1865.2	17.47	-0.1447	1062.42	1866.5	16.86	-0.1165
36.0	1094.39	1860.6	17.50	-0.1486	1064.96	1860.8	16.90	-0.1216
37.0	1096.60	1856.2	17.54	-0.1524	1067.45	1855.3	16.95	-0.1265
38.0	1098.78	1852.0	17.58	-0.1561	1069.89	1850.0	16.99	-0.1312
39.0	1100.92	1847.9	17.61	-0.1596	1072.30	1845.0	17.03	-0.1357
40.0	1103.04	1843.9	17.65	-0.1632	1074.66	1840.2	17.07	-0.1401
41.0	1105.12	1840.1	17.68	-0.1664	1076.99	1835.5	17.11	-0.1443
42.0	1107.17	1836.5	17.72	-0.1696	1079.27	1831.1	17.15	-0.1484
43.0	1109.20	1832.9	17.75	-0.1727	1081.52	1826.8	17.19	-0.1524

44.0	1111.19	1829.5	17.78	-0.1757	1083.74	1822.7	17.22	-0.1561
45.0	1113.16	1826.3	17.81	-0.1785	1085.92	1818.7	17.26	-0.1597
46.0	1115.11	1823.1	17.84	-0.1814	1088.08	1814.9	17.30	-0.1634
47.0	1117.03	1820.0	17.87	-0.1841	1090.20	1811.2	17.33	-0.1667
48.0	1118.92	1817.1	17.90	-0.1866	1092.29	1807.7	17.37	-0.1700
49.0	1120.80	1814.3	17.93	-0.1892	1094.35	1804.3	17.40	-0.1732
50.0	1122.65	1811.5	17.96	-0.1917	1096.38	1801.0	17.43	-0.1764
51.0	1124.47	1808.9	17.99	-0.1941	1098.39	1797.8	17.46	-0.1794
52.0	1126.28	1806.3	18.02	-0.1964	1100.37	1794.8	17.50	-0.1823
53.0	1128.06	1803.8	18.05	-0.1985	1102.32	1791.8	17.53	-0.1850
54.0	1129.83	1801.4	18.07	-0.2008	1104.25	1789.0	17.56	-0.1878
55.0	1131.57	1799.1	18.10	-0.2028	1106.15	1786.2	17.59	-0.1905
56.0	1133.30	1796.9	18.13	-0.2050	1108.04	1783.6	17.62	-0.1931
57.0	1135.01	1794.7	18.15	-0.2070	1109.90	1781.0	17.65	-0.1955
58.0	1136.70	1792.7	18.18	-0.2088	1111.73	1778.5	17.68	-0.1980
59.0	1138.37	1790.6	18.21	-0.2107	1113.55	1776.2	17.70	-0.2004
60.0	1140.02	1788.7	18.23	-0.2126	1115.34	1773.8	17.73	-0.2027
61.0	1141.66	1786.8	18.25	-0.2144	1117.12	1771.6	17.76	-0.2048
62.0	1143.28	1785.0	18.28	-0.2161	1118.87	1769.5	17.79	-0.2069
63.0	1144.89	1783.3	18.30	-0.2177	1120.61	1767.4	17.81	-0.2091
64.0	1146.48	1781.6	18.33	-0.2194	1122.33	1765.4	17.83	-0.2112
65.0	1148.05	1780.0	18.35	-0.2210	1124.03	1763.5	17.86	-0.2132
66.0	1149.61	1778.4	18.37	-0.2226	1125.71	1761.6	17.89	-0.2150
67.0	1151.16	1776.9	18.40	-0.2240	1127.37	1759.8	17.91	-0.2170
68.0	1152.69	1775.4	18.41	-0.2256	1129.02	1758.0	17.93	-0.2188
69.0	1154.21	1774.0	18.44	-0.2270	1130.65	1756.3	17.96	-0.2205
70.0	1155.71	1772.6	18.46	-0.2283	1132.27	1754.7	17.98	-0.2223
71.0	1157.20	1771.3	18.48	-0.2297	1133.86	1753.1	18.01	-0.2240
72.0	1158.68	1770.0	18.50	-0.2310	1135.45	1751.6	18.03	-0.2256
73.0	1160.15	1768.8	18.53	-0.2323	1137.02	1750.2	18.05	-0.2272
74.0	1161.60	1767.6	18.54	-0.2335	1138.57	1748.7	18.08	-0.2287
75.0	1163.04	1766.5	18.57	-0.2347	1140.11	1747.4	18.10	-0.2302
76.0	1164.47	1765.4	18.58	-0.2359	1141.64	1746.1	18.12	-0.2317
77.0	1165.89	1764.4	18.61	-0.2371	1143.15	1744.8	18.14	-0.2332
78.0	1167.29	1763.4	18.63	-0.2382	1144.65	1743.6	18.16	-0.2346
79.0	1168.69	1762.4	18.65	-0.2392	1146.14	1742.4	18.18	-0.2359

80.0	1170.07	1761.5	18.67	-0.2403	1147.61	1741.2	18.20	-0.2373
81.0	1171.44	1760.6	18.69	-0.2413	1149.07	1740.1	18.23	-0.2385
82.0	1172.81	1759.7	18.71	-0.2423	1150.52	1739.1	18.24	-0.2399
83.0	1174.16	1758.9	18.73	-0.2433	1151.96	1738.1	18.26	-0.2411
84.0	1175.50	1758.1	18.74	-0.2442	1153.38	1737.1	18.28	-0.2423
85.0	1176.83	1757.3	18.76	-0.2452	1154.79	1736.2	18.30	-0.2435
86.0	1178.16	1756.6	18.78	-0.2461	1156.20	1735.2	18.33	-0.2445
87.0	1179.47	1755.9	18.80	-0.2470	1157.59	1734.4	18.34	-0.2457
88.0	1180.77	1755.3	18.82	-0.2479	1158.97	1733.5	18.36	-0.2468
89.0	1182.07	1754.6	18.83	-0.2487	1160.34	1732.7	18.38	-0.2478
90.0	1183.35	1754.0	18.85	-0.2495	1161.69	1732.0	18.40	-0.2488
91.0	1184.63	1753.5	18.87	-0.2503	1163.04	1731.2	18.41	-0.2499
92.0	1185.90	1752.9	18.89	-0.2510	1164.38	1730.5	18.44	-0.2508
93.0	1187.16	1752.4	18.90	-0.2519	1165.71	1729.9	18.45	-0.2518
94.0	1188.41	1751.9	18.92	-0.2526	1167.03	1729.2	18.47	-0.2527
95.0	1189.65	1751.5	18.94	-0.2532	1168.34	1728.6	18.49	-0.2536
96.0	1190.88	1751.0	18.96	-0.2539	1169.64	1728.0	18.51	-0.2545
97.0	1192.11	1750.6	18.97	-0.2546	1170.93	1727.5	18.52	-0.2554
98.0	1193.33	1750.2	18.99	-0.2553	1172.21	1726.9	18.54	-0.2562
99.0	1194.54	1749.9	19.00	-0.2559	1173.49	1726.4	18.56	-0.2570
100.0	1195.74	1749.6	19.02	-0.2565	1174.75	1726.0	18.57	-0.2578
101.0	1196.94	1749.2	19.04	-0.2572	1176.01	1725.5	18.59	-0.2586
102.0	1198.13	1749.0	19.06	-0.2577	1177.25	1725.1	18.61	-0.2593
103.0	1199.31	1748.7	19.07	-0.2584	1178.49	1724.7	18.62	-0.2600
104.0	1200.48	1748.4	19.08	-0.2589	1179.72	1724.3	18.64	-0.2608
105.0	1201.65	1748.2	19.10	-0.2594	1180.95	1724.0	18.65	-0.2615
106.0	1202.81	1748.0	19.11	-0.2600	1182.16	1723.6	18.67	-0.2622
107.0	1203.97	1747.9	19.13	-0.2605	1183.37	1723.3	18.69	-0.2628
108.0	1205.11	1747.7	19.14	-0.2610	1184.57	1723.0	18.70	-0.2635
109.0	1206.25	1747.6	19.16	-0.2614	1185.76	1722.8	18.72	-0.2641
110.0	1207.39	1747.4	19.18	-0.2619	1186.95	1722.5	18.73	-0.2648
111.0	1208.51	1747.3	19.20	-0.2623	1188.12	1722.3	18.75	-0.2654
112.0	1209.64	1747.3	19.21	-0.2628	1189.29	1722.1	18.76	-0.2659
113.0	1210.75	1747.2	19.22	-0.2632	1190.46	1721.9	18.78	-0.2665
114.0	1211.86	1747.2	19.24	-0.2636	1191.61	1721.8	18.79	-0.2671
115.0	1212.96	1747.1	19.25	-0.2641	1192.76	1721.6	18.81	-0.2676

116.0	1214.06	1747.1	19.26	-0.2645	1193.91	1721.5	18.83	-0.2681
117.0	1215.15	1747.1	19.28	-0.2649	1195.04	1721.4	18.84	-0.2686
118.0	1216.24	1747.2	19.29	-0.2653	1196.17	1721.3	18.85	-0.2692
119.0	1217.32	1747.2	19.31	-0.2655	1197.30	1721.2	18.87	-0.2696
120.0	1218.39	1747.3	19.33	-0.2659	1198.41	1721.2	18.89	-0.2700
121.0	1219.46	1747.4	19.34	-0.2663	1199.52	1721.2	18.89	-0.2706
122.0	1220.52	1747.4	19.35	-0.2667	1200.63	1721.2	18.91	-0.2710
123.0	1221.58	1747.6	19.37	-0.2669	1201.73	1721.2	18.93	-0.2714
124.0	1222.63	1747.7	19.38	-0.2673	1202.82	1721.2	18.94	-0.2718
125.0	1223.68	1747.8	19.40	-0.2675	1203.91	1721.2	18.95	-0.2722
126.0	1224.72	1748.0	19.41	-0.2677	1204.99	1721.3	18.97	-0.2726
127.0	1225.76	1748.1	19.42	-0.2681	1206.06	1721.3	18.98	-0.2730
128.0	1226.79	1748.3	19.44	-0.2683	1207.13	1721.4	18.99	-0.2734
129.0	1227.82	1748.5	19.45	-0.2686	1208.20	1721.5	19.01	-0.2737
130.0	1228.84	1748.7	19.47	-0.2688	1209.25	1721.6	19.02	-0.2741
131.0	1229.86	1749.0	19.48	-0.2690	1210.31	1721.7	19.03	-0.2745
132.0	1230.87	1749.2	19.50	-0.2693	1211.36	1721.9	19.05	-0.2747
133.0	1231.88	1749.5	19.51	-0.2695	1212.40	1722.0	19.06	-0.2751
134.0	1232.88	1749.7	19.52	-0.2697	1213.44	1722.2	19.07	-0.2754
135.0	1233.88	1750.0	19.53	-0.2700	1214.47	1722.4	19.09	-0.2757
136.0	1234.87	1750.3	19.54	-0.2702	1215.49	1722.6	19.10	-0.2760
137.0	1235.86	1750.6	19.55	-0.2704	1216.52	1722.8	19.11	-0.2763
138.0	1236.85	1750.9	19.57	-0.2705	1217.53	1723.0	19.12	-0.2766
139.0	1237.83	2027.8	19.58	-0.2707	1218.55	1723.3	19.14	-0.2768
140.0	1238.81	2015.5	19.60	-0.2708	1219.55	1723.5	19.15	-0.2771
141.0	1239.78	2003.9	19.61	-0.2710	1220.56	1723.8	19.17	-0.2773
142.0	1240.75	1993.0	19.63	-0.2711	1221.55	1724.1	19.18	-0.2775
143.0	1241.71	1982.6	19.64	-0.2713	1222.55	1724.4	19.19	-0.2778
144.0	1242.67	1972.8	19.65	-0.2714	1223.54	1724.7	19.20	-0.2780
145.0	1243.63	1963.5	19.66	-0.2717	1224.52	1725.0	19.22	-0.2782
146.0	1244.58	1954.6	19.67	-0.2717	1225.50	1725.3	19.23	-0.2784
147.0	1245.53	1946.2	19.69	-0.2718	1226.48	1725.6	19.24	-0.2786
148.0	1246.47	1938.2	19.70	-0.2719	1227.45	1726.0	19.25	-0.2787
149.0	1247.41	1930.5	19.72	-0.2720	1228.41	1726.3	19.26	-0.2790
150.0	1248.35	1923.2	19.73	-0.2721	1229.38	1726.7	19.28	-0.2791
151.0	1249.28	1916.2	19.74	-0.2722	1230.33	1727.1	19.29	-0.2793

152.0	1250.21	1909.5	19.76	-0.2723	1231.29	1727.5	19.30	-0.2794
153.0	1251.13	1903.1	19.77	-0.2724	1232.24	1727.9	19.31	-0.2797
154.0	1252.05	1897.0	19.78	-0.2724	1233.18	1728.3	19.33	-0.2798
155.0	1252.97	1891.2	19.79	-0.2725	1234.13	1728.7	19.34	-0.2799
156.0	1253.89	1885.5	19.80	-0.2726	1235.06	1729.2	19.35	-0.2800
157.0	1254.80	1880.1	19.81	-0.2727	1236.00	1729.6	19.36	-0.2802
158.0	1255.71	1875.0	19.82	-0.2727	1236.93	1730.1	19.37	-0.2803
159.0	1256.61	1870.0	19.84	-0.2727	1237.85	1730.5	19.38	-0.2804
160.0	1257.51	1865.2	19.85	-0.2728	1238.78	1731.0	19.40	-0.2805
161.0	1258.41	1860.6	19.86	-0.2729	1239.70	1731.5	19.41	-0.2806
162.0	1259.30	1856.2	19.88	-0.2728	1240.61	1732.0	19.42	-0.2807
163.0	1260.19	1852.0	19.89	-0.2729	1241.52	1732.5	19.43	-0.2808
164.0	1261.08	1847.9	19.89	-0.2730	1242.43	1733.0	19.44	-0.2809
165.0	1261.96	1843.9	19.91	-0.2729	1243.33	1733.5	19.45	-0.2810
166.0	1262.84	1840.1	19.93	-0.2729	1244.23	1734.0	19.47	-0.2809
167.0	1263.72	1836.5	19.93	-0.2729	1245.13	1734.6	19.48	-0.2810
168.0	1264.60	1832.9	19.95	-0.2729	1246.03	1735.1	19.49	-0.2811
169.0	1265.47	1829.5	19.96	-0.2730	1246.92	1735.7	19.50	-0.2812
170.0	1266.34	1826.3	19.97	-0.2729	1247.80	1736.3	19.52	-0.2811
171.0	1267.20	1823.1	19.99	-0.2729	1248.69	1736.8	19.53	-0.2812
172.0	1268.06	1820.0	19.99	-0.2729	1249.57	1737.4	19.53	-0.2813
173.0	1268.92	1817.1	20.01	-0.2729	1250.44	1738.0	19.55	-0.2813
174.0	1269.78	1814.3	20.02	-0.2728	1251.32	1738.6	19.56	-0.2814
175.0	1270.63	1811.5	20.03	-0.2728	1252.19	1739.2	19.58	-0.2813
176.0	1271.49	1808.9	20.05	-0.2727	1253.05	1739.8	19.58	-0.2814
177.0	1272.33	1806.3	20.05	-0.2728	1253.92	1740.5	19.60	-0.2814
178.0	1273.18	1803.8	20.06	-0.2727	1254.78	1741.1	19.60	-0.2814
179.0	1274.02	1801.4	20.08	-0.2727	1255.64	1741.7	19.62	-0.2814
180.0	1274.86	1799.1	20.09	-0.2726	1256.49	1742.4	19.63	-0.2813
181.0	1275.70	1796.9	20.10	-0.2726	1257.34	1743.1	19.64	-0.2814
182.0	1276.53	1794.7	20.11	-0.2725	1258.19	1743.7	19.65	-0.2814
183.0	1277.36	1792.7	20.12	-0.2724	1259.04	1744.4	19.67	-0.2813
184.0	1278.19	1790.6	20.13	-0.2724	1259.88	1745.1	19.67	-0.2814
185.0	1279.02	1788.7	20.14	-0.2723	1260.72	1745.8	19.68	-0.2813
186.0	1279.84	1786.8	20.16	-0.2721	1261.56	1746.5	19.70	-0.2813
187.0	1280.66	1785.0	20.17	-0.2721	1262.39	1747.2	19.71	-0.2812

188.0	1281.48	1783.3	20.18	-0.2720	1263.23	1747.9	19.72	-0.2812
189.0	1282.30	1781.6	20.19	-0.2720	1264.05	1748.6	19.73	-0.2811
190.0	1283.11	1780.0	20.20	-0.2719	1264.88	1749.3	19.74	-0.2811
191.0	1283.92	1778.4	20.22	-0.2717	1265.70	1750.0	19.76	-0.2810
192.0	1284.73	1776.9	20.23	-0.2717	1266.52	1750.8	19.77	-0.2810
193.0	1285.54	1775.4	20.24	-0.2716	1267.34	1751.5	19.78	-0.2809
194.0	1286.34	1774.0	20.25	-0.2716	1268.16	1752.3	19.79	-0.2809
195.0	1287.14	1772.6	20.27	-0.2714	1268.97	1753.0	19.80	-0.2808
		T= 283.15 K				T= 293.15 K		
14.0	948.92	2170.7	14.61	0.1845	899.79	2286.3	13.73	0.3413
15.0	954.53	2141.6	14.73	0.1615	907.12	2242.6	13.87	0.3060
16.0	959.87	2115.2	14.84	0.1403	914.00	2203.6	14.01	0.2740
17.0	964.97	2091.1	14.95	0.1207	920.50	2168.5	14.13	0.2448
18.0	969.86	2069.0	15.05	0.1026	926.66	2136.9	14.25	0.2180
19.0	974.55	2048.7	15.14	0.0858	932.51	2108.1	14.36	0.1935
20.0	979.06	2030.0	15.23	0.0701	938.10	2081.9	14.47	0.1708
21.0	983.40	2012.7	15.32	0.0554	943.43	2057.9	14.57	0.1498
22.0	987.60	1996.6	15.40	0.0417	948.54	2035.9	14.67	0.1302
23.0	991.65	1981.6	15.48	0.0289	953.45	2015.6	14.76	0.1121
24.0	995.58	1967.6	15.56	0.0167	958.17	1996.8	14.85	0.0951
25.0	999.38	1954.5	15.63	0.0051	962.72	1979.3	14.93	0.0792
26.0	1003.08	1942.2	15.70	-0.0056	967.11	1963.1	15.01	0.0642
27.0	1006.67	1930.6	15.77	-0.0160	971.36	1948.0	15.09	0.0502
28.0	1010.16	1919.7	15.83	-0.0257	975.47	1933.8	15.17	0.0370
29.0	1013.55	1909.4	15.90	-0.0349	979.45	1920.5	15.24	0.0244
30.0	1016.87	1899.7	15.96	-0.0436	983.31	1908.1	15.31	0.0126
31.0	1020.10	1890.6	16.02	-0.0521	987.07	1896.4	15.38	0.0014
32.0	1023.25	1881.9	16.08	-0.0599	990.72	1885.3	15.44	-0.0093
33.0	1026.33	1873.6	16.13	-0.0677	994.27	1874.9	15.50	-0.0194
34.0	1029.34	1865.7	16.19	-0.0749	997.73	1865.1	15.57	-0.0289
35.0	1032.29	1858.3	16.24	-0.0819	1001.10	1855.7	15.63	-0.0381
36.0	1035.17	1851.2	16.29	-0.0885	1004.39	1846.9	15.68	-0.0468
37.0	1037.99	1844.4	16.34	-0.0949	1007.61	1838.5	15.74	-0.0551
38.0	1040.76	1837.9	16.39	-0.1011	1010.75	1830.5	15.79	-0.0631
39.0	1043.47	1831.7	16.44	-0.1069	1013.82	1822.9	15.85	-0.0706
40.0	1046.13	1825.8	16.48	-0.1125	1016.83	1815.7	15.90	-0.0780

41.0	1048.74	1820.1	16.53	-0.1180	1019.77	1808.8	15.95	-0.0849
42.0	1051.30	1814.7	16.57	-0.1231	1022.65	1802.2	16.00	-0.0917
43.0	1053.82	1809.5	16.61	-0.1282	1025.48	1795.9	16.05	-0.0979
44.0	1056.29	1804.6	16.66	-0.1330	1028.25	1789.9	16.09	-0.1042
45.0	1058.73	1799.8	16.70	-0.1377	1030.97	1784.1	16.14	-0.1102
46.0	1061.12	1795.2	16.74	-0.1422	1033.63	1778.6	16.18	-0.1158
47.0	1063.47	1790.8	16.78	-0.1466	1036.25	1773.3	16.23	-0.1213
48.0	1065.79	1786.5	16.81	-0.1507	1038.82	1768.2	16.27	-0.1266
49.0	1068.07	1782.5	16.85	-0.1548	1041.35	1763.3	16.31	-0.1317
50.0	1070.31	1778.5	16.89	-0.1588	1043.84	1758.7	16.35	-0.1366
51.0	1072.52	1774.8	16.92	-0.1625	1046.28	1754.2	16.39	-0.1414
52.0	1074.70	1771.1	16.96	-0.1663	1048.69	1749.8	16.43	-0.1459
53.0	1076.85	1767.6	16.99	-0.1697	1051.05	1745.7	16.47	-0.1504
54.0	1078.97	1764.2	17.02	-0.1732	1053.38	1741.6	16.50	-0.1547
55.0	1081.06	1761.0	17.06	-0.1765	1055.68	1737.8	16.54	-0.1589
56.0	1083.12	1757.8	17.09	-0.1798	1057.94	1734.1	16.57	-0.1629
57.0	1085.15	1754.8	17.12	-0.1829	1060.16	1730.5	16.61	-0.1667
58.0	1087.16	1751.9	17.15	-0.1859	1062.36	1727.0	16.64	-0.1705
59.0	1089.14	1749.1	17.19	-0.1889	1064.52	1723.7	16.68	-0.1742
60.0	1091.09	1746.3	17.22	-0.1917	1066.66	1720.4	16.71	-0.1777
61.0	1093.02	1743.7	17.25	-0.1944	1068.76	1717.3	16.74	-0.1810
62.0	1094.93	1741.2	17.27	-0.1972	1070.84	1714.3	16.78	-0.1843
63.0	1096.82	1738.7	17.30	-0.1998	1072.89	1711.4	16.80	-0.1876
64.0	1098.68	1736.3	17.33	-0.2023	1074.91	1708.6	16.83	-0.1908
65.0	1100.52	1734.0	17.36	-0.2049	1076.91	1705.9	16.87	-0.1938
66.0	1102.34	1731.8	17.39	-0.2072	1078.88	1703.3	16.89	-0.1967
67.0	1104.14	1729.7	17.41	-0.2096	1080.83	1700.7	16.92	-0.1995
68.0	1105.92	1727.6	17.44	-0.2117	1082.76	1698.3	16.95	-0.2023
69.0	1107.68	1725.6	17.46	-0.2140	1084.66	1695.9	16.98	-0.2051
70.0	1109.42	1723.6	17.49	-0.2161	1086.54	1693.6	17.01	-0.2078
71.0	1111.14	1721.8	17.51	-0.2183	1088.39	1691.4	17.03	-0.2102
72.0	1112.85	1720.0	17.54	-0.2202	1090.23	1689.2	17.06	-0.2127
73.0	1114.53	1718.2	17.57	-0.2222	1092.05	1687.1	17.09	-0.2152
74.0	1116.20	1716.5	17.59	-0.2241	1093.84	1685.1	17.11	-0.2176
75.0	1117.86	1714.9	17.61	-0.2261	1095.62	1683.1	17.14	-0.2199
76.0	1119.49	1713.3	17.63	-0.2279	1097.38	1681.2	17.16	-0.2220

77.0	1121.11	1711.8	17.66	-0.2297	1099.12	1679.4	17.19	-0.2243
78.0	1122.72	1710.3	17.68	-0.2315	1100.84	1677.6	17.21	-0.2264
79.0	1124.31	1708.9	17.70	-0.2331	1102.54	1675.9	17.23	-0.2285
80.0	1125.88	1707.5	17.72	-0.2347	1104.23	1674.2	17.26	-0.2304
81.0	1127.44	1706.1	17.75	-0.2364	1105.89	1672.6	17.28	-0.2324
82.0	1128.99	1704.9	17.76	-0.2380	1107.55	1671.1	17.31	-0.2343
83.0	1130.52	1703.6	17.79	-0.2394	1109.18	1669.5	17.33	-0.2362
84.0	1132.04	1702.4	17.81	-0.2409	1110.80	1668.1	17.35	-0.2380
85.0	1133.54	1701.2	17.83	-0.2424	1112.41	1666.7	17.37	-0.2399
86.0	1135.04	1700.1	17.85	-0.2438	1114.00	1665.3	17.39	-0.2415
87.0	1136.51	1699.0	17.87	-0.2451	1115.57	1663.9	17.41	-0.2432
88.0	1137.98	1698.0	17.89	-0.2466	1117.14	1662.7	17.43	-0.2448
89.0	1139.44	1697.0	17.91	-0.2479	1118.68	1661.4	17.45	-0.2466
90.0	1140.88	1696.0	17.93	-0.2492	1120.22	1660.2	17.47	-0.2481
91.0	1142.31	1695.1	17.95	-0.2503	1121.74	1659.0	17.50	-0.2496
92.0	1143.73	1694.2	17.97	-0.2516	1123.24	1657.9	17.51	-0.2511
93.0	1145.13	1693.3	17.99	-0.2527	1124.74	1656.8	17.53	-0.2525
94.0	1146.53	1692.5	18.00	-0.2540	1126.22	1655.8	17.55	-0.2539
95.0	1147.92	1691.7	18.02	-0.2551	1127.68	1654.7	17.57	-0.2553
96.0	1149.29	1690.9	18.04	-0.2562	1129.14	1653.8	17.59	-0.2567
97.0	1150.66	1690.2	18.06	-0.2572	1130.58	1652.8	17.60	-0.2581
98.0	1152.01	1689.5	18.07	-0.2583	1132.02	1651.9	17.63	-0.2593
99.0	1153.35	1688.8	18.09	-0.2593	1133.44	1651.0	17.64	-0.2607
100.0	1154.69	1688.2	18.11	-0.2604	1134.85	1650.1	17.66	-0.2619
101.0	1156.01	1687.5	18.12	-0.2614	1136.25	1649.3	17.68	-0.2631
102.0	1157.33	1687.0	18.14	-0.2623	1137.63	1648.5	17.70	-0.2642
103.0	1158.63	1686.4	18.16	-0.2633	1139.01	1647.8	17.71	-0.2654
104.0	1159.93	1685.8	18.18	-0.2641	1140.38	1647.0	17.73	-0.2666
105.0	1161.21	1685.3	18.19	-0.2650	1141.73	1646.3	17.74	-0.2677
106.0	1162.49	1684.8	18.21	-0.2658	1143.08	1645.6	17.76	-0.2687
107.0	1163.76	1684.4	18.22	-0.2667	1144.42	1645.0	17.78	-0.2697
108.0	1165.02	1683.9	18.24	-0.2676	1145.74	1644.3	17.80	-0.2708
109.0	1166.27	1683.5	18.26	-0.2683	1147.06	1643.7	17.81	-0.2718
110.0	1167.52	1683.1	18.27	-0.2691	1148.37	1643.1	17.82	-0.2728
111.0	1168.75	1682.8	18.29	-0.2699	1149.66	1642.6	17.84	-0.2737
112.0	1169.98	1682.4	18.30	-0.2707	1150.95	1642.1	17.85	-0.2747

113.0	1171.20	1682.1	18.32	-0.2713	1152.23	1641.6	17.87	-0.2756
114.0	1172.41	1681.8	18.33	-0.2721	1153.51	1641.1	17.89	-0.2765
115.0	1173.61	1681.5	18.35	-0.2727	1154.77	1640.6	17.90	-0.2773
116.0	1174.81	1681.2	18.36	-0.2735	1156.02	1640.2	17.92	-0.2782
117.0	1176.00	1681.0	18.38	-0.2741	1157.27	1639.7	17.93	-0.2790
118.0	1177.18	1680.7	18.39	-0.2747	1158.50	1639.3	17.95	-0.2799
119.0	1178.35	1680.5	18.41	-0.2754	1159.73	1639.0	17.96	-0.2807
120.0	1179.52	1680.4	18.42	-0.2760	1160.96	1638.6	17.98	-0.2814
121.0	1180.68	1680.2	18.43	-0.2766	1162.17	1638.3	17.98	-0.2823
122.0	1181.83	1680.0	18.45	-0.2772	1163.37	1638.0	18.00	-0.2829
123.0	1182.98	1679.9	18.46	-0.2778	1164.57	1637.7	18.02	-0.2836
124.0	1184.12	1679.8	18.48	-0.2783	1165.76	1637.4	18.03	-0.2843
125.0	1185.25	1679.7	18.49	-0.2789	1166.95	1637.1	18.04	-0.2851
126.0	1186.38	1679.6	18.50	-0.2793	1168.12	1636.9	18.05	-0.2858
127.0	1187.50	1679.6	18.51	-0.2799	1169.29	1636.7	18.07	-0.2863
128.0	1188.61	1679.5	18.53	-0.2804	1170.45	1636.5	18.08	-0.2870
129.0	1189.72	1679.5	18.55	-0.2808	1171.61	1636.3	18.10	-0.2877
130.0	1190.82	1679.5	18.56	-0.2813	1172.76	1636.1	18.11	-0.2883
131.0	1191.91	1679.5	18.57	-0.2817	1173.90	1636.0	18.12	-0.2888
132.0	1193.00	1679.5	18.59	-0.2822	1175.03	1635.8	18.13	-0.2895
133.0	1194.08	1679.5	18.60	-0.2826	1176.16	1635.7	18.15	-0.2900
134.0	1195.16	1679.6	18.61	-0.2831	1177.28	1635.6	18.16	-0.2907
135.0	1196.23	1679.6	18.62	-0.2835	1178.39	1635.5	18.17	-0.2912
136.0	1197.30	1679.7	18.63	-0.2839	1179.50	1635.5	18.18	-0.2917
137.0	1198.36	1679.8	18.65	-0.2842	1180.61	1635.4	18.20	-0.2922
138.0	1199.41	1679.9	18.66	-0.2847	1181.70	1635.4	18.21	-0.2926
139.0	1200.46	1680.0	18.67	-0.2851	1182.79	1635.3	18.22	-0.2932
140.0	1201.51	1680.2	18.68	-0.2854	1183.88	1635.3	18.23	-0.2936
141.0	1202.55	1680.3	18.70	-0.2857	1184.95	1635.3	18.24	-0.2941
142.0	1203.58	1680.5	18.71	-0.2861	1186.03	1635.3	18.25	-0.2946
143.0	1204.61	1680.7	18.72	-0.2864	1187.09	1635.4	18.26	-0.2951
144.0	1205.63	1680.9	18.74	-0.2867	1188.16	1635.4	18.28	-0.2954
145.0	1206.65	1681.1	18.74	-0.2871	1189.21	1635.5	18.29	-0.2959
146.0	1207.66	1681.3	18.75	-0.2874	1190.26	1635.6	18.31	-0.2962
147.0	1208.67	1681.5	18.77	-0.2877	1191.31	1635.6	18.31	-0.2967
148.0	1209.67	1681.7	18.78	-0.2879	1192.34	1635.7	18.33	-0.2970

149.0	1210.67	1682.0	18.79	-0.2882	1193.38	1635.9	18.33	-0.2975
150.0	1211.66	1682.2	18.80	-0.2885	1194.41	1636.0	18.35	-0.2978
151.0	1212.65	1682.5	18.81	-0.2888	1195.43	1636.1	18.36	-0.2982
152.0	1213.64	1682.8	18.83	-0.2889	1196.45	1636.3	18.37	-0.2985
153.0	1214.62	1683.1	18.84	-0.2892	1197.46	1636.4	18.37	-0.2989
154.0	1215.59	1683.4	18.85	-0.2894	1198.47	1636.6	18.39	-0.2992
155.0	1216.56	1683.7	18.87	-0.2896	1199.48	1636.8	18.40	-0.2996
156.0	1217.53	1684.1	18.87	-0.2898	1200.47	1637.0	18.41	-0.2999
157.0	1218.49	1684.4	18.88	-0.2901	1201.47	1637.2	18.42	-0.3002
158.0	1219.45	1684.8	18.90	-0.2902	1202.46	1637.4	18.43	-0.3005
159.0	1220.41	1685.1	18.91	-0.2905	1203.44	1637.7	18.45	-0.3006
160.0	1221.35	1685.5	18.92	-0.2906	1204.42	1637.9	18.45	-0.3010
161.0	1222.30	1685.9	18.94	-0.2907	1205.40	1638.2	18.46	-0.3012
162.0	1223.24	1686.3	18.94	-0.2910	1206.37	1638.5	18.47	-0.3015
163.0	1224.18	1686.7	18.95	-0.2911	1207.33	1638.7	18.49	-0.3017
164.0	1225.11	1687.1	18.97	-0.2912	1208.30	1639.0	18.49	-0.3020
165.0	1226.04	1687.5	18.97	-0.2915	1209.25	1639.3	18.50	-0.3023
166.0	1226.97	1688.0	18.98	-0.2916	1210.21	1639.6	18.51	-0.3025
167.0	1227.89	1688.4	19.00	-0.2917	1211.16	1640.0	18.52	-0.3027
168.0	1228.81	1688.9	19.01	-0.2918	1212.10	1640.3	18.53	-0.3029
169.0	1229.72	1689.3	19.02	-0.2919	1213.04	1640.6	18.55	-0.3030
170.0	1230.63	1689.8	19.03	-0.2920	1213.98	1641.0	18.55	-0.3033
171.0	1231.54	1690.3	19.04	-0.2921	1214.91	1641.4	18.56	-0.3035
172.0	1232.44	1690.8	19.05	-0.2922	1215.84	1641.7	18.58	-0.3036
173.0	1233.34	1691.3	19.06	-0.2923	1216.76	1642.1	18.58	-0.3039
174.0	1234.23	1691.8	19.07	-0.2925	1217.68	1642.5	18.59	-0.3040
175.0	1235.12	1692.3	19.08	-0.2926	1218.60	1642.9	18.60	-0.3042
176.0	1236.01	1692.8	19.10	-0.2925	1219.51	1643.3	18.61	-0.3043
177.0	1236.90	1693.4	19.11	-0.2926	1220.42	1643.7	18.62	-0.3044
178.0	1237.78	1693.9	19.11	-0.2927	1221.33	1644.2	18.63	-0.3046
179.0	1238.66	1694.5	19.12	-0.2928	1222.23	1644.6	18.64	-0.3047
180.0	1239.53	1695.1	19.14	-0.2928	1223.13	1645.1	18.65	-0.3048
181.0	1240.40	1695.6	19.15	-0.2929	1224.02	1645.5	18.66	-0.3050
182.0	1241.27	1696.2	19.15	-0.2930	1224.91	1646.0	18.67	-0.3051
183.0	1242.14	1696.8	19.17	-0.2930	1225.80	1646.5	18.68	-0.3052
184.0	1243.00	1697.4	19.17	-0.2931	1226.68	1646.9	18.68	-0.3053

185.0	1243.86	1698.0	19.19	-0.2930	1227.56	1647.4	18.69	-0.3055
186.0	1244.71	1698.6	19.19	-0.2931	1228.44	1647.9	18.71	-0.3054
187.0	1245.56	1699.2	19.21	-0.2931	1229.31	1648.4	18.72	-0.3056
188.0	1246.41	1699.8	19.22	-0.2930	1230.18	1649.0	18.72	-0.3057
189.0	1247.26	1700.5	19.23	-0.2931	1231.05	1649.5	18.73	-0.3058
190.0	1248.10	1701.1	19.24	-0.2931	1231.91	1650.0	18.74	-0.3058
191.0	1248.94	1701.8	19.25	-0.2932	1232.77	1650.6	18.75	-0.3059
192.0	1249.78	1702.4	19.26	-0.2931	1233.62	1651.1	18.77	-0.3059
193.0	1250.61	1703.1	19.27	-0.2931	1234.48	1651.7	18.77	-0.3060
194.0	1251.44	1703.8	19.29	-0.2930	1235.33	1652.2	18.78	-0.3060
195.0	1252.27	1704.5	19.29	-0.2931	1236.17	1652.8	18.79	-0.3061
		T= 304.21 K				T= 313.15 K		
14.0	837.55	2489.5	12.76	0.5766	779.81	2734.6	11.96	0.8260
15.0	847.58	2419.9	12.92	0.5216	792.90	2630.5	12.15	0.7493
16.0	856.87	2359.1	13.08	0.4725	804.87	2541.4	12.32	0.6809
17.0	865.52	2305.5	13.23	0.4281	815.90	2464.2	12.48	0.6195
18.0	873.61	2257.8	13.37	0.3877	826.12	2396.9	12.64	0.5644
19.0	881.21	2215.3	13.50	0.3509	835.62	2337.6	12.78	0.5142
20.0	888.39	2177.1	13.62	0.3174	844.51	2285.0	12.92	0.4688
21.0	895.17	2142.5	13.74	0.2866	852.84	2238.0	13.06	0.4272
22.0	901.62	2111.2	13.85	0.2581	860.70	2195.9	13.18	0.3891
23.0	907.76	2082.6	13.96	0.2318	868.12	2157.9	13.30	0.3540
24.0	913.61	2056.4	14.06	0.2074	875.16	2123.4	13.42	0.3218
25.0	919.21	2032.4	14.16	0.1848	881.84	2092.1	13.52	0.2919
26.0	924.58	2010.2	14.25	0.1636	888.22	2063.4	13.63	0.2643
27.0	929.74	1989.7	14.35	0.1440	894.30	2037.1	13.73	0.2385
28.0	934.70	1970.7	14.43	0.1255	900.13	2012.9	13.83	0.2146
29.0	939.49	1953.1	14.52	0.1082	905.71	1990.5	13.92	0.1921
30.0	944.10	1936.6	14.59	0.0918	911.08	1969.8	14.01	0.1711
31.0	948.56	1921.2	14.67	0.0766	916.25	1950.6	14.10	0.1515
32.0	952.88	1906.8	14.75	0.0621	921.22	1932.6	14.18	0.1331
33.0	957.07	1893.3	14.82	0.0485	926.03	1915.9	14.26	0.1157
34.0	961.13	1880.6	14.89	0.0355	930.67	1900.3	14.34	0.0993
35.0	965.07	1868.6	14.96	0.0232	935.16	1885.6	14.41	0.0838
36.0	968.90	1857.4	15.02	0.0116	939.52	1871.9	14.49	0.0692
37.0	972.63	1846.7	15.09	0.0005	943.74	1858.9	14.56	0.0555

38.0	976.26	1836.6	15.15	-0.0100	947.84	1846.7	14.63	0.0422
39.0	979.80	1827.1	15.21	-0.0199	951.82	1835.2	14.69	0.0297
40.0	983.25	1818.0	15.27	-0.0295	955.70	1824.3	14.76	0.0179
41.0	986.62	1809.4	15.32	-0.0387	959.47	1814.0	14.82	0.0066
42.0	989.91	1801.2	15.38	-0.0475	963.15	1804.2	14.88	-0.0040
43.0	993.13	1793.4	15.43	-0.0557	966.73	1794.9	14.94	-0.0143
44.0	996.27	1785.9	15.49	-0.0636	970.23	1786.1	15.00	-0.0241
45.0	999.35	1778.8	15.54	-0.0714	973.65	1777.7	15.05	-0.0335
46.0	1002.37	1772.0	15.59	-0.0786	976.98	1769.7	15.11	-0.0424
47.0	1005.32	1765.6	15.64	-0.0857	980.25	1762.0	15.16	-0.0510
48.0	1008.21	1759.3	15.69	-0.0925	983.44	1754.7	15.22	-0.0592
49.0	1011.05	1753.4	15.73	-0.0990	986.57	1747.7	15.27	-0.0671
50.0	1013.84	1747.7	15.78	-0.1053	989.63	1741.0	15.31	-0.0748
51.0	1016.57	1742.2	15.82	-0.1113	992.63	1734.6	15.37	-0.0819
52.0	1019.26	1737.0	15.86	-0.1170	995.57	1728.5	15.41	-0.0891
53.0	1021.89	1731.9	15.90	-0.1228	998.45	1722.6	15.46	-0.0957
54.0	1024.49	1727.1	15.95	-0.1281	1001.28	1716.9	15.50	-0.1023
55.0	1027.03	1722.4	15.99	-0.1333	1004.06	1711.5	15.55	-0.1085
56.0	1029.54	1717.9	16.03	-0.1383	1006.79	1706.2	15.59	-0.1144
57.0	1032.01	1713.5	16.06	-0.1433	1009.47	1701.2	15.63	-0.1202
58.0	1034.43	1709.4	16.10	-0.1480	1012.11	1696.3	15.67	-0.1259
59.0	1036.82	1705.3	16.14	-0.1525	1014.70	1691.7	15.71	-0.1312
60.0	1039.17	1701.5	16.18	-0.1569	1017.25	1687.1	15.75	-0.1366
61.0	1041.49	1697.7	16.21	-0.1612	1019.76	1682.8	15.79	-0.1415
62.0	1043.77	1694.1	16.25	-0.1654	1022.22	1678.6	15.83	-0.1464
63.0	1046.02	1690.6	16.28	-0.1693	1024.65	1674.5	15.87	-0.1512
64.0	1048.24	1687.2	16.31	-0.1732	1027.05	1670.6	15.90	-0.1557
65.0	1050.43	1683.9	16.35	-0.1770	1029.40	1666.8	15.94	-0.1603
66.0	1052.58	1680.8	16.38	-0.1806	1031.73	1663.2	15.97	-0.1645
67.0	1054.71	1677.7	16.41	-0.1842	1034.01	1659.6	16.01	-0.1687
68.0	1056.81	1674.7	16.44	-0.1876	1036.27	1656.2	16.04	-0.1729
69.0	1058.89	1671.9	16.47	-0.1909	1038.50	1652.8	16.08	-0.1767
70.0	1060.93	1669.1	16.50	-0.1942	1040.69	1649.6	16.11	-0.1805
71.0	1062.95	1666.4	16.53	-0.1974	1042.86	1646.5	16.14	-0.1843
72.0	1064.95	1663.8	16.56	-0.2004	1044.99	1643.4	16.17	-0.1879
73.0	1066.92	1661.3	16.59	-0.2034	1047.10	1640.5	16.20	-0.1913

74.0	1068.87	1658.8	16.62	-0.2063	1049.19	1637.6	16.23	-0.1947
75.0	1070.79	1656.4	16.65	-0.2091	1051.24	1634.9	16.26	-0.1981
76.0	1072.69	1654.1	16.67	-0.2119	1053.27	1632.2	16.29	-0.2013
77.0	1074.57	1651.9	16.70	-0.2146	1055.28	1629.6	16.31	-0.2046
78.0	1076.43	1649.7	16.72	-0.2173	1057.26	1627.0	16.34	-0.2076
79.0	1078.27	1647.6	16.75	-0.2197	1059.22	1624.6	16.37	-0.2104
80.0	1080.09	1645.6	16.77	-0.2222	1061.15	1622.2	16.40	-0.2135
81.0	1081.89	1643.6	16.80	-0.2247	1063.07	1619.8	16.42	-0.2163
82.0	1083.67	1641.7	16.82	-0.2269	1064.96	1617.6	16.45	-0.2189
83.0	1085.43	1639.8	16.85	-0.2292	1066.83	1615.4	16.47	-0.2218
84.0	1087.17	1638.0	16.87	-0.2315	1068.68	1613.2	16.50	-0.2244
85.0	1088.90	1636.2	16.89	-0.2338	1070.51	1611.1	16.52	-0.2268
86.0	1090.60	1634.5	16.91	-0.2359	1072.32	1609.1	16.55	-0.2293
87.0	1092.29	1632.8	16.94	-0.2380	1074.11	1607.1	16.57	-0.2317
88.0	1093.97	1631.2	16.96	-0.2399	1075.88	1605.2	16.59	-0.2342
89.0	1095.62	1629.7	16.98	-0.2420	1077.64	1603.4	16.62	-0.2364
90.0	1097.26	1628.1	17.00	-0.2439	1079.38	1601.5	16.64	-0.2388
91.0	1098.89	1626.7	17.02	-0.2458	1081.09	1599.8	16.66	-0.2409
92.0	1100.50	1625.2	17.05	-0.2475	1082.80	1598.0	16.68	-0.2431
93.0	1102.10	1623.8	17.06	-0.2494	1084.48	1596.4	16.71	-0.2452
94.0	1103.68	1622.5	17.09	-0.2511	1086.15	1594.7	16.73	-0.2472
95.0	1105.24	1621.2	17.11	-0.2528	1087.80	1593.1	16.75	-0.2493
96.0	1106.80	1619.9	17.12	-0.2545	1089.44	1591.6	16.77	-0.2513
97.0	1108.34	1618.7	17.14	-0.2562	1091.07	1590.1	16.79	-0.2531
98.0	1109.86	1617.4	17.16	-0.2578	1092.67	1588.6	16.80	-0.2552
99.0	1111.37	1616.3	17.18	-0.2593	1094.27	1587.2	16.82	-0.2570
100.0	1112.87	1615.1	17.20	-0.2608	1095.85	1585.8	16.85	-0.2587
101.0	1114.36	1614.1	17.22	-0.2624	1097.41	1584.4	16.86	-0.2605
102.0	1115.83	1613.0	17.23	-0.2639	1098.96	1583.1	16.88	-0.2621
103.0	1117.30	1612.0	17.26	-0.2652	1100.50	1581.8	16.90	-0.2640
104.0	1118.75	1610.9	17.27	-0.2667	1102.02	1580.6	16.92	-0.2656
105.0	1120.19	1610.0	17.29	-0.2681	1103.53	1579.3	16.94	-0.2671
106.0	1121.61	1609.0	17.30	-0.2694	1105.03	1578.1	16.95	-0.2687
107.0	1123.03	1608.1	17.32	-0.2707	1106.52	1577.0	16.97	-0.2703
108.0	1124.43	1607.2	17.34	-0.2719	1107.99	1575.9	16.99	-0.2718
109.0	1125.83	1606.4	17.35	-0.2732	1109.46	1574.8	17.01	-0.2732

110.0	1127.21	1605.6	17.37	-0.2744	1110.91	1573.7	17.02	-0.2747
111.0	1128.58	1604.7	17.38	-0.2757	1112.35	1572.7	17.04	-0.2761
112.0	1129.95	1604.0	17.40	-0.2768	1113.77	1571.7	17.05	-0.2775
113.0	1131.30	1603.2	17.42	-0.2780	1115.19	1570.7	17.06	-0.2790
114.0	1132.64	1602.5	17.43	-0.2791	1116.60	1569.7	17.08	-0.2802
115.0	1133.97	1601.8	17.45	-0.2802	1117.99	1568.8	17.10	-0.2815
116.0	1135.30	1601.1	17.47	-0.2812	1119.37	1567.9	17.11	-0.2829
117.0	1136.61	1600.5	17.48	-0.2823	1120.75	1567.0	17.13	-0.2841
118.0	1137.91	1599.8	17.49	-0.2833	1122.11	1566.2	17.14	-0.2853
119.0	1139.21	1599.2	17.50	-0.2844	1123.47	1565.3	17.15	-0.2866
120.0	1140.50	1598.6	17.52	-0.2854	1124.81	1564.5	17.17	-0.2876
121.0	1141.77	1598.1	17.53	-0.2863	1126.14	1563.8	17.18	-0.2888
122.0	1143.04	1597.5	17.55	-0.2872	1127.47	1563.0	17.20	-0.2899
123.0	1144.30	1597.0	17.56	-0.2882	1128.78	1562.3	17.21	-0.2911
124.0	1145.55	1596.5	17.57	-0.2891	1130.09	1561.6	17.22	-0.2921
125.0	1146.80	1596.0	17.59	-0.2899	1131.39	1560.9	17.24	-0.2932
126.0	1148.03	1595.6	17.60	-0.2908	1132.67	1560.2	17.25	-0.2942
127.0	1149.26	1595.1	17.62	-0.2916	1133.95	1559.5	17.26	-0.2953
128.0	1150.48	1594.7	17.62	-0.2925	1135.22	1558.9	17.28	-0.2963
129.0	1151.69	1594.3	17.64	-0.2933	1136.49	1558.3	17.29	-0.2973
130.0	1152.89	1593.9	17.65	-0.2940	1137.74	1557.7	17.30	-0.2981
131.0	1154.09	1593.6	17.66	-0.2950	1138.98	1557.2	17.31	-0.2992
132.0	1155.28	1593.2	17.67	-0.2957	1140.22	1556.6	17.32	-0.3002
133.0	1156.46	1592.9	17.68	-0.2965	1141.45	1556.1	17.34	-0.3010
134.0	1157.63	1592.6	17.70	-0.2970	1142.67	1555.6	17.35	-0.3018
135.0	1158.80	1592.3	17.71	-0.2978	1143.89	1555.1	17.36	-0.3027
136.0	1159.96	1592.0	17.72	-0.2985	1145.09	1554.6	17.37	-0.3037
137.0	1161.11	1591.8	17.73	-0.2993	1146.29	1554.2	17.38	-0.3045
138.0	1162.26	1591.5	17.75	-0.2998	1147.48	1553.7	17.39	-0.3053
139.0	1163.40	1591.3	17.75	-0.3006	1148.66	1553.3	17.41	-0.3060
140.0	1164.53	1591.1	17.77	-0.3011	1149.84	1552.9	17.42	-0.3068
141.0	1165.66	1590.9	17.78	-0.3017	1151.01	1552.5	17.42	-0.3076
142.0	1166.78	1590.7	17.79	-0.3024	1152.17	1552.1	17.43	-0.3084
143.0	1167.89	1590.6	17.80	-0.3030	1153.33	1551.8	17.45	-0.3091
144.0	1169.00	1590.4	17.81	-0.3036	1154.48	1551.4	17.45	-0.3099
145.0	1170.10	1590.3	17.82	-0.3041	1155.62	1551.1	17.47	-0.3105

146.0	1171.19	1590.2	17.84	-0.3047	1156.75	1550.8	17.47	-0.3113
147.0	1172.28	1590.1	17.85	-0.3052	1157.88	1550.5	17.48	-0.3119
148.0	1173.36	1590.0	17.85	-0.3058	1159.00	1550.3	17.50	-0.3126
149.0	1174.44	1589.9	17.86	-0.3063	1160.12	1550.0	17.51	-0.3132
150.0	1175.51	1589.8	17.87	-0.3069	1161.23	1549.7	17.52	-0.3138
151.0	1176.58	1589.8	17.89	-0.3072	1162.33	1549.5	17.53	-0.3144
152.0	1177.64	1589.7	17.89	-0.3078	1163.43	1549.3	17.54	-0.3150
153.0	1178.69	1589.7	17.91	-0.3082	1164.52	1549.1	17.54	-0.3156
154.0	1179.74	1589.7	17.91	-0.3087	1165.61	1548.9	17.55	-0.3163
155.0	1180.78	1589.7	17.93	-0.3091	1166.69	1548.7	17.56	-0.3169
156.0	1181.82	1589.7	17.93	-0.3096	1167.76	1548.6	17.57	-0.3175
157.0	1182.85	1589.8	17.95	-0.3100	1168.83	1548.4	17.57	-0.3181
158.0	1183.88	1589.8	17.95	-0.3105	1169.89	1548.3	17.59	-0.3185
159.0	1184.90	1589.9	17.96	-0.3109	1170.95	1548.2	17.59	-0.3191
160.0	1185.92	1589.9	17.97	-0.3113	1172.00	1548.1	17.60	-0.3195
161.0	1186.93	1590.0	17.98	-0.3116	1173.04	1548.0	17.61	-0.3201
162.0	1187.94	1590.1	17.99	-0.3120	1174.08	1547.9	17.62	-0.3206
163.0	1188.94	1590.2	18.00	-0.3123	1175.12	1547.8	17.62	-0.3212
164.0	1189.94	1590.3	18.01	-0.3127	1176.15	1547.8	17.63	-0.3216
165.0	1190.93	1590.5	18.02	-0.3130	1177.17	1547.7	17.64	-0.3220
166.0	1191.92	1590.6	18.03	-0.3134	1178.19	1547.7	17.65	-0.3224
167.0	1192.90	1590.7	18.04	-0.3138	1179.20	1547.7	17.66	-0.3228
168.0	1193.88	1590.9	18.04	-0.3141	1180.21	1547.7	17.66	-0.3234
169.0	1194.85	1591.1	18.05	-0.3145	1181.22	1547.7	17.67	-0.3238
170.0	1195.82	1591.3	18.07	-0.3146	1182.22	1547.7	17.68	-0.3242
171.0	1196.78	1591.5	18.07	-0.3150	1183.21	1547.7	17.68	-0.3246
172.0	1197.74	1591.7	18.08	-0.3153	1184.20	1547.8	17.69	-0.3250
173.0	1198.70	1591.9	18.09	-0.3155	1185.18	1547.8	17.70	-0.3254
174.0	1199.65	1592.1	18.09	-0.3159	1186.17	1547.9	17.71	-0.3256
175.0	1200.60	1592.3	18.11	-0.3161	1187.14	1547.9	17.72	-0.3261
176.0	1201.54	1592.6	18.11	-0.3164	1188.11	1548.0	17.72	-0.3265
177.0	1202.48	1592.8	18.12	-0.3166	1189.08	1548.1	17.73	-0.3269
178.0	1203.41	1593.1	18.12	-0.3169	1190.04	1548.2	17.74	-0.3271
179.0	1204.34	1593.4	18.14	-0.3171	1191.00	1548.3	17.74	-0.3275
180.0	1205.27	1593.7	18.15	-0.3173	1191.95	1548.5	17.75	-0.3278
181.0	1206.19	1594.0	18.15	-0.3176	1192.90	1548.6	17.76	-0.3281

182.0	1207.11	1594.3	18.16	-0.3178	1193.84	1548.8	17.76	-0.3284
183.0	1208.03	1594.6	18.17	-0.3179	1194.78	1548.9	17.77	-0.3287
184.0	1208.94	1594.9	18.18	-0.3181	1195.72	1549.1	17.77	-0.3291
185.0	1209.84	1595.2	18.19	-0.3183	1196.65	1549.3	17.78	-0.3293
186.0	1210.75	1595.6	18.19	-0.3186	1197.58	1549.4	17.79	-0.3295
187.0	1211.64	1595.9	18.19	-0.3188	1198.50	1549.6	17.79	-0.3299
188.0	1212.54	1596.3	18.20	-0.3189	1199.42	1549.9	17.80	-0.3301
189.0	1213.43	1596.7	18.21	-0.3191	1200.34	1550.1	17.81	-0.3303
190.0	1214.32	1597.1	18.22	-0.3192	1201.25	1550.3	17.81	-0.3306
191.0	1215.20	1597.4	18.22	-0.3194	1202.16	1550.5	17.82	-0.3309
192.0	1216.09	1597.8	18.23	-0.3196	1203.07	1550.8	17.83	-0.3310
193.0	1216.96	1598.3	18.25	-0.3196	1203.97	1551.0	17.83	-0.3313
194.0	1217.84	1598.7	18.25	-0.3197	1204.86	1551.3	17.84	-0.3315
195.0	1218.71	1599.1	18.26	-0.3199	1205.76	1551.6	17.85	-0.3316

Table S6. Comparison between the experimental results for several thermodynamic properties of the system CO_2 + CH_3OH with x_{CO_2}= 0.9700 and the values calculated using the PC-SAFT and GERG EoSs. Properties: speed of sound, c, at pressures up to p = 194.49 MPa; density, ρ, up to p = 20.00 MPa~~; bubble pressure, p_b; and density of the liquid phase at *VLE*, ρ_L.~~

$MRD_x(\%)$	EoS	T / K						
		263.15	273.15	283.15	293.15	304.21	313.15	$\overline{MRD_x}(\%)$
$MRD_c(\%)$	PC-SAFT	3.08	2.91	2.85	2.70	2.53	2.51	2.77
	GERG	3.62	3.44	2.74	2.37	2.05	1.73	2.65
$MRD_\rho(\%)$	PC-SAFT	2.23	2.75	3.51	4.13	5.18	5.95	3.81
	GERG	0.10	0.15	0.23	0.58	0.83	1.56	0.52
~~$MRD_{p_b}(\%)$~~	~~PC-SAFT~~	~~1.62~~	~~0.27~~	~~3.98~~	~~4.15~~	~~1.14~~	~~---~~	~~2.23~~
	~~GERG~~	~~8.88~~	~~6.38~~	~~8.84~~	~~0.13~~	~~4.14~~	~~---~~	~~5.67~~
~~$MRD_{\rho_L}(\%)$~~	~~PC-SAFT~~	~~3.76~~	~~4.36~~	~~5.61~~	~~7.99~~	~~8.46~~	~~---~~	~~6.04~~
	~~GERG~~	~~0.11~~	~~0.65~~	~~0.98~~	~~0.86~~	~~4.25~~	~~---~~	~~1.37~~

$MRD_x(\%) = \frac{10^2}{N}\sum_{i=1}^{N}\left|\frac{x_{i,\mathrm{EoS}}-x_{i,\mathrm{exp}}}{x_{i,\mathrm{exp}}}\right|$; $\overline{MRD_x}(\%) = \frac{1}{N_T}\sum_{i=1}^{N_T} MRD_{x,i}(\%)$

$x_{i,\mathrm{exp}}$: experimental values; $x_{i,\mathrm{EoS}}$: calculated values using the PC-SAFT or GERG EoS; N: number of points; N_T: number of temperatures.

Table S7. Comparison between experimental results obtained in this work for the speed of sound, c, in CO_2 + CH_3OH mixtures with several compositions at pressures up to 194.49 MPa and the values calculated using the PC-SAFT and GERG EoSs.

$MRD_c(\%)$	EoS	T/ K			
		263.15	298.15	323.15	$\overline{MRD_c}(\%)$
x_{CO_2} =0.7534	PC-SAFT	1.95	2.54	2.98	2.49
	GERG	13.3	15.3	13.7	14.1
x_{CO_2} =0.8502	PC-SAFT	1.48	3.30	4.20	2.99
	GERG	10.2	10.7	9.77	10.2
x_{CO_2} =0.9250	PC-SAFT	2.26	1.67	1.49	1.83
	GERG	5.50	5.60	4.56	5.25
x_{CO_2} =0.9803	PC-SAFT	3.23	2.82	2.34	2.80
	GERG	3.00	1.75	1.47	2.07

$MRD_c(\%) = \frac{10^2}{N}\sum_{i=1}^{N}\left|\frac{c_{i,\mathrm{EoS}}-c_{i,\mathrm{exp}}}{c_{i,\mathrm{exp}}}\right|$; $\overline{MRD_c}(\%) = \frac{1}{N_T}\sum_{i=1}^{N_T} MRD_{c,i}(\%)$

$c_{i,\mathrm{exp}}$: experimental values; $c_{i,\mathrm{EoS}}$: values calculated using the PC-SAFT or GERG EoS; N: number of points; N_T: number of temperatures.

Table S9. Comparison between values for several properties calculated in this work and those obtained using the PC-SAFT and GERG EoSs for the CO_2 + CH_3OH mixture with $x_{CO_2} = 0.9700$ in the pressure range p= 14.0-195.0 MPa at temperatures T. Properties: density, ρ; isobaric specific heat capacity, c_p; volume-dependent solubility parameter, δ_V; and Joule-Thomson coefficient, μ_{JT}.

$MRD_x(\%)$ or $AAD_{\mu_{JT}}$	EoS	T/ K						$\overline{MRD_c}(\%)$ or $\overline{AAD_{\mu_{JT}}}$
		263.15	273.15	283.15	293.15	304.21	313.15	
$MRD_\rho(\%)$	PC-SAFT	1.70	1.82	1.88	1.94	2.02	2.03	1.90
	GERG	0.50	0.43	0.43	0.45	0.46	0.52	0.46
$MRD_{C_p}(\%)$	PC-SAFT	16.3	14.5	11.7	8.86	6.22	4.11	10.3
	GERG	3.41	2.69	1.69	1.44	2.12	3.44	2.47
$MRD_{\delta_V}(\%)$	PC-SAFT	2.10	2.54	3.10	3.62	4.04	4.31	3.28
	GERG	1.23	1.17	1.29	1.63	2.02	2.26	1.60
$AAD_{\mu_{JT}}$ (K/MPa)	PC-SAFT	0.074	0.065	0.056	0.050	0.047	0.046	0.056
	GERG	0.019	0.013	0.009	0.008	0.011	0.018	0.013

$$MRD_x(\%) = \frac{10^2}{N}\sum_{i=1}^{N}\left|\frac{x_{i,\mathrm{cal}} - x_{i,\mathrm{EoS}}}{x_{i,\mathrm{EoS}}}\right|; \quad AAD_{\mu_{JT}} = \frac{1}{N}\sum_{i=1}^{N}\left|\left(\mu_{JT}\right)_{i,\mathrm{cal}} - \left(\mu_{JT}\right)_{i,\mathrm{EoS}}\right|$$

$$\overline{MRD_c}(\%) = \frac{1}{N_T}\sum_{i=1}^{N_T} MRD_{c,i}(\%); \quad \overline{AAD_{\mu_{JT}}} = \frac{1}{N_T}\sum_{i=1}^{N_T} AAD_{\mu_{JT},i}$$

$x_{i,\mathrm{cal}}$: calculated values; $x_{i,\mathrm{EoS}}$: values obtained using the PC-SAFT or GERG EoS; N: number of points; N_T: number of temperatures.

Figure S1. Relative deviation between the experimentally determined speeds of sound and the values calculated using different EoSs for CO_2 + CH_3OH with x_{CO_2}= 0.9700. Solid line PC-SAFT EoS; Dot line, GERG EoS. ● , T=263.15 K; ● , T=273.15 K; ● , T=283.15 K; ● , T=293.15 K; ● , T=304.21 K; ● , T=313.15 K.

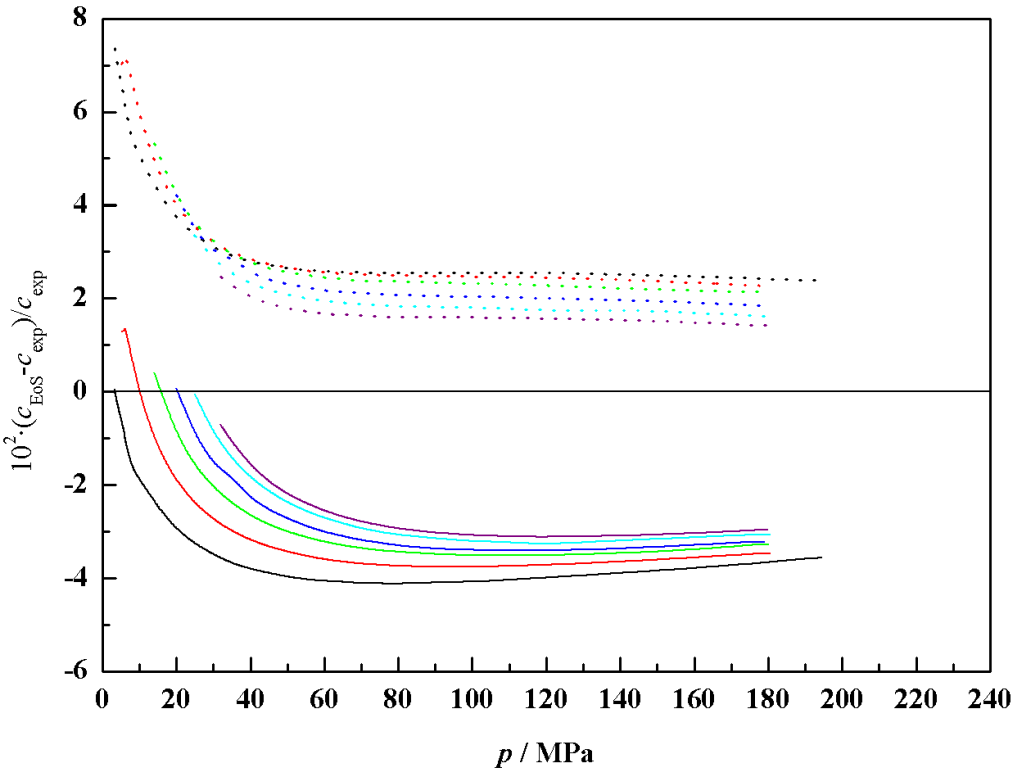

Figure S2. Relative deviation between the experimentally determined densities and the values calculated using different EoSs for CO_2 + CH_3OH with x_{CO_2}= 0.9700. Solid line PC-SAFT EoS; Dot line, GERG EoS. ● , T=263.15 K; ● , T=273.15 K; ● , T=283.15 K; ● , T=293.15 K; ● , T=304.21 K; ● , T=313.15 K.

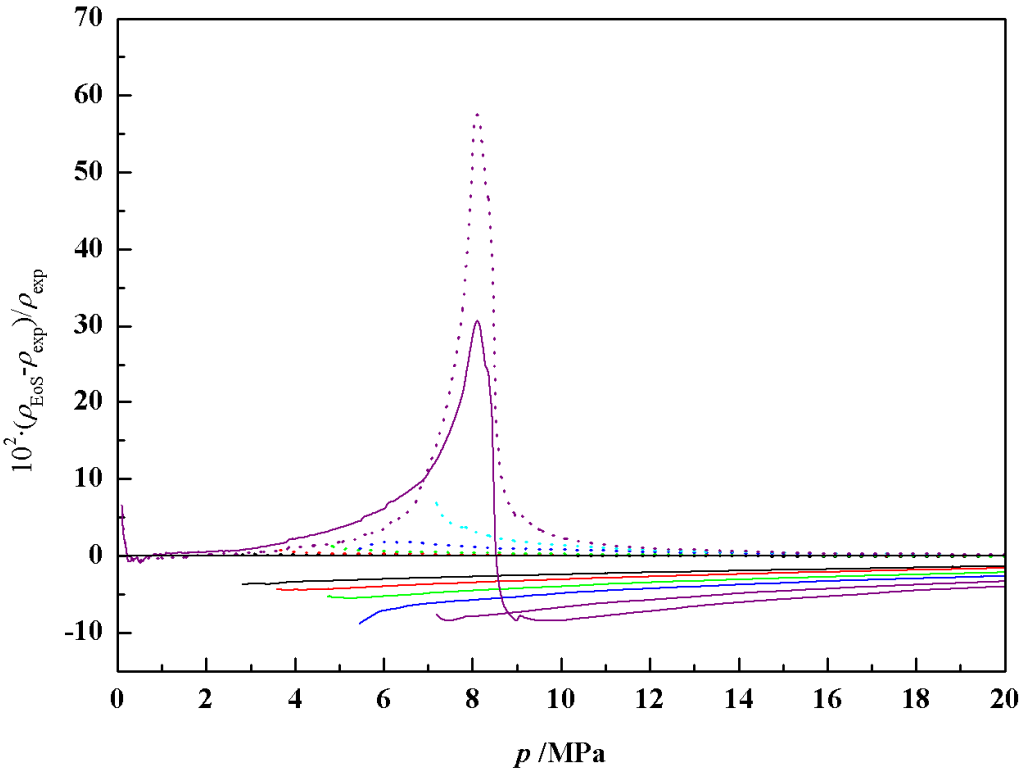

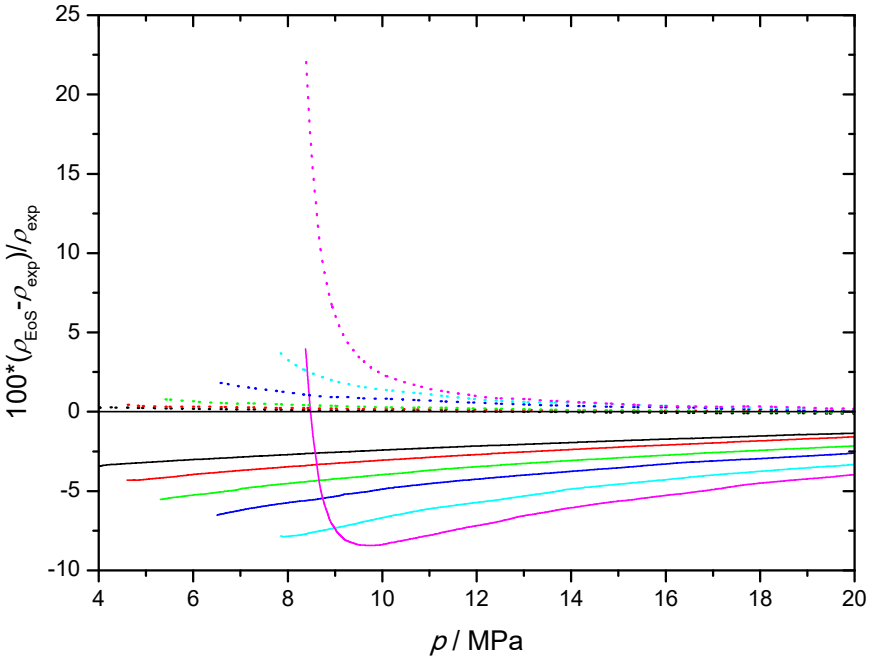

Figure S3. Relative deviation between the calculated densities and the values obtained using different EoSs for CO_2 + CH_3OH with x_{CO_2}= 0.9700. Solid line PC-SAFT EoS; Dot line, GERG EoS. ● , T=263.15 K; ● , T=273.15 K; ● , T=283.15 K; ● , T=293.15 K; ● , T=304.21 K; ● , T=313.15 K.

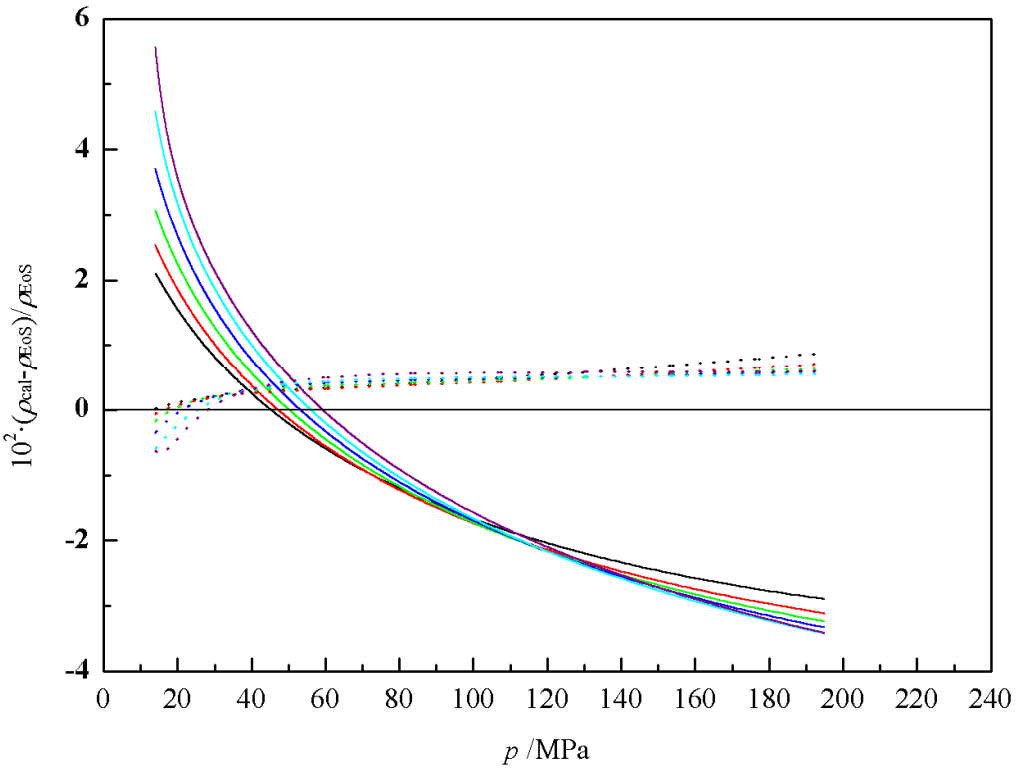

Figure S4. Relative deviation between the calculated isobaric specific heat capacities and the values obtained using different EoSs for CO_2 + CH_3OH with x_{CO_2}= 0.9700. Solid line PC-SAFT EoS; Dot line, GERG EoS. ● , T=263.15 K; ● , T=273.15 K; ● , T=283.15 K; ● , T=293.15 K; ● , T=304.21 K; ● , T=313.15 K.

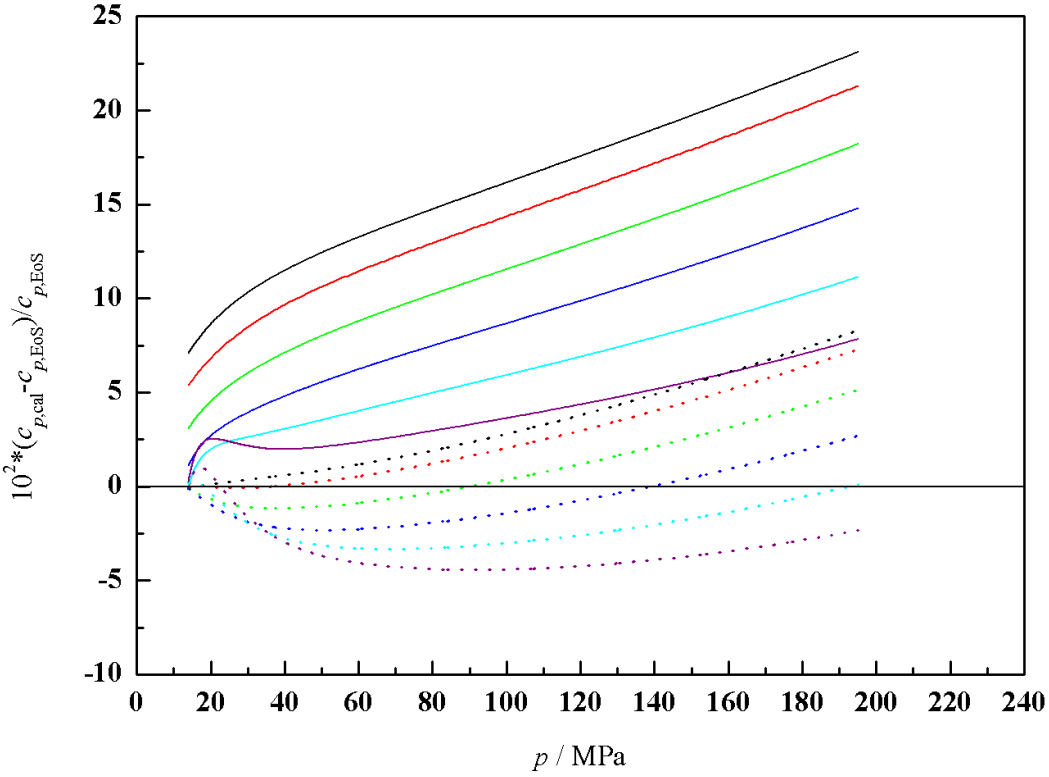

Figure S5. Relative deviation between the calculated volume-dependent solubility parameters and the values obtained using different EoSs for CO_2 + CH_3OH with x_{CO_2} = 0.9700. Solid line PC-SAFT EoS; Dot line, GERG EoS. ● , T=263.15 K; ● , T=273.15 K; ● , T=283.15 K; ● , T=293.15 K; ● , T=304.21 K; ● , T=313.15 K.

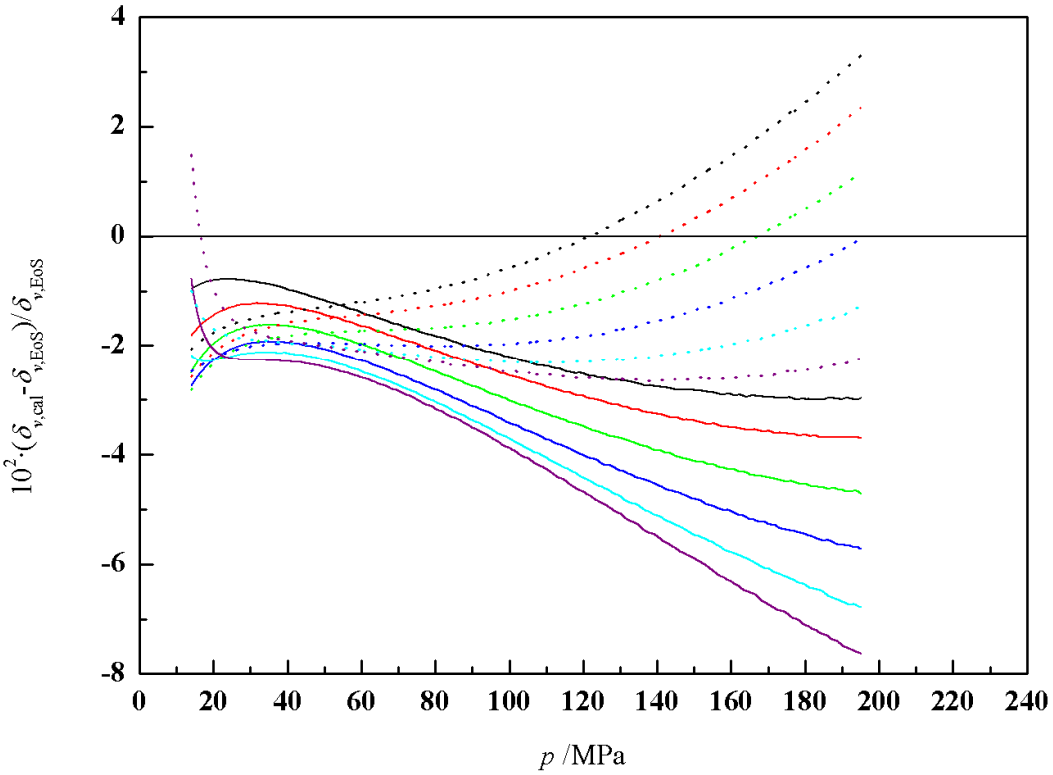

Figure S6. Relative deviation between the calculated Joule-Thomson coefficients and the values obtained using different EoSs for CO_2 + CH_3OH with x_{CO_2}= 0.9700. Solid line PC-SAFT EoS; Dot line, GERG EoS. ● , T=263.15 K; ● , T=273.15 K; ● , T=283.15 K; ● , T=293.15 K; ● , T=304.21 K; ● , T=313.15 K.

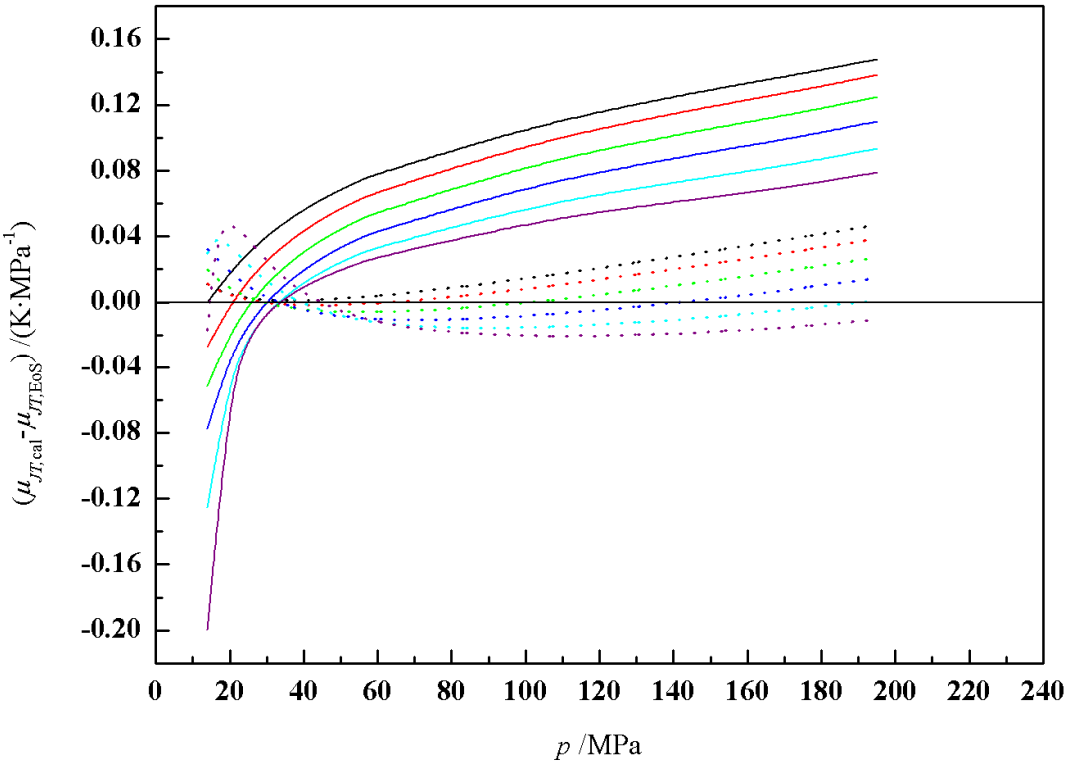
0.16
0.12
0.08
0.04
0.00
-0.04
-0.08
-0.12
-0.16
-0.20
0
20
40
60
80
100
120
140
160
180
200
220
240
p /MPa
(μJT,cal-μJT,EoS) /(K·MPa-1)